ELSEVIER

Coordination Chemistry Reviews
168 (1998) 177–231

COORDINATION CHEMISTRY REVIEWS

Annual survey of organometallic metal cluster chemistry for the year 1996

Michael G. Richmond *

Center for Organometallic Research and Education, Department of Chemistry, University of North Texas, Denton, TX 76203, USA

Received 2 September 1997; accepted 5 September 1997

Contents

1. Dissertations

The reaction of Cp_2TiCl_2 with excess H_2Se in the presence of triethylamine afforded the polynuclear complex $(CpTi)_4(\mu_2\text{-}Se)_3(\mu_3\text{-}Se)_3$. Use of $(CpTiCl_2)_n \cdot 2THF$ as the starting material gives the seleno-bridged complex $(CpTi)_5(\mu_3\text{-}Se)_6$. The synthesis of $(CpTi)_8(\mu\text{-}O)_{12}$ is also described. The reduction

* *Tel: +1 940 5653548; Fax: +1 940 5654318; e-mail: cobalt@CASI.UNT.EDU*

PII S0010-8545(97)00069-6

chemistry of these and related clusters has been examined and the results discussed. The reaction chemistry of $Cp_2Ti(CO)_2$ and H_2S in the presence of traces of H_2O affords a variety of polynuclear sulfido and oxo clusters [1].

The desulfurization catalysis and redox chemistry of several Mo_2Co_2 clusters have been explored. $(C_5Me_4Et)_2Mo_2Co_2S_4(CO)_4$ has been allowed to react with thiiranes and thietanes. Besides the corresponding organic alkenes, the insoluble solids that accompany these reactions analyze for $(C_5Me_4Et)_2Mo_2Co_2S_x$ (where $x = 5–8$). Treatment of these sulfide clusters with CO gives back the original Mo_2Co_2 cluster. The hydrogenation properties of $(C_5Me_4Et)_2Mo_2Co_2S_4(CO)_4$ have also been examined and the relationship of this catalyst to the conventional Co Mo S/Al_2O_3 catalyst discussed. The synthesis and X-ray diffraction structures of $(C_5Me_4Et)_2Mo_2M_2S_4(NO)_2$, $(C_5Me_4Et)_2W_2M_2S_4(NO)_2$ (where M = Fe, Co) and $(C_5Me_4Et)_2W_2Co_2S_3(CO)_5$ are presented. The first four clusters exhibit a cubane skeletal core [2]. The synthesis of the cubic clusters $Cp^*_3CpCr_3MO_4$ (where M = Cr, V) are reported from the starting material $[Cp^*Cr(\mu_3\text{-}O)]_3(\mu_3\text{-}O)$. The electrochemical properties and the temperature dependence of the magnetic susceptibilities of these clusters were investigated [3]. Sundry Cp*Cr- and Cp*Mo-oxide clusters have been prepared and characterized by X-ray crystallography and traditional solution spectroscopic methods [4].

Group VII and VIII metal clusters have been employed in studies involving the activation and catalytic cyclooligomerization of thietane. Treatment of 3,3-dimethylthietane and thietane with $Re_3(CO)_{10}(MeCN)_2(\mu_3\text{-}H)_3$ yields the new cluster complexes $Re_3(CO)_{10}(\overline{SCH_2CMe_2CH_2})(\mu_3\text{-}H)_3$ and $Re_3(CO)_{10}(\overline{SCH_2CH_2CH_2})(\mu_3\text{-}H)_3$, respectively. The nucleophilic ring opening of the thietane ring has been studied by using halide anions and Me_3N. The resulting products were fully characterized in solution and by X-ray analysis. Me_2S addition to $Re_3(CO)_{10}(\mu\text{-}\overline{SCH_2CH_2CH_2})(\mu_3\text{-}H)_3$ gives the zwitterionic cluster $Re_3(CO)_{10}(\mu\text{-}SCH_2CH_2CH_2SMe_2)(\mu\text{-}H)_3$, which contains a sulfonium-substituted thiolate ligand that bridges one edge of the cluster. The reaction of $Os_4(CO)_{11}(MeCN)(\mu\text{-}H)_4$ and $Ru_4(CO)_{12}(\mu\text{-}H)_4$ with thietane has also been investigated. The X-ray structures of the product clusters are presented and the cyclooligomerization activity of these ruthenium and osmium derivatives discussed [5]. The oxidation of $[Pt_3\{Re(CO)_3\}(\mu\text{-dppm})_3]^+$ using Me_3NO, O_2 and H_2O_2 is shown to yield the oxo clusters $[Pt_3\{Re(CO)_3\}(\mu_3\text{-}O)_n(\mu\text{-dppm})_3]^+$ (where $n = 1–3$), along with the hexa-oxo cluster $[Pt_3(ReO_3)(\mu_3\text{-}O)_3(\mu\text{-dppm})_3]^+$. The direct synthesis of $[Pt_3(ReO_3)(\mu\text{-dppm})_3]^+$ from $MeReO_3$ and $[Pt_3(\mu\text{-dppm})_3(\mu_3\text{-}H)]^+$ is presented. Reactivity studies involving nucleophilic additions to $[Pt_3\{Re(CO)_3\}(\mu\text{-dppm})_3]^+$ and $[Pt_3(ReO_3)(\mu\text{-dppm})_3]^+$ show site selectivity related to the formal oxidation of the coordinated rhenium center. The use of these clusters as models for oxide-supported PtRe catalysts is discussed. Data from extended Hückel MO calculations and XPS studies are presented and used in a discussion on the bonding in Pt_3Re clusters [6]. The isolation of $KRe_3(CO)_{10}$, $Re_4(CO)_{12}(OH)_2(OEt)_2 \cdot 2EtOH$, $Re_4(CO)_{12}(OH)_4 \cdot 8H_2O$ and $KRe_3(CO)_9(OH)_4$ from the reaction between

$Re(CO)_5Cl$ and KOH under a variety of conditions has been demonstrated. The molecular structure of each of these clusters was established by X-ray crystallography [7]. A higher yield synthesis of the known cluster $Mn_{15}(CO)_{24}(THF)_{12}$ has been reported. The reaction of this Mn_{15} cluster with $Fe(CO)_5$ gives the mixed-metal cluster $[\mu\text{-}Mn(THF)_2]_2Fe_2(CO)_8$ [8]. The temperature-programmed reaction (TPR) profile of $[Re(CO)_3OH]_4$ supported on Al_2O_3 has been explored. IR spectroscopic measurements revealed the presence of $Re(CO)_3(OAl)(HOAl)_2$ after activation at 480 K. Similar studies have also been conducted with the carbide clusters $[Re_7IrC(CO)_{23}]^-$ and $[Re_5IrC(CO)_{17}\{Re(CO)_3\}_2]^-$ [9].

The synthesis and electrochemical properties of $H_2Ru_3(RC_2R')(CO)_{9-n}(PR'_3)_n$ have been published. The reaction of $Ru_3(CO)_{12}$ with 3,5-di-*tert*-butyl-1,2-benzoquinone and catechol affords the tetraruthenium clusters $Ru_4(CO)_8(\mu_3\text{-}O_2C_6H_2R_2)_2$, which contain μ_3-semiquinone ligands that bridge the cluster by terminal and bridging oxygen atoms and an η^6-aryl ring. The ligand substitution chemistry and fragmentation reactivity are also reported. The activation volume for the conversion of $(\mu\text{-}H)_2Ru_3(CO)_9(\mu_3\text{-}\eta^3\text{-}EtSCCMeCMe)$ to $Ru_3(CO)_9(\mu\text{-}SEt)(\mu_3\text{-}\eta^3\text{-}CCMeCHMe)$ has been determined. On the basis of the kinetic data, it is proposed that this reaction proceeds by a dissociative rate-limiting step involving either a C–S bond or Ru–Ru bond cleavage [10]. The clusters $(\mu\text{-}H)Ru_4(CO)_9(\mu_3\text{-}COMe)\{(PPh_2)_3CH\}$ and $(\mu\text{-}H)_3Ru_3(CO)_7(\mu_3\text{-}CPh)\{(PPh_2)_2CHPPh_2\}$ have been prepared and characterized in solution. The kinetics and activation parameters for the reaction of $(\mu\text{-}H)_3Ru_3(CO)_9(\mu_3\text{-}CSEt)$ to $(\mu\text{-}H)Ru_3(CO)_9(\mu_3\text{-}CH_2SEt)$ have been measured. The proposed mechanism is based on a rapid, reversible loss of CO, followed by the formation of an agostic Ru–H–C bond. The rate-determining cleavage of the agostic bond is also supported by the measured volume of activation. The reactivity of hydrogen with $(\mu\text{-}H)_2Ru_3(CO)_8[\mu\text{-}PBu^t_2]_2$ and the results of detailed mechanistic studies are presented. The synthesis and spectroscopic characterization of the new clusters $(\mu\text{-}H)_2Ru_3(CO)_8[\mu\text{-}PCy_2]_2$ and $(\mu\text{-}H)Ru_3(CO)_8[\mu\text{-}PCy_2]_3$ are included [11]. The reaction between 1-phenylthiocyclobutene and $Os_3(CO)_{10}(MeCN)_2$ gives two new products, whose thermolysis reactivity has been explored. The compound 4-*tert*-butyl-4-methyl-1-phenylthiocyclobutene has been allowed to react with $Os_3(CO)_{10}(MeCN)_2$ and $Ru_3(CO)_{12}$. All new products were isolated and thoroughly characterized. The reactivity of 1-iodo-2-methylcyclobutene, 1-bromocyclobutene and benzothiophene with $Os_3(CO)_{10}(MeCN)_2$ has been investigated [12]. The reaction of polysulfides and polyselenides with $Fe(CO)_5$ affords the anionic clusters $[Fe_6(CO)_{12}S_6]^{2-}$ and $[Fe_5(CO)_{14}Se_2]^{2-}$. When these clusters are treated with nickel and palladium complexes, mixed-metal clusters have been isolated [13].

The phosphido clusters $Ru_4(CO)_{13}(\mu\text{-}PR_2)_2$, $Ru_4(CO)_{13}(\mu_3\text{-}PPh)$, $H_2Ru_4(CO)_{12}(\mu_3\text{-}PPh)$, $Os_4(CO)_{13}(\mu_3\text{-}PPh)$ and $Ru_4(CO)_{13}(\mu_3\text{-}PNPr^i_2)$ have been prepared and their reactivity studied. It is shown that $[Ru_4(CO)_{13}]^{2-}$ reacts with added R_2PCl to give the electron rich butterfly clusters $Ru_4(CO)_{13}(\mu\text{-}PR_2)_2$, which in the case of R = Ph is shown to undergo a reversible skeletal transformation to yield $(\mu\text{-}H)Ru_4(CO)_{10}(\mu\text{-}PPh_2)[\mu_4\text{-}(C_6H_4)PPh]$. This latter cluster represents the first example of a triply bridging bis(aryl)phosphido ligand. The reaction of 1,3-diynes

with $Ru_4(CO)_{13}(\mu_3\text{-PPh})$ has been fully investigated. The products of the diyne insertion reactions have been characterized by solution and solid-state methods. Evidence for diyne trimerization and co-dimerization with added alkynes is discussed [14]. The hydroboration of various osmium clusters has been explored. Catecholborane reacts with $[Os_3(CO)_{11}]^{2-}$ to give $[(\mu\text{-H})Os_3(CO)_{11}]^-$ while $BH_3\cdot THF$ reacts with the same starting cluster to produce $[(\mu\text{-H})Os_3(CO)_9(\mu_3\text{-}\eta^2\text{-HC}{=}{-}CH)]^-$. The cluster $[Os_3(CO)_9(\mu_3\text{-CCO})]^{2-}$ reacts with $BH_3\cdot THF$ to give a quantitative yield of the previous acetylene-coordinated cluster. When the same reaction is conducted with excess $BH_3\cdot THF$, the alkylidyne cluster $(\mu\text{-H})_3Os_3(CO)_9(\mu_3\text{-CMe})$ may be isolated. Included in this dissertation are the X-ray structures of $[Ph_3PMe]_2[M_3(CO)_{11}]\cdot CH_2Cl_2$ (where M = Ru, Os), $[PPN][(\mu\text{-H})Os_3(CO)_9(\mu_3\text{-}\eta^2\text{-HC}{=}CH)]$ and $(\mu\text{-H})_3Os_3(CO)_9(\mu_3\text{-CMe})$. Results from the use of $Fe_3(CO)_{12}$, $Ru_3(CO)_{12}$ and $H_2FeRu_3(CO)_{12}$ as CVD reagents are presented. The metallic films were analyzed by the usual arsenal of surface science methods [15]. Treatment of the tantalum carbene complex $Cp_2Ta(CH_2)(Me)$ with $Ru_3(CO)_{12}$ leads to the cluster $Cp_2Ta(\mu\text{-O})Ru_3(C_4H_4)(CO)_9$, which is shown to possess a bridging 4-carbon cumulene moiety. Spectral and structural data pertaining to the early steps of this reaction are presented and discussed [16].

The synthesis and study of sterically demanding compounds that contain multiple cluster moieties have been published. The use of the trichloroacetate esters $p\text{-}C_6H_4(O_2CCCl_3)_2$ and $C(CH_2O_2CCCl_3)_4$ in the construction of the multi-cobalt cluster complexes $p\text{-}C_6H_4[O_2CCCo_3(CO)_9]_2$ and $C[CH_2O_2CCCo_3(CO)_9]_3(CH_2O_2CCCl_3)$ is described [17]. The two clusters $[Bi_4Co_9(CO)_8(\mu\text{-CO})_8]^{2-}$ and $[Bi_8Co_{14}(CO)_{12}(\mu\text{-CO})_8]^{2-}$ have been obtained from the reaction between $[Bi_2Co_4(CO)_{11}]^-$ and $(\eta^6\text{-}C_6H_5Me)Mo(CO)_3$ upon oxidative work-up. $MePCl_2$ has been shown to function as a halogenation reagent in the reaction with $[Bi_4Fe_4(CO)_{13}]^{2-}$. The use of $MePCl_2$ (one equiv.) leads to $[Fe_2(CO)_6(\mu\text{-H})Bi_2\{Fe(CO)_4\}]^-$ and $[Bi_3Cl_4(\mu\text{-Cl})_4\{\mu_3\text{-Fe}(CO)_3\}]^{3-}$. Bromination of $Te_2Fe_3(CO)_9$ with CBr_4 initially proceeds to give $Te_2Fe_3(CO)_6$, which upon reaction with additional CBr_4 gives the novel cubane-like cluster $Fe_3(CO)_9Te_4(\mu_3\text{-CTeBr}_4)$. The results of extended Hückel MO calculations on model cluster systems related to these clusters have been reported [18].

2. Homometallic clusters

2.1. Group 4 clusters

The low-yield synthesis of $(CpTi)_6(\mu_3\text{-Te})_6(\mu_3\text{-O})_2$ from $Cp_2Ti(TeSiPh_3)_2$ with excess PPh_3 has been published. The solid-state structure of this cluster was established by X-ray crystallography [19]. Various allylic Grignard reagents have been allowed to react with $\{Cp^*Ti(\mu\text{-O})Cl\}_3$ to give the allyl oxotrimers $[Cp^*Ti(\mu\text{-O})]_3R_nCl_{3-n}$ (where $n = 1$–3, R = allyl; $n = 3$, R = crotyl). The thermal stability of these complexes has been examined and the resulting products characterized by solution and X-ray methods [20]. The redox properties of cyclopentadienyl(oxo)-

titanium complexes in non-aqueous solvents have been explored. The cluster $[(C_5H_4TMS)Ti]_4(\mu\text{-}O)_6$ exhibits an electrochemically and chemically reversible $0/1^-$ redox couple, followed by a multi-electron reduction process. An EECCEE mechanism is proposed and substantiated by a comparison with the related compound $[(C_5H_4TMS)TiCl(\mu\text{-}O)]_4$. The electrochemical properties of the mixed-metal complex $[(MeCp)_2Ti(\mu\text{-}MoO_4)_2]_2$ have also been examined. The presence of the molybdate bridges increases the stability of the electrogenerated reduction products. It is concluded that these poly-oxo clusters do not function as good models for electron reservoirs [21].

2.2. Group 5 clusters

Sodium amalgam reduction of $[Cp^*VCl(\mu\text{-}N)]_2$ gives the diamagnetic cubane cluster $[Cp^*V(\mu_3\text{-}N)]_4$, which was characterized in solution by NMR spectroscopy (^1H, ^{13}C and ^{51}V) and by X-ray crystallography. On the basis of the observed V–V and V–N bond lengths, it was concluded that strong V–N bonds exist. An electrochemical study reveals a stable one-electron reduction process [22].

2.3. Group 6 clusters

Site-selective hydrogenolysis, hydrogenation and alcoholysis have been documented in the octahedral cluster $W_6(\mu\text{-}H)_4H(\mu\text{-}CPr^i)(\mu\text{-}OPr^i)_5(OPr^i)_5$ [23]. The trinuclear cluster $Mo_3(\mu\text{-}PyS)_2(\mu_3\text{-}PyS)_2(CO)_6$ has been isolated in trace amounts from the reaction between $Mo(CO)_3(MeCN)_3$ and pyridine-2-thione. The X-ray structure of this cluster reveals a bent open geometry involving the three molybdenum centers with two doubly bridging and two triply bridging PyS ligands [24]. The thermolysis reaction of $CpMo(CO)_3H$ with Me_2S gives, as one of the products, the trinuclear cluster $CpMo(CO)(\mu\text{-}SMe)_2Mo(CO)_2(\mu\text{-}SMe)Mo(CO)_2Cp$. X-ray diffraction data confirm the make-up of the metallic core [25]. Treatment of $(\eta^5\text{-}MeO_2CCp)_2Mo_2(CO)_4$ with $(\mu\text{-}SEt)_2Fe_2(CO)_6$ in refluxing xylene produces the cluster $(\eta^5\text{-}MeO_2CCp)_4Mo_4(\mu_3\text{-}S)_2(\mu\text{-}CO)_4$, whose structure has been established by X-ray crystallography [26]. Amalgam reduction of $Cp^*Mo(SBu^t)_3$ affords the cluster complex $(Cp^*Mo)_3S_4$ in high yield. X-ray diffraction analysis (Fig. 1) has confirmed the nature of the metallic core. Extended Hückel MO calculations indicate that this cluster possesses seven cluster electrons, allowing for a comparison with the known six-electron cation $[(CpMo)_3S_4]^+$ previously prepared by Dahl. Cluster expansion is shown to arise from the population of an anti-bonding orbital of e symmetry [27].

2.4. Group 7 clusters

Disproportionation of $Mn_2(CO)_{10}$ in methanol or THF in the presence of Na_2Se gives $[Mn(CO)_5]^-$ and $[Mn_3Se_2(CO)_9]^{2-}$. The X-ray structure of the Mn_3 cluster, as the $[PPh_4]^+$ salt, provides unambiguous evidence for the first manganese complex with a mixed carbonyl–selenido ligand sphere. The paramagnetic nature of this cluster and the role of the asymmetric carbonyl bridge in controlling the

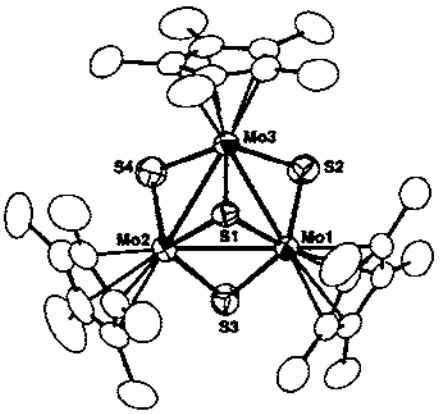

Fig. 1. X-ray structure of $(Cp^*Mo)_3S_4$. Reprinted with permission from Inorganic Chemistry. Copyright 1996 American Chemical Society.

coordination polyhedron are discussed [28]. Cluster catalysis in hydrogenation and isomerization reactions has been explored in rhenium phosphido complexes. Treatment of $Re_2[\mu\text{-}P(p\text{-}XC_6H_4)_2]_2(CO)_8$ (where X = H, F) with H_2 in xylene at 220 C gives the unsaturated rhenium clusters containing delocalized π bonds: $Re_3(\mu_3\text{-}H)_2[\mu\text{-}P(p\text{-}XC_6H_4)_2]_3(CO)_6$, $Re_4(\mu\text{-}H)_4[\mu\text{-}P(p\text{-}XC_6H_4)_2]_4[\mu_4\text{-}P(p\text{-}XC_6H_4)](CO)_8$ and $Re_4(\mu\text{-}H)_2[\mu\text{-}P(p\text{-}XC_6H_4)_2]_3[\mu_4\text{-}P(p\text{-}XC_6H_4)]_2(CO)_8$. In addition to the full solution characterization of these clusters, the X-ray structure of the second cluster was determined. These clusters are reported to hydrogenate and isomerize 1-hexene without any cluster fragmentation up to 180 C. The effect of the X substituent on the catalytic reactivity is discussed [29]. Reaction of orthomanganated *N,N*-dimethylbenzamide with SO_2 gives the tetra-manganese complex $Mn_4(CO)_{16}(\text{thiosalicylate})_2$, which is shown by X-ray analysis to contain four $Mn(CO)_4$ groups linked by two triply bridging thiosalicylate moieties [30]. $Re_3(CO)_{10}(MeCN)_2(\mu\text{-}H)_3$ reacts with *N,N*-diethyl-*N'*-*p*-tolylthiourea to produce $Re_3(CO)_{10}[\mu\text{-}SC(NEt_2)NH(p\text{-tolyl})](\mu\text{-}H)_3$ in quantitative yield. X-ray crystallography confirms that this is the first example of an S-coordinated bridging thiourea moiety [31].

The details associated with the expeditious synthesis of $Re_3(CO)_{11}(MeCN)(\mu\text{-}H)_3$ from $Re_2(CO)_8(MeCN)_2$ have appeared [32]. The reduction of $[^{188}ReO_4]$ to $[^{188}ReCl_3(CO)_3]^2$ and $^{188}Re_3(CO)_{12}(\mu\text{-}H)_3$ is described. Similar procedures have been employed with $[^{99}TcO_4]$ to give the first prepared and structurally characterized μ-hydrido bridged technetium cluster $Tc_3(CO)_{12}(\mu\text{-}H)_3$ [33]. The anionic cluster $[H_4Re_3(CO)_9][Re(CO)_3(DMF)_3]$ forms in quantitative yield when $H_4Re_4(CO)_{12}$ is treated with DMF in $CHCl_3$. The three rhenium atoms of this 44-electron cluster form an isosceles triangle, as determined by X-ray analysis. Two hydrides are shown to bridge the two long Re–Re single bonds, with the other two hydrides bridging the Re–Re double bond. This unsaturated cluster reacts with ligands to give $[H_4Re_3(CO)_9L]$ (where L = CO, Py, PPh_3,

MeCN). Variable-temperature NMR data on $[H_4Re_3(CO)_9]^-$ are discussed relative to the observed solid-state structure [34]. Spectroscopic titration of $H_4Re_4(CO)_{12}$ with chloride ions has provided evidence for the intervention of an electron-precise cluster as an intermediate in the fragmentation reaction to unsaturated triangular rhenium anions [35]. The phosphorus longitudinal relaxation times (T_1) in a series of $H_3Re_3(CO)_{11}P$ clusters have been measured in order to probe the ^{31}P coordination geometry about the cluster polyhedron. The T_1 values are dominated by relaxation by the scalar coupling process. Dipolar relaxation in these complexes is irrelevant [36]. The addition of $[M(CO)_5]^-$ (where M = Mn, Re) to the unsaturated dimer $Re_2(CO)_8(\mu\text{-}H)_2$ furnishes the trinuclear anionic clusters $[ReM(CO)_9(\mu\text{-}H)ReH(CO)_4]^-$. X-ray diffraction analysis of the Re_3 cluster (Fig. 2) reveals the presence of a fully staggered L-shaped core. Variable-temperature ^1H and ^{13}C NMR studies of this Re_3 cluster indicate the presence of a hydride/carbonyl exchange that involves a windshield-wiper motion about the $H_2Re(CO)$ fragment. Thermolysis of the same cluster gives the known cluster $[Re_3(CO)_{12}(\mu\text{-}H)_2]^-$, while protonation with strong acid yields $HRe(CO)_5$ and $Re_2(CO)_8(\mu\text{-}H)_2$ [37].

2.5. *Group 8 clusters*

Both molecular mechanics and atom–atom pair potential calculations on the solid-state dynamics of $Fe_3(CO)_{12}$ have been carried out [38]. Hydrogen bonding in organometallic cluster compounds has been investigated by analyzing the neutron and/or X-ray diffraction data deposited in the Cambridge Structural Database. Significant M–H···O interactions have been found and discussed with respect to C–H···O hydrogen bonds [39]. Structural and bonding trends in binary osmium

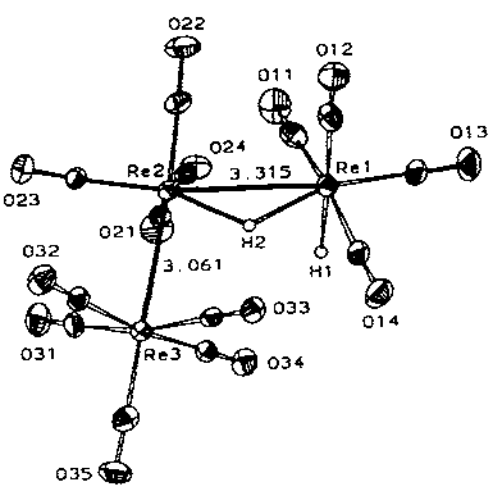

Fig. 2. X-ray structure of $[Re_3(CO)_9(\mu\text{-}H)ReH(CO)_4]^-$. Reprinted with permission from Organometallics. Copyright 1996 American Chemical Society.

carbonyl clusters have been examined by using available structural and enthalpy (M–M) data [40].

The use of $Ru_3(CO)_{12}$ as a catalyst precursor in the addition of aromatic imines at the *ortho* carbon–hydrogen bonds to olefins has been described. Aldimines and ketimines may also be employed in place of imines [41]. Regioselective acylation of the imidazole ring using $Ru_3(CO)_{12}$, CO and olefins has been achieved. These reactions proceed by activation of the imidazole C–H bond, followed by carbonylation and olefin coupling [42]. A report describing the allylic amination of cyclohexene via an intermolecular C–H bond functionalization sequence has appeared. The reaction employs $Ru_3(CO)_{12}$ as the catalyst precursor and an aryl nitro compound in the presence of CO [43]. The catalyst system composed of $Ru_3(CO)_{12}$/bpy supported on SiO_2 has been examined by FT-IR spectroscopy. Cluster fragmentation to new ruthenium/bpy surface species was observed. The role played by the solvent is crucial in determining the nature of the surface species [44].

$Ru_3(CO)_{12}$ reacts with isopropenylbenzene to give several products including the allyl clusters $Ru_3(\mu_2\text{-}H)(CO)_9(\mu_3\text{-}\eta^1\text{:}\eta^1\text{:}\eta^3\text{-}C_3H_2Ph)$ and $Ru_5(\mu_5\text{-}H)(CO)_{14}(\mu_4\text{-}\eta^1\text{:}\eta^1\text{:}\eta^3\text{:}\eta^3\text{-}C_3H_2Ph)$. X-ray diffraction analysis indicates that the isopropenyl side arm interacts with the cluster core. The polyhedral core of the latter cluster contains a Ru_4-butterfly arrangement with a wing tip-hinge edge bridged by the remaining ruthenium atom. Thermolysis of the former cluster affords the known alkyne cluster $Ru_6C(CO)_{15}(\mu_3\text{-}\eta^1\text{:}\eta^1\text{:}\eta^2\text{-}C_2HPh)$ [45]. The reaction between diazoindene and $Ru_3(CO)_{12}$ gives $Ru_3(CO)_{10}(\eta^5\text{-}C_9H_6)$, as a result of the insertion of "C_9H_6" into one of the Ru–Ru bonds of $Ru_3(CO)_{12}$. The clusters $Ru_3(CO)_8(\eta^5\text{-}C_9H_6)_2$ and $Ru_3(CO)_6(\eta^5\text{-}C_9H_6)_3$ (two different metallocyclic forms) are also produced. Three X-ray structures accompany this report [46]. The activation of C–H bonds via Ru–Ru bond scission has been examined in the thermolysis reaction of the isopropenylbenzene cluster $Ru_3(CO)_8(C_9H_{10})$. Of the several products formed in low yield, the new cluster $Ru_3(CO)_8(C_9H_8)$ has been isolated and fully characterized in solution and by X-ray crystallography [47]. The use of an arene ligand as a template for cluster formation has been investigated by allowing $Ru_3(CO)_{12}$ to react with 1,4-diisopropenylbenzene. When the reaction is carried out in refluxing octane, the following clusters may be isolated: $Ru_4(CO)_{10}(C_{12}H_{14})$, $Ru_3(CO)_8(C_{12}H_{12})$, $Ru_6H(CO)_{15}(C_{12}H_{11})$, $Ru_6H(CO)_{15}(C_{12}H_{13})$, $Ru_2(CO)_6(C_{12}H_{12})$, $Ru_5C(CO)_{16}(C_{12}H_{12})$, $Ru_3H(CO)_9(C_{12}H_{11})$, $Ru_5H(CO)_{14}(C_{12}H_{11})$ and $Ru_6C(CO)_{15}(C_{11}H_{10})$. Four X-ray structures are presented and the pathway for ligand-moderated modular cluster build-up discussed [48]. Thermolysis of $Ru_3(CO)_{12}$ with 1,3,5-trisisopropenylbenzene affords two isomeric clusters having the formula $Ru_4(CO)_9(C_{15}H_{20})$. Each of these clusters has had their molecular structure established by X-ray analysis [49]. Reaction of either *cis*-cyclooctene or *trans*-cyclododecene with $Ru_3(CO)_{12}$ at 100°C gives $Ru_3(\mu\text{-}H)(CO)_9(\mu_3\text{-}\eta^2\text{-}C_8H_{12})$ and $Ru_3(\mu\text{-}H)(CO)_9(\mu_3\text{-}\eta^2\text{-}C_8H_{14})$, respectively. Both products have been characterized in solution and by X-ray crystallography. Prolonged heating of $Ru_3(CO)_{12}$ and *cis*-cyclooctene yields $HRu_3(CO)_9(C_8H_{11})$, as determined by IR and NMR analyses [50]. Treatment of $Fe_3(CO)_{12}$ with 1,2-(3,5-cyclohexadieno)-buckminsterfullerene in refluxing benzene leads to cluster fragmentation and

[η^4-1,2-(3,5-cyclohexadieno)buckminsterfullerene]$Fe(CO)_3$, whose X-ray structure has been determined [51]. Refluxing buckminsterfullerene (C_{60}) with $Ru_3(CO)_{12}$ yields a black precipitate, whose identity was established as $Ru_3(CO)_9(C_{60})$, on the basis of FAB mass spectrometry and IR spectroscopy. X-ray diffraction analysis confirmed the presence of the face-capping arene ligand and the exact nature of the cluster as $Ru_3(CO)_9(\mu_3\text{-}\eta^2,\eta^2,\eta^2\text{-}C_{60})$ (Fig. 3) [52].

A thorough mechanistic study of the phase-transfer-catalyzed reduction of nitrobenzene to aniline using $Fe_3(CO)_{12}$ has been published. It is demonstrated that hydroxide reacts with $Fe_3(CO)_{12}$ to give the radical anion cluster $[Fe_3(CO)_{12}]^-$ and not the hydrido cluster $[HFe_3(CO)_{11}]^-$. In the presence of nitrobenzene it is the radical anion that functions as the reducing agent. The hydrido cluster is completely unreactive under comparable reaction conditions [53]. Treatment of $Ru_3(CO)_{12}$ with (4*S*, 5*S*)-(−)-2-methyl-5-phenyl-2-oxazoline-4-methanol (L) furnishes the chiral ruthenium cluster $H_2Ru_6(CO)_{14}L_2$. X-ray analysis shows that the metal frame consists of two Ru_3 triangles having weak interactions between two edges [54]. The reaction between $Ru_3(CO)_{12}$ and $Ni[\eta^1,\eta^2\text{-}C_5H_5C_2(CO_2Me)_2]Cp$ gives the dinuclear complex $Ru_2[\mu\text{-}\eta^1\text{-}O{:}\eta^2\text{-}C(CO_2Me)\text{-}CHC(O)OMe]Cp$ as the only isolable product. X-ray diffraction analysis reveals that the $C(CO_2Me)\text{-}CHC(O)OMe$ moiety bridges the two ruthenium centers by a $\mu\text{-}\eta^1{:}\eta^2$-vinyl interaction and ester coordination [55]. $Os_3(CO)_{12}$ is readily protonated in anhydrous HF, which upon addition of WF_6 produces single crystals of $[HOs_3(CO)_{12}][W_2O_2F_9]$. The solid-state structure has been determined and the hydride located by difference Fourier techniques and the geometry of the CO ligands [56]. A detailed study of alkyne activation at several

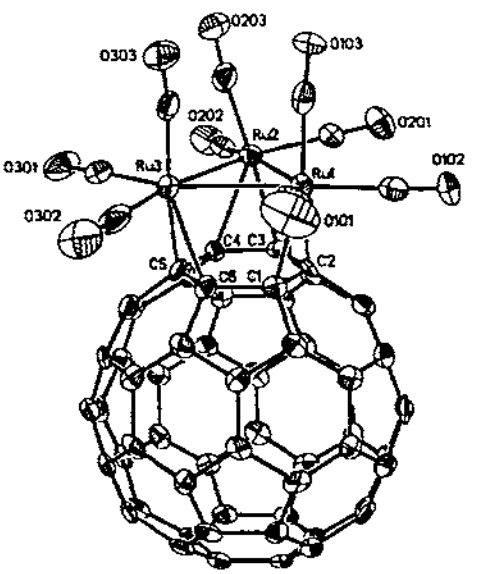

Fig. 3. X-ray structure of $Ru_3(CO)_9(\mu_3\text{-}\eta^2,\eta^2,\eta^2\text{-}C_{60})$. Reprinted with permission from Journal of American Chemical Society. Copyright 1996 American Chemical Society.

triruthenium clusters has been published. Methanol catalyzes the elimination of chloride ion from $[PPN][Ru_3(\mu\text{-}Cl)(\mu\text{-}PhCCPh)(CO)_9]$ in the presence of dppm to afford the unsaturated cluster $Ru_3(\mu\text{-}PhCCPh)(CO)_7(dppm)$ and/or the corresponding octacarbonyl cluster. The 46-electron cluster is extremely active towards ligand substitution, which has been extensively examined. Alkyne C–C bond scission reactions and alkyne coupling sequences are discussed. The X-ray structures of four complexes are presented. Mechanistic schemes for alkyne activation are shown, and the involvement of intramolecular bridge opening/closing reactions as a route to productive chemistry is discussed [57]. The reactivity of the charge-compensated carboranes *nido*-7-NR_3-7-$CB_{10}H_{12}$ (where R = various alkyl groups) with $Ru_3(CO)_{12}$ in refluxing toluene has been investigated. The major products from these reactions are the triruthenium clusters $Ru_3(CO)_8(\eta^5\text{-}7\text{-}NR_3\text{-}7\text{-}CB_{10}H_{10})$. The structure of the NMe_3 derivative has been solved by X-ray crystallography, and the solution NMR data discussed relative to the structure of each cluster [58]. The carborane *nido*-7,8-Me_2-7,8-$C_2B_9H_9$ reacts with $Ru_3(CO)_{12}$ in CH_2Cl_2 to produce both $Ru(CO)_3(\eta^5\text{-}7,8\text{-}Me_2\text{-}7,8\text{-}C_2B_9H_9)$ and $Ru_3(CO)_8(\eta^5\text{-}7,8\text{-}Me_2\text{-}7,8\text{-}C_2B_9H_9)$. The reactivity of the latter complex with phosphines has been explored. Four X-ray structures accompany this report [59]. Diene activation at three metal centers has been demonstrated in the reaction between $(Cp^*Ru)_3(\mu\text{-}H)_3(\mu_3\text{-}H)_2$ and 1,3-butadiene or isoprene. The final 1,3-dimetalloallyl cluster $(Cp^*Ru)_3(\mu\text{-}H)_4[\mu_3\text{-}\eta^3\text{-}C(Me)CHC(R)]$ has been fully characterized in solution and by X-ray crystallography in the case of the isoprene derivative (Fig. 4). NMR analyses reveal the presence of an intermediary triruthenium $\mu\text{-}\eta^2{:}\eta^2$-*s-cis*-isoprene complex, which converts to the 1,3-dimetalloallyl end-product over the course of one week. The role of an agostic C–H interaction in the intermediate complex and the results of variable-temperature NMR studies are discussed [60].

The study of $Os_3(CO)_{10}(MeCN)_2$ and $Os_3(CO)_{11}(MeCN)$ with HD or with a

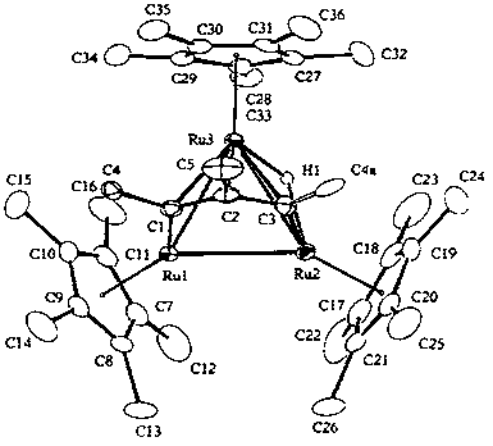

Fig. 4. X-ray structure of $(Cp^*Ru)_3(\mu\text{-}H)_4[\mu\text{-}\eta^3{:}\eta^2\text{-}C(Me)C(Me)CH]$. Reprinted with permission from Organometallics. Copyright 1996 American Chemical Society.

mixture of H_2 D_2 has been carried out in order to study the H–D isotopic exchange at osmium clusters. The kinetics and activation parameters for these reactions are reported and a mechanism involving the reversible oxidative addition and reductive elimination of H_2 from $H_2Os_3(CO)_{10}$ by way of a fluxional tetra(hydrido, deuterio) species is discussed [61]. The synthesis and use of $Os_3(CO)_{10}(\mu_3\text{-}\eta^2\text{-}$succinimido 4-pentynoate) in protein labeling reactions are described. The Os_3 cluster functions as the Bolton–Hunter-like reagent, as verified by various spectroscopic techniques. An average coupling ratio between the Os_3 marker and bovine serum albumin is ca. 20 [62]. Reaction of the carbene cluster $Os_3(CO)_9(\mu_3\text{-}\eta^2\text{:}\eta^2\text{:}\eta^2\text{-}C_6H_6Ph)$ with either S_8 or cyclohexenesulfide takes place to give the corresponding thioketone cluster $Os_3(CO)_9(\mu_3\text{-}\eta^2\text{:}\eta^2\text{:}\eta^2\text{-}C_6H_5PhS)$. Solution NMR data confirm the presence of a coordinated cyclohexadienyl ring and thioketone moiety. Reactivity studies involving protonation and hydride reduction are described, and the chemistry of the ambivalent thiol group is discussed [63]. Both $Ru_3(CO)_{12}$ and $Ru_3(CO)_{10}(MeCN)_2$ have been examined for their reactivity with 1,4-diphenylbuta-1,3-diyne. Besides the several mono- and bimetallic ruthenium complexes isolated, the two clusters $Ru_3(CO)_9(\mu\text{-}CO)(\mu_3\text{-}PhC_2C{=}CPh)$ and $Ru_4(CO)_{12}(\mu_4\text{-}PhC_2C{=}CPh)$ were also isolated. The X-ray structure of the Ru_4 cluster has been solved. Reaction schemes involving mono-yne intermediates are presented and discussed [64]. The linking and fragmentation of alkynes at $Ru_3(CO)_3(\mu\text{-}CO)(\mu_3\text{-}CO)[\mu_3\text{-}C_2(CF_3)_2]Cp_2$ have been thoroughly investigated with added alkynes. Over ten new complexes have been prepared and their spectroscopic properties reported. The X-ray structures of four triruthenium clusters are included in this report. It is demonstrated that the reactivity pathway observed is dependent on the nature of the substituents attached to the alkyne linkage [65]. Protonation of $Os_3(CO)_9(\mu\text{-}CO)(\mu_3\text{-}2\sigma,\eta^2\text{-}HC{\equiv}CR)$ (where $R=CH_2OH$, CMe_2OH) and $Os_3(\mu\text{-}H)(CO)_9(\mu\text{-}CO)(\mu_3\text{-}\sigma,2\eta^2\text{-}C{\equiv}CR)$ (where $R=CH_2OH$, CMe_2OH, $CMe{=}CH_2$) leads to the cationic clusters $[Os_3(CO)_9(\mu\text{-}CO)(\mu_3\text{-}3\sigma,\eta^2\text{-}HC{-}CCR'_2)]^+$ (where $R'=H$, Me) and $[Os_3(\mu\text{-}H)(CO)_9(\mu\text{-}CO)(\mu_3\text{-}2\sigma,2\eta^2\text{-}CCCR'_2)]^+$ (where $R'=H$, Me), respectively. PPh_3 reacts with these clusters to give phosphonium complexes. Synthetic details and spectroscopic data are presented along with the X-ray structure of $Os_3(CO)_8(\mu\text{-}CO)[HC_2(CMe{=}CH_2)COC(CMe{=}CH_2)CH]$ [66]. The reaction of $Ru_3(CO)_{12}$ with Me_3NO in the presence of nitriles leads to $Ru_3(CO)_{12-n}(RCN)_n$ (RCN = acetonitrile, adiponitrile, phenylenediacetonitrile; $n=1$–3). It is shown that the number of coordinated nitrile ligands depends on the nitrile concentration and to a lesser extent on the Me_3NO:Ru_3 ratio. Conditions related to the high yield synthesis and isolation of $Ru_3(CO)_9(MeCN)_3$ are presented. The fluxional behavior of the ancillary CO and MeCN ligands about the cluster polyhedron has been studied by variable-temperature NMR spectroscopy. Exchange pathways are discussed and it is shown that the activation energy for CO exchange is related to the number of RCN ligands present [67]. The isomerization kinetics for the transformation of $Ru_3(CO)_9(\mu\text{-}H)_3(\mu_3\text{-}CCO_2Me)$ to $Ru_3(CO)_9(\mu\text{-}H)_2(\mu_3\text{-}\eta^2\text{-}CHCO_2Me)$ and of $Ru_3(CO)_9(\mu\text{-}H)_3(\mu_3\text{-}CSEt)$ to $Ru_3(CO)_9(\mu\text{-}H)(\mu_3\text{-}\eta^2\text{-}CH_2SEt)$ have been measured by IR spectroscopy. While the former starting cluster undergoes isomerization in a process that does not involve dissociative CO loss, the latter starting cluster reacts

by a different mechanism. CO inhibition data, the entropy of activation, and activation volume suggest a mechanism involving reversible CO loss prior to the rate-limiting step but following an intramolecular rearrangement in $Ru_3(CO)_9(\mu\text{-}H)_3(\mu_3\text{-}CSEt)$. The role played by the methylidyne substituent in determining the extent of anchimeric assistance in the intramolecular rearrangement reaction is outlined. The relevance of these C–H bond formation reactions to those that take place on metal surfaces is discussed [68]. Borane reduction of the ketenylidene moiety in $Os_3(CO)_9(\mu\text{-}H)_2(\mu_3\text{-}CCO)$ gives the methylidyne-capped cluster $Os_3(CO)_9(\mu\text{-}H)_3(\mu_3\text{-}CMe)$ in moderate yield. Depending upon the nature of the reducing agent employed, the intermediate vinylidene cluster $Os_3(CO)_9(\mu\text{-}H)_2(\mu_3\text{-}\eta^2\text{-}C{-}{-}CH_2)$ could be observed by NMR analysis. Use of the isotopically labeled $Os_3(CO)_9(\mu\text{-}H)_2(\mu_3\text{-}^{13}CCO)$ in the reduction reaction gives $Os_3(CO)_9(\mu\text{-}H)_3(\mu_3\text{-}^{13}CMe)$ without any evidence of isotope scrambling. The X-ray structure (Fig. 5) of $Os_3(CO)_9(\mu\text{-}H)_3(\mu_3\text{-}CMe)$ is included in this report [69].

Heating $Fe_3(CO)_{12}$ with $[Na]_2[Te]$ and $[Ph_4P][Br]$ in MeOH at 80°C affords the tellurium-capped cluster $[Ph_4P]_2[Fe_4Te_2(CO)_{14}]$. Use of $[Cs]_2[Te]_3$ in H_2O leads to the hydrido cluster $[Cs][HFe_3Te(CO)_9]$. The X-ray structures of these clusters are reported, and the ^{125}Te NMR chemical shifts have been recorded [70]. Treatment of $Fe_3(CO)_{12}$ with SnR_2 (where R = 2,4,6-triisopropylphenyl, 2,6-diethylphenyl, pentamethylphenyl) gives the diiron complexes $Fe_2(CO)_8(\mu\text{-}SnR_2)$. Two X-ray structures are presented and the details of the Mössbauer data are interpreted with respect to other related systems [71]. The new lead–iron cluster $[Ph_4P][Fe_3(CO)_9(\mu\text{-}CO)(PbPPh_3)]$ has been obtained from the reaction between $[Ph_4P]_2[Fe_3(CO)_{11}]$ and $ClPbPPh_3$. The open and linear Fe–Fe–Pb linkage was confirmed by X-ray crystallography. The redox chemistry of this cluster was explored and the nature of the HOMO was established by MO calculations. The site preference for attack by the "$PbPPh_3^+$" fragment on $[Fe_3(CO)_{11}]^{2-}$ is contrasted with that of attack by a "$AuPPh_3^+$" fragment using MO data [72]. Photolysis of $Os(CO)_4(GeMe_2)_2$ in hexane gives the triosmium cluster $[Os(CO)_3(GeMe_2)]_3$ and

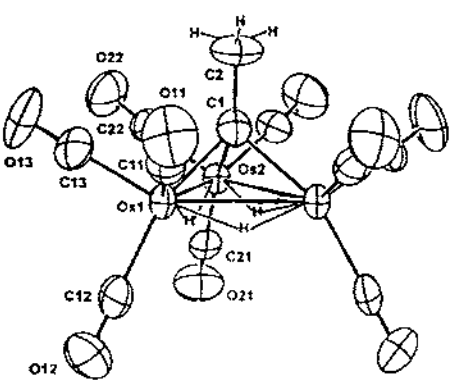

Fig. 5. X-ray structure of $Os_3(CO)_9(\mu\text{-}H)_3(\mu_3\text{-}CMe)$. Reprinted with permission from Inorganic Chemistry. Copyright 1996 American Chemical Society.

$Os_4(CO)_{12}(GeMe_2)_4$. The molecular structure of each cluster has been crystallographically determined. Cluster build-up schemes using an osmium germylene species (Os–Ge) are discussed [73]. $Ru_3(CO)_{12}$ reacts with SnR_2 (where R = 2,4,6-triisopropylphenyl) at low temperature or with the corresponding trimer $(SnR_2)_3$ at high temperature to produce $Ru_3(CO)_{10}(\mu\text{-}SnR_2)_2$ and $Ru_3(CO)_9(\mu\text{-}SnR_2)_3$. Use of $Ru_3(CO)_{10}$(dppm) in place of the parent cluster and $(SnR_2)_3$ leads to $Ru_3(CO)_8$(dppm)$(\mu\text{-}SnR_2)_2$. When the monomeric tin reagent is used, only the diruthenium complex $Ru_2(CO)_6$(dppm)$(\mu\text{-}SnR_2)$ is obtained. Four X-ray structures are presented and discussed [74].

The electron-transfer catalyzed substitution of PPh_3 for CO in $Ru_3(CO)_{12}$ using dibenzoylethene has been investigated by using a factorial design experiment. Maximum turnover numbers were observed when high concentrations of $Ru_3(CO)_{12}$ and PPh_3 were employed. The use of other phosphines and Bu^tNC display analogous substitution reactivity [75]. The previously assigned solution structures for $Fe_3(CO)_9[P(OR)_3]_3$ (where R = Me, Pr^i) have been checked by X-ray crystallography. The solid-state structures were found to be in complete agreement with the predicted structures. The isopropyl derivative possesses pseudo D_3 symmetry and is analogous to that observed in related ruthenium and osmium clusters [76]. Thermolysis of $Ru_3(CO)_{12}$ and (9-anthracyl)diphenylphosphine affords the bow-tie cluster $Ru_5(CO)_{13}(\mu_5\text{-}\eta^1\text{:}\eta^2\text{:}\eta^3\text{:}\eta^3\text{-}C_{14}H_8\text{-}\eta^1\text{-PPh})$, whose X-ray structure confirms the unique μ_5 interaction of the ligand with the pentaruthenium core. Also isolated from this reaction were the triruthenium cluster $Ru_3(CO)_8(\mu\text{-}H)_2(\mu_3\text{-}C_{14}H\text{-}PPh_2)$ and the tetraruthenium cluster $Ru_4(CO)_{11}(\mu_4\text{-}C_{14}H\text{-}PPh_2)$. Both of these clusters may be considered as anthracyne complexes derived by double metalation of one of the unsubstituted aryl rings [77]. Oxidation of $Ph_2PNP(Ph)_2P(Ph)_2NPPh_2$ by selenium gives the diselenide ligand $Ph_2P(Se)NP(Ph)_2P(Ph)_2NP(Se)Ph_2$, which when allowed to react with $Ru_3(CO)_{12}$ in the presence of Me_3NO yields the seleno-bridged cluster $Ru_3(CO)_6(\mu_3\text{-}Se)_2(\mu\text{-}PPh_2)[Ph_2PNP(Ph)_2NPPh_2]$. ^{31}P NMR and X-ray diffraction analyses confirm the identity of the product [78]. The unsaturated cluster $Os_3(CO)_7(PhC_2Ph)$(dppm) reacts with P-donor ligands to yield $Os_3(CO)_7(PhC_2Ph)$(dppm)L [where L = PBu_3, PPh_3, PMe_2Ph, $P(OMe)_3$]. Solution spectroscopic data reveal that these products exist in three isomeric forms, the ratio of which depends on the polarity of the solvent employed in the reaction. The X-ray structures of the isolated PBu_3 isomers and one of the $P(OMe)_3$ isomers have been solved. The $P(OMe)_3$-substituted clusters undergo facile decarbonylation to give the unsaturated cluster $Os_3(CO)_6(PhC_2Ph)$(dppm)$[P(OMe)_3]$. The other phosphine clusters show no tendency to undergo a similar decarbonylation [79]. Pyrolysis of $Ru_3(CO)_9(\mu\text{-dppm})(PPh_3)$ in toluene solution gives as the major products $Ru_4(\mu_4\text{-PPh})(\mu_4\text{-}PPh_2C_6H_4CO)(\mu\text{-}PPh_2CH_2)(CO)_8$ and $Ru_3[\mu_3\text{-}PPh(C_6H_4)](\mu\text{-}PPh_2CH_2)(\mu\text{-}PPh_2)(CO)_6$, along with minor amounts of $Ru_3[\mu_3\text{-}PPhCH_2PPh(C_6H_4)](CO)_9$ and $Ru_2(\mu\text{-}PPhC_6H_4PPhCH_2)(CO)_{6-n}(PPh_3)_n$ (where $n = 0, 1$). The role played by the oxidative addition of the aryl C–H bond and P–C bonds to the cluster, benzene elimination and carbonylation of the aryl–Ru bond in these transformations is discussed. The X-ray structures of the major products and $Ru_2(\mu\text{-}PPhC_6H_4PPhCH_2)(CO)_6$ are reported [80]. The electron-deficient cluster $Os_3(CO)_8(\mu_3\text{-}H)(\mu\text{-}H)(\mu\text{-}PBu^t_2)_2(\mu\text{-dppm})$ has been obtained

from $Os_3(CO)_{10}(\mu\text{-dppm})$ and PBu^t_2H in refluxing diglyme. X-ray crystallography confirms the unsaturated state of this cluster. The resistance of this cluster to add CO even under high pressure conditions suggests that the unsaturation is a result of the high steric demands exerted on the metallic core by the two phosphido ligands [81]. COT has been allowed to react with $Ru_3(CO)_{10}(\mu\text{-dppm})$ in refluxing THF to afford the new clusters $Ru_3(CO)_6(\mu\text{-dppm})(\mu\text{-}C_8H_8)$, $Ru_3(CO)_5(\mu_3\text{-}PPhCH_2PPh_2)(\mu_3\text{-}C_8H_8)(Ph)$, $Ru_3[\mu_3\text{-}PPhCH_2PPh(C_6H_4)](\mu\text{-}C_8H_8)(\mu\text{-}CO)(CO)_4$ and $Ru_3(\mu\text{-}H)[\mu_3\text{-}PPh_2CHPPh(C_6H_4)](\mu\text{-}C_8H_9)(\mu\text{-}CO)(CO)_4$, all of which have been structurally characterized by X-ray crystallography. The bonding mode adopted by the ancillary ligands is discussed [82]. Phosphine substitution at the alkylidyne capping ligand in $Os_3(CO)_9(\mu\text{-}H)_3(\mu_3\text{-}CCl)$ is observed when dppm, dppe or dppp is allowed to react with the cluster in the presence of added DBU. The isolated clusters include $Os_3(CO)_9(\mu\text{-}H)_2(\mu_3\text{-}CPPh_2CH_2PPh_2)$, $Os_3(CO)_9(\mu\text{-}H)_2(\mu_3\text{-}CPPh_2CH_2CH_2PPh_2)$ and $[Os_3(CO)_9(\mu\text{-}H)_2(\mu_3\text{-}C_2)]_2(\mu\text{-dppp})$. The intramolecular ring closure found in the first two clusters yields $Os_3(CO)_8(\mu\text{-}H)_2(\mu_3\text{-}CPPh_2CH_2PPh_2)$ and $Os_3(CO)_8(\mu\text{-}H)_2(\mu_3\text{-}CPPh_2CH_2CH_2PPh_2)$. The solid-state structures of the linked dppp cluster and the ring-closed dppm cluster have been determined by X-ray analysis [83].

The tetrahedral cluster $Ru_4(CO)_8(\mu\text{-}H)(\mu_3\text{-}PPhCH_2PPh_2)(\mu\text{-}\eta^1\text{:}\eta^5\text{-}CH_2C_5Me_4)$ has been obtained as the major isolable product from the thermolysis reaction of $Ru_3(CO)_{10}(\mu\text{-dppm})$ with pentamethylcyclopentadiene. The molecular structure of the product was ascertained by X-ray crystallography [84]. Bulky secondary phosphines have been studied for their reactivity with $Ru_3(CO)_{10}(\mu\text{-dppm})$. The use of R_2PH (where R = Bu^t, 1-Ad) leads to the electron-deficient clusters $Ru_3(CO)_4(\mu\text{-}CO)(\mu_3\text{-}H)(\mu\text{-}H)(\mu\text{-}PR_2)_2(\mu\text{-dppm})$ in good yields. The expected monophosphine intermediates $Ru_3(CO)_9(R_2PH)(\mu\text{-dppm})$ could be isolated under controlled conditions. When the less sterically demanding ligand Cy_2PH is used, the electronically saturated cluster $Ru_3(CO)_8(\mu\text{-}H)_2(\mu\text{-}PCy_2)_2(\mu\text{-dppm})$ was obtained. The structural features of two of these clusters are discussed in detail [85]. The hydrido cluster $Os_3(CO)_{10}(H)_2$ has been allowed to react with dppm and Ph_2PPy to yield the monodentate P-bonded complexes $Os_3(CO)_{10}(H)_2$(dppm) and $Os_3(CO)_{10}(H)_2(Ph_2PPy)$, respectively. The dppm-linked cluster $(H)_2(CO)_{10}Os_3(\mu\text{-dppm})Os_3(CO)_{10}(H)_2$ may be isolated by using a 2:1 stoichiometry of cluster to ligand. All of these compounds have been characterized in solution by IR and NMR (^1H and ^{31}P) spectroscopies. The reaction of $Os_3(CO)_{10}(H)_2$ with $(\eta^6\text{-}C_6H_6)RuCl_2(dppm)$ furnishes the mixed-metal cluster $(\eta^6\text{-}C_6H_6)RuCl_2(\mu\text{-dppm})Os_3(CO)_{10}(H)_2$ [86]. The kinetics for H_2 addition to $Ru_3(CO)_8(\mu\text{-}H)_2(\mu\text{-}PBu^t_2)_2$ have been examined. The reaction displays a rate law that is first-order in cluster and hydrogen and inverse order in CO. The rate-limiting step involves the oxidative addition of H_2 by a three-center transition state at a single ruthenium center after the reversible dissociation of CO. Given that the related cyclohexyl and phenyl phosphido clusters do not react with hydrogen, it is suggested that the steric bulk of the *tert*-butyl groups promote the prerequisite CO loss. Activation parameters and the results of deuterium kinetic isotope studies allow for

the formulation of a working mechanism. The energy of the unbridged Ru–Ru bond of the starting cluster has been estimated to be ca. 47–59 kJ mol^{-1}, on the basis of the temperature dependence of the equilibrium constant for hydrogenation [87]. The reaction of the activated clusters $Os_3(CO)_{12-n}(MeCN)_n$ (where $n=1, 2$) with diphenylvinylphosphine gives the corresponding phosphine-substituted clusters $Os_3(CO)_{12-n}(Ph_2PCH{=}CH_2)_n$, while the use of $Os_3(CO)_{10}(H)_2$ yields $Os_3(CO)_{10}(\mu\text{-}H)H(Ph_2PCH{=}CH_2)$. The ruthenium clusters $Ru_3(CO)_{12-n}(Ph_2PCH{=}CH_2)_n$ (where $n=1, 2$) have been prepared by using $Ru_3(CO)_{12}$ with a catalytic amount of sodium benzophenone ketyl. Thermolysis of $Os_3(CO)_{11}(Ph_2PCH{=}CH_2)$ occurs with activation of the terminal vinyl C–H bond and formation of $Os_3(CO)_9(\mu\text{-}H)(\mu_3\text{-}Ph_2PCH{=}CH)$. Analogous vinyl activations were also observed in the ruthenium clusters. The details of the solution spectroscopic data and the X-ray structures of $Os_3(CO)_{11}(Ph_2PCH{=}CH_2)$ and $Os_3(CO)_9(\mu\text{-}H)(\mu_3\text{-}Ph_2PCH{=}CH)$ are presented [88]. The two isomers of $Os_3(CO)_8(\mu\text{-}H)(PPh_3)(\mu\text{-}\eta^2\text{-}CH{=}CH_2)$, which are obtained from the reaction between acetylene and $Os_3(CO)_9(\mu\text{-}H)_2(PPh_3)$, have been isolated and crystallographically characterized. The solution structures and the slow interconversion of these isomers have been investigated by variable-temperature NMR measurements. These same isomers have also been obtained by treating $Os_3(CO)_9(\mu\text{-}H)_2(PPh_3)$ with high pressures of ethylene, by way of the intermediate cluster $Os_3(CO)_9(\mu\text{-}H)_2(PPh_3)(\mu\text{-}CHCH_3)$ [89].

The use of $Os_3(CO)_{11}(PH_3)$ in the construction of hexaosmium clusters has been published. This phosphine-substituted cluster reacts with $Os_3(CO)_{11}(MeCN)$ to give the phosphido-bridged cluster $Os_6(CO)_{22}(\mu\text{-}H)(\mu\text{-}PH_2)$ and the phosphinidene-capped cluster $Os_6(CO)_{21}(\mu\text{-}H)_2(\mu\text{-}PH)$. Use of the bis(acetonitrile) cluster $Os_3(CO)_{10}(MeCN)_2$ gives $Os_6(CO)_{21}(MeCN)(\mu\text{-}H)(\mu\text{-}PH_2)$. Each of these hexaosmium clusters was characterized by IR and NMR spectroscopies and X-ray crystallography in the case of $Os_6(CO)_{22}(\mu\text{-}H)(\mu\text{-}PH_2)$, which indicates that the phosphido moiety serves as a linking ligand that joins both Os_3 triangles. Further phosphine ligand activation has been observed when $Os_6(CO)_{22}(\mu\text{-}H)(\mu\text{-}PH_2)$ and $Os_6(CO)_{21}(MeCN)(\mu\text{-}H)(\mu\text{-}PH_2)$ are refluxed in xylene solution. Here the clusters $[Os_6(CO)_{18}(\mu_6\text{-}P)]^-$ and $Os_6(CO)_{18}(\mu\text{-}H)(\mu_6\text{-}P)$ have been isolated [90]. A report describing the systematic synthesis of substituted hexaosmium phosphide and phosphinidene clusters has appeared. Treatment of either $Os_3(CO)_{11}(PH_3)$ or $Os_3(CO)_{10}(\mu\text{-}H)(\mu\text{-}PH_2)$ with $Os_3(CO)_{11-n}L_n(MeCN)$ [where $n=1$, L = PMe_3, Bu^tNC; $n=2$, L = $P(OMe)_3$] furnishes hexaosmium clusters. Full solution characterization and the X-ray structures of three clusters are presented. Structural differences found in the two $P(OMe)_3$-substituted clusters relative to other phosphine-substituted derivatives are attributed to the steric influence associated with the bulky phosphite ligands [91]. Cyclophosphane reactivity with $Os_3(CO)_{11}(MeCN)$ and $Os_3(CO)_{10}(\mu\text{-}H)_2$ has been investigated. $(F_3CP)_4$ and $(F_3CP)_5$ react with the acetonitrile cluster to give $Os_3(CO)_{11}(\mu\text{-}PHCF_3)Os_3(CO)_{11}(\mu\text{-}H)$ while reaction with the hydrido cluster furnishes both $Os_3(CO)_{10}(\mu\text{-}H)(\mu\text{-}PHCF_3)$ and $Os_3(CO)_9(\mu\text{-}H)_2(\mu_4\text{-}F_3CPPCF_3)Os_3(CO)_9(\mu\text{-}H)_2$. Pyrolysis of $(F_3CP)_4$ with $Os_3(CO)_{12}$ at 209°C yields the tetraosmium cluster $Os_4(CO)_{13}(\mu_3\text{-}PCF_3)_2$. When the

same cyclophosphanes were allowed to react with $Ru_3(CO)_{12}$, the clusters $Ru_4(CO)_{12}(\mu_3\text{-}PCF_3)_4$ and $Ru_5(CO)_{15}(\mu_4\text{-}PCF_3)$ were obtained depending upon the cluster/cyclophosphane ratio employed. Use of the hydrido cluster $Ru_4H_4(CO)_{12}$ allows for the isolation of $Ru_4(CO)_{12}(\mu\text{-}H)_2(\mu\text{-}PCF_3)(\mu_3\text{-}PCF_3)_2$. Details of solution IR and NMR data are discussed. The X-ray structures of six products accompany this report [92]. Treatment of $Os_3(CO)_{10}(\mu\text{-}H)_2$ with $(EtP)_5$ at 80 C gives $Os_3(CO)_8(\mu\text{-}H)(\mu\text{-}\eta^3\text{-}P_5Et_5H)$ and $Os_3(CO)_{10}[1,3\text{-}(EtP)_5]$, while the use of $(PhP)_5$ at room temperature produces $Os_3(CO)_8(\mu\text{-}H)(\mu\text{-}\eta^3\text{-}P_5Ph_5H)$. The bis(acetonitrile) cluster $Os_3(CO)_{10}(MeCN)_2$ reacts with $(EtP)_5$ at room temperature to yield $Os_3(CO)_{10}[1,2\text{-}(EtP)_5]$. All compounds have been characterized by IR and NMR (^1H and ^{31}P) spectroscopies. Three X-ray structures are included in this report [93]. A pair of inversion isomers having the formula $Os_3(CO)_{10}(PPh)_5$ have been isolated from the reaction between $(PPh)_5$ and $Os_3(CO)_{10}(MeCN)_2$. The cluster $Os_3(CO)_{10}[(PPh)_5]_2$ has been isolated when a 3:1 ratio of cyclophosphane to cluster was employed. Treatment of $Os_3(CO)_{11}(PPh)_5$ with $Ru_3(CO)_{11}(MeCN)$ generates the cluster $(OC)_{11}Os_3[(PPh)_5]Ru_3(CO)_{11}$. The interconversion of the two inversion isomers and mode of cyclophosphane chelation have been examined by two-dimensional ^{31}P NMR spectroscopy [94]. Tetrakis(trifluoromethyl) diphosphine reacts with $Ru_3(CO)_{12}$ in refluxing xylene to give $Ru_4(CO)_{13}[\mu\text{-}P(CF_3)_2]_2$, $Ru_4(CO)_{14}[\mu\text{-}P(CF_3)_2]_2$ and $Ru_4(CO)_{11}[\mu\text{-}P(CF_3)_2]_4$. Treatment of $H_4Ru_4(CO)_{12}$ with $(CF_3)_2PP(CF_3)_2$ under identical reaction conditions affords $Ru_4(CO)_{12}(\mu\text{-}H)_3[\mu\text{-}P(CF_3)_2]$. Variable-temperature ^1H NMR measurements have been carried out on the last cluster in order to study the fluxional behavior of the three hydride ligands. All four products have been structurally characterized by X-ray crystallography. Several of these products are also obtained from the thermolysis of $Ru_3(CO)_{12}$ and $(CF_3)_2PH$ [95].

Site-selective basal substitution occurs in $Ru_3(CO)_6(\mu_3\text{-}S)_2$ when treated with the redox-active ligand bpcd in the presence of Me_3NO. The product cluster $Ru_3(CO)_5(bpcd)(\mu_3\text{-}S)_2$ represents the first example of a cluster derived from $Ru_3(CO)_6(\mu_3\text{-}S)_2$ that contains a chelating diphosphine ligand. The X-ray structure of the product confirms that the bpcd ligand chelates one of the basal ruthenium sites. Cyclic voltammetry studies show the existence of a reversible one-electron reduction and an irreversible metal-based oxidation. The nature of the HOMO and LUMO in the cluster was established by carrying out extended Hückel MO calculations on the model cluster $Ru_3(CO)_5(H_4\text{-}bpcd)(\mu_3\text{-}S)_2$ [96]. The reaction of Ph_3PSe with $Fe_3(CO)_{12}$ yields six products belonging to three different families of clusters. A complicated mixture of products is also obtained when the same reaction is conducted with $Ru_3(CO)_{12}$. A discussion of the solid-state structures of four clusters is presented. HPLC was used to separate the six iron complexes, whose elution was dependent on the degree of phosphine substitution and the type of cluster framework present [97]. The first example of a structurally characterized complex possessing a μ_3-P S moiety has been published. Treatment of the triferriophosphonium salts $[Cp_3Fe_3(CO)_6(\mu_3\text{-}PH)][FeCl_4]$ and $[\{Cp_2Fe_2(CO)_2(\mu\text{-}CO)\}CpFe(CO)_2(\mu_3\text{-}PH)][FeCl_4]$ with DBU, followed by reaction with sulfur gives the triferriophosphane complexes $[Cp_3Fe_3(CO)_6](\mu_3\text{-}P{-}S)$ and

$[\{Cp_2Fe_2(CO)_2(\mu\text{-}CO)\}CpFe(CO)_2](\mu_3\text{-}P\cdots S)$, respectively. The X-ray structure of the latter complex confirms the presence of the μ_3-P···S moiety [98].

The imido-capped cluster $Ru_3(CO)_{10}(\mu_3\text{-}NPh)$ reacts with PPh_3 under thermal and Me_3NO activation to give $Ru_3(CO)_9(PPh_3)(\mu_3\text{-}NPh)$ and $Ru_3(CO)_8(PPh_3)_2(\mu_3\text{-}NPh)$. Both ^{31}P NMR analysis and X-ray crystallography reveal that each substitution reaction proceeds in a regio- and stereoselective fashion. The mono-substituted cluster has an axial PPh_3 group while the bis-substituted derivative contains an axial and an equatorial PPh_3 group at adjacent ruthenium centers. The redox properties of these derivatives and the parent cluster were explored by cyclic voltammetry, with the stability of the 0/1− redox couple decreasing as the number of PPh_3 groups increases [99]. Cluster build-up schemes starting from $Ru_3(CO)_{10}(\mu_3\text{-}NOMe)$ are described. Thermolysis of $Ru_3(CO)_{10}(\mu_3\text{-}NOMe)$ in octane solution gives $Ru_6(CO)_{13}(\mu\text{-}CO)(\mu_3\text{-}NH)(\mu_5\text{-}N)(\mu_3\text{-}OMe)[\mu_2\text{-}\eta^2\text{-}C(O)OMe]$ as the major product, along with a minor amount of $Ru_4(CO)_{12}(\mu_4\text{-}N)(\mu\text{-}OMe)$. The molecular structure of the Ru_6 cluster reveals a distorted square-pyramidal core composed of a $Ru_5(\mu_5\text{-}N)$ frame. The remaining ruthenium center caps one of the triruthenium planes through some of the bridging organic ligands. Vacuum thermolysis of $Ru_3(CO)_{10}(\mu_3\text{-}NOMe)$ affords both $Ru_6(CO)_{16}(\mu\text{-}CO)_2(\mu_4\text{-}NH)(\mu\text{-}OMe)_2$ and $Ru_6(CO)_{16}(\mu\text{-}CO)_2(\mu_4\text{-}NH)(\mu\text{-}OMe)(\mu\text{-}NCO)$ in moderate yields [100]. Nitrosobenzene reacts with $Ru_3(CO)_{10}(\mu_3\text{-}NPh)$ to give $Ru_3(CO)_7(\mu_3\text{-}NPh)_2(\mu\text{-}\eta^2\text{-}ONPh)_2$, whose molecular structure is shown to consist of a triruthenium core that is capped on two sides by two phenylimido moieties and two nitrosobenzene bridging ligands across the two non-bonding Ru···Ru edges [101]. The reactivity of $[Ru_3(CO)_{10}(NO)]^-$ has been fully examined as a route to μ_4-nitrene clusters. Methylation using CF_3SO_3Me leads to both $Ru_3(CO)_{10}(\mu_3\text{-}NOMe)$ and $Ru_6(CO)_{16}(\mu\text{-}CO)(\mu\text{-}H)(\mu_4\text{-}NH)[\mu_3\text{-}\eta^2\text{-}C(O)OMe]$. Hydrogenation of this former cluster gives $Ru_3(CO)_{10}(\mu_3\text{-}NH)$ and $Ru_3(CO)_9(\mu\text{-}H)_2(\mu_3\text{-}NOMe)$. When the hydrogenation is carried out with added $Ru_3(CO)_{12}$, both $Ru_6(CO)_{16}(\mu\text{-}CO)_2(\mu\text{-}H)(\mu_4\text{-}NH)(\mu\text{-}OMe)$ and $Ru_5(CO)_{13}(\mu\text{-}H)_3(\mu_4\text{-}NH)(\mu_3\text{-}OMe)$ may be isolated. Thermolysis reactions have been carried out and the products fully characterized is solution. Ten X-ray structures have been solved and are presented in this report [102]. Kinetic studies on phosphine ligand substitution in the activated triruthenium clusters $[PPN][Ru_3(CO)_9(\mu_3\text{-}\eta^2\text{-}XPy)]$ (where X = 2-substituted pyridyl group: PhN, MeN, S) are reported. These reactions are first-order in cluster and ligand concentrations, suggesting an associative nucleophilic attack of the entering ligand on the ruthenium center, coupled with opening of the μ-X bridge. This process produces adducts of the form $[PPN][Ru_3(CO)_9(\mu\text{-}\eta^2\text{-}XPy)L]$. The influence of the ancillary bridging ligand on the reactivity of the cluster is discussed [103]. 3-*N*-Diphenylprop-2-enimine reacts with $Ru_3(CO)_{12}$ in refluxing heptane to afford $Ru_2(CO)_6(PhC{=}CHCH{=}NPh)_2$, $Ru_3(CO)_9(\mu\text{-}H)(\mu_3\text{-}\eta^2\text{-}PhCH_2CH_2C{=}NPh)$, $Ru_3(CO)_6(PhC{=}CHCH{=}NPh)_2$ and $Ru_4(CO)_{10}(PhC{=}CHCH{=}NPh)_2$. Solution IR and NMR data are presented and the X-ray structures of all four products are discussed relative to the bonding mode adopted by the nitrogen ligand [104]. New 1,3-diaryltriazenido clusters of ruthenium and osmium have been synthesized.

$Ru_3(CO)_{12}$ reacts with RN=NNHR (where R = *p*-C_6H_4X and X = F, Br, H) to produce $Ru_3(CO)_{10}(\mu\text{-H})(\mu\text{-RNNNR})$. Treatment of $Os_3(CO)_{11}(MeCN)$ in CH_2Cl_2 with the above triazenes affords the linear osmium clusters $Os_3(CO)_{11}(Cl)(\eta^2\text{-RNNNR})$. Spectroscopic data and a working mechanism accounting for the opening of the triosmium core are presented. The X-ray structures of $Ru_3(CO)_{10}(\mu\text{-H})(\mu\text{-}C_6F_5NNNC_6F_5)$ and $Os_3(CO)_{11}(Cl)(\eta^2\text{-}C_6F_5NNNC_6F_5)$ are included in this report [105]. New anthracene-containing supramolecular osmium complexes have been synthesized from $Os_3(CO)_9(\mu\text{-H})_3(\mu_3\text{-CCl})$ and pyridyl-substituted anthracenes. The three complexes isolated include $Os_3(CO)_9(\mu\text{-H})_2(\mu_3\text{-}CNC_5H_4CH{=}CHC_{14}H_9)$, $Os_3(CO)_9(\mu\text{-H})_2(\mu_3\text{-}CNC_5H_4CH_2CH_2C_{14}H_9)$ and $Os_3(CO)_9(\mu\text{-H})(\mu_3\text{-}CNC_5H_4CH{=}CHC_{14}H_9)$, of which the X-ray structures of the latter two clusters have been determined. UV/vis spectroscopic data indicate the existence of significant Os_3–anthracene interaction in the ground state of the first of these products [106]. Reaction of $Os_3(CO)_{10}(MeCN)_2$ with [PPN][NO_2] yields the nitrite cluster $[PPN][Os_3(CO)_{10}(\mu\text{-}\eta^2\text{-}NO_2)]$, which undergoes protonation by $HBF_4\cdot Et_2O$ to give $Os_3(CO)_{10}(\mu\text{-H})(\mu\text{-}\eta^2\text{-}NO_2)$. X-ray crystallography confirms the presence of the μ-η^2-nitrite ligand in both clusters [107]. The linear osmium cluster $Os_3(CO)_{11}(H)(\eta^2\text{-}C_6F_5NNNC_6F_5)$ reacts with $Os_3(CO)_{11}(MeCN)$ in hexane at 60°C under vacuum to produce the "spiked" tetraosmium cluster $Os_4(CO)_{14}(\mu\text{-H})(\eta^2\text{-}C_6F_5NNNC_6F_5)$, while reaction with $Os_3(CO)_{10}(MeCN)_2$ in CH_2Cl_2 at room temperature gives the "spiked" hexaosmium cluster complex $Os_6(CO)_{21}(\mu\text{-H})(MeCN)(\eta^2\text{-}C_6F_5NNNC_6F_5)$. Thermolysis of this last cluster proceeds to afford $Os_5(CO)_{15}(\mu\text{-H})(\eta^2\text{-}C_6F_5NNNC_6F_5)$ and $Os_5(CO)_{16}$. The transformations exhibited by these clusters and their polyhedral shapes are discussed in detail [108]. 1-Hydroxypyridine-2-thione reacts with $Os_3(CO)_{11}(MeCN)$ to yield $Os_3(CO)_{10}(\mu\text{-H})[\mu\text{-}\eta^1\text{-}SC_5H_4N(O)]$, $Os_3(CO)_{10}(\mu\text{-H})[\eta^2\text{-}SC_5H_4N(O)]$ and $Os_3(CO)_9(\mu\text{-H})[\mu\text{-}\eta^2\text{:}\eta^1\text{-}SC_5H_4N(O)]$. Use of $Os_3(CO)_{10}(MeCN)_2$ yields primarily the first product along with a trace amount of the last product. Reaction of the same pyridine compound with the isocyanide clusters $Os_3(CO)_{10}(CNR)(MeCN)$ (where R = benzyl, Pr) leads to the formation of $Os_3(CO)_9(\mu\text{-H})(CNR)[\eta^2\text{-}SC_5H_4N(O)]$, $Os_3(CO)_{10}(\mu\text{-}\eta^1\text{-}C{-}NHCH_2Ph)[\eta^2\text{-}SC_5H_4N(O)]$ and $Os_3(CO)_9(\mu\text{-H})(CNR)[\mu\text{-}\eta^1\text{-}SC_5H_4N(O)]$. Thermolysis of $Os_3(CO)_{10}(\mu\text{-H})[\mu\text{-}\eta^1\text{-}SC_5H_4N(O)]$ at 80°C generates $Os_3(CO)_9(\mu\text{-H})(\mu_3\text{-SPy})$, $Os_3(CO)_9(\mu\text{-OH})(\mu_3\text{-SPy})$ and CO_2. Four X-ray structures have been solved, of which $Os_3(CO)_{10}(\mu\text{-H})[\mu\text{-}\eta^1\text{-}SC_5H_4N(O)]$ is shown below in Fig. 6. The versatile bonding modes exhibited by the N-oxide group are discussed [109].

The catalytic hydrogenation of diphenylacetylene to *cis*- and *trans*-stilbene is reported to be catalyzed by the cluster $[Ru_3(CO)_8(\mu\text{-H})(\mu_3\text{-ampy})(\mu,\eta^1\text{:}\eta^2\text{-PhC}{=}CHPh)][BF_4]$. On the basis of kinetic studies and spectroscopic data, it is proposed that catalysis takes place via a cationic triruthenium species. A working mechanism is presented and discussed [110]. The reaction of neutral and anionic nucleophiles with $[Ru_3(CO)_8(\mu\text{-H})(\mu_3\text{-ampy})(\mu\text{-PhC}{=}CHPh)][BF_4]$ has been studied. Monodentate ligands add readily to the cluster to give $[Ru_3(CO)_{8-n}L_n(\mu\text{-H})(\mu_3\text{-ampy})(\mu\text{-PhC}{=}CHPh)][BF_4]$ (where $n = 1$–3), while dppm causes the reductive elimination of *cis*-stilbene and production of

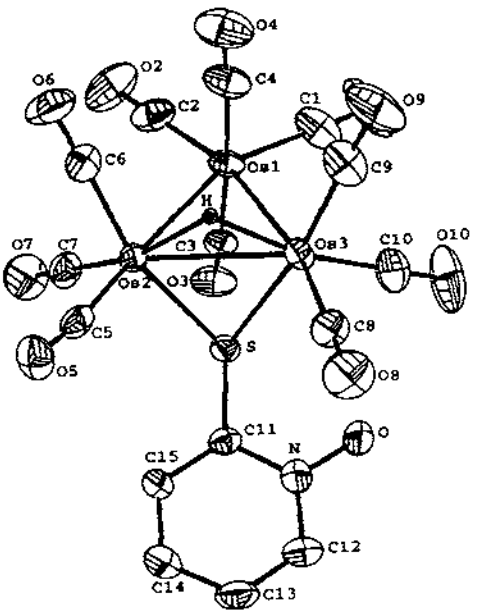

34

Fig. 6. X-ray structure of $Os_3(CO)_{10}(\mu\text{-}H)[\mu\text{-}\eta^1\text{-}SC_5H_4N(O)]$. Reprinted with permission from Organometallics. Copyright 1996 American Chemical Society.

$[Ru_3(CO)_7(\mu\text{-dppm})(\mu_3\text{-ampy})][BF_4]$. NaOMe deprotonation of the starting cluster gives $Ru_3(CO)_8(\mu_3\text{-ampy})(\mu\text{-PhC}{-}\text{CHPh})$ while reaction with NaOH yields *cis*-stilbene and $Ru_3(CO)_9(\mu\text{-H})(\mu_3\text{-ampy})$ [111]. Two alternative routes for the synthesis of $Ru_3(CO)_9(\mu\text{-H})(\mu,\eta^2\text{-}o\text{-}HNC_6H_2Me_2NH_2)$ and $Ru_3(CO)_8(\mu_3,\eta^2\text{-}o\text{-}OC_6H_4NH_2)$ are reported from $Ru_3(CO)_{12}$ and $RuCl_3 \cdot nH_2O$. The thiol derivative $Ru_3(CO)_9(\mu\text{-H})(\mu,\eta^2\text{-}o\text{-}SC_6H_4NH_2)$ is best prepared from 2-aminothiophenol and $Ru_3(CO)_{12}$. The molecular structure of this last cluster was established by X-ray crystallography [112]. The synthesis and reactivity of ruthenium clusters containing a bridging 1-azavinylidene ligand have been published. $Ru_3(CO)_{12}$ reacts with the lithium salt of benzophenone imine to afford $[Ru_3(CO)_{10}(\mu\text{-N}{=}\text{CPh}_2)]^-$, which after protonation gives the corresponding bridged cluster $Ru_3(CO)_{10}(\mu\text{-H})(\mu\text{-N}{=}\text{CPh}_2)$. The direct reaction of benzophenone imine and $Ru_3(CO)_{12}$ cannot be used as a route to the desired product. Dppm reacts with $Ru_3(CO)_{10}(\mu\text{-H})(\mu\text{-N}{=}\text{CPh}_2)$ to produce $Ru_3(CO)_8(\mu\text{-dppm})(\mu\text{-H})(\mu\text{-N}{=}\text{CPh}_2)$ and $Ru_3(CO)_7(\mu\text{-dppm})$-$(\text{dppm})(\mu\text{-H})(\mu\text{-N}{=}\text{CPh}_2)$. In each of these clusters the dppm ligand bridges the same Ru–Ru edge. The latter cluster was examined by X-ray diffraction analysis, which proved the presence of the η^1-dppm ligand. The thermolysis chemistry of these clusters was also investigated, with orthometalation of the azavinylidene's phenyl group being observed [113].

Thermolysis of $Ru_3(CO)_{12}$ with pyridine gave a mixture of

$Ru_3(CO)_{10}(\mu\text{-}H)(\mu\text{-}NC_5H_4)$ and $Ru_3(CO)_8(\mu\text{-}H)_2(\mu\text{-}NC_5H_4)_2$. X-ray analysis of the latter cluster confirms that it is the first crystallographically characterized Ru_3 cluster containing two orthometalated N-heterocycle ligands. Dppm reacts with $Ru_3(CO)_{10}(\mu\text{-}H)(\mu\text{-}NC_5H_4)$ to give a mixture of products, along with $Ru_3(CO)_8(\mu_3\text{-}\eta^2\text{-}PPhCH_2PPh_2)(\mu\text{-}NC_5H_4)$, whose solid-state structure was established by X-ray analysis. This same product is also obtained in low yield from the reaction between pyridine and $Ru_3(CO)_{10}(\mu\text{-dppm})$. Use of dppe, with its more flexible chain, leads to more complex mixtures of products. Whereas the thermolysis of $Ru_3(CO)_{10}(\mu\text{-}H)(\mu\text{-}NC_5H_4)$ gives $[Ru_2(CO)_4(\mu\text{-}H)(\mu\text{-}NC_5H_4)_2]$-$[Ru_{10}(CO)_{21}(\mu\text{-}H)(\mu_6\text{-}C)]$, thermolyses of the other pyridine-containing clusters afford only intractable mixtures [114]. Treatment of $Os_3(CO)_{10}(MeCN)_2$ with 4-methylthiazole yields $Os_3(CO)_{10}(\mu\text{-}H)(\mu\text{-}2,3\text{-}\eta^2\text{-}\overline{C=NCMe=CHS})$, which displays a thiazolide ligand that is coordinated to the cluster core via the nitrogen and carbon atoms of the C=N bond. The reactivity of this cluster has been examined in PPh_3 substitution reactions. An additional reaction occurs with 4-methylthiazole at 110°C to give $Os_3(CO)_8(\mu\text{-}H)_2(\mu\text{-}2,3\text{-}\eta^2\text{-}\overline{C=NCMe=CHS})(\mu\text{-}2,3\text{-}\eta^2\text{-}\overline{C=NCMe=CHS})$ and $Os_3(CO)_8(\mu\text{-}H)_2(\mu\text{-}2,3\text{-}\eta^2\text{-}\overline{C=NCMe=CHS})_2$. $Ru_3(CO)_{12}$ has been allowed to react with 4-methylthiazole in the presence of sodium benzophenone to give $Ru_3(CO)_{10}(\mu\text{-}H)(\mu\text{-}2,3\text{-}\eta^2\text{-}\overline{C=NCMe=CHS})$ and $Ru_3(CO)_8(\mu\text{-}H)_2(\mu\text{-}2,3\text{-}\eta^2\text{-}\overline{C=NCMe=CHS})$, depending on the amount of heterocyclic ligand used. All new complexes were characterized in solution by IR and NMR spectroscopies. The molecular structures of three clusters are presented [115]. A detailed study describing the molecular transformations of bicyclic nitrogen heterocycles with triosmium clusters has been published. Indoline reacts with $Os_3(CO)_{10}(MeCN)_2$ to initially give $Os_3(CO)_{10}(\mu\text{-}H)(\mu\text{-}\eta^2\text{-}C_8H_7NH)$, which decarbonylates thermally to afford the corresponding nonacarbonyl cluster. $Os_3(CO)_9(\mu\text{-}H)_2(\mu_3\text{-}\eta^2\text{-}C_8H_7N)$ exists as a tautomeric mixture involving μ-alkylidene imino and μ-amido aryl bonding modes. The kinetics and equilibrium constant associated with the decarbonylation have been measured. Dehydrogenation of these tautomers furnishes $Os_3(CO)_9(\mu\text{-}H)_2$-$(\mu_3\text{-}\eta^2\text{-}C_8H_4NH)$. Tetrahydroquinoline reacts with $Os_3(CO)_{10}(MeCN)_2$ to give a related tautomeric pair having the formula $Os_3(CO)_9(\mu\text{-}H)(\mu_3\text{-}\eta^2\text{-}C_9H_6N)$, along with $Os_3(CO)_{10}(\mu\text{-}H)[\mu\text{-}\eta^1\text{-}C_9H_{10}N(Me)CN]$. This latter cluster results from the nucleophilic attack of the quinoline's nitrogen atom on a coordinated MeCN ligand. The reactivity differences between the indoline-, tetrahydroquinoline- and isotetrahydroquinoline-substituted clusters are discussed [116]. The synthesis and characterization of triosmium clusters containing μ-η^1 and μ-η^1:η^6-phenyl groups have been described. Treatment of $Os_3(CO)_9(\mu\text{-}H)_2[\mu\text{-}\eta^2\text{-}\overline{C=N(CH_2)}]Br$ with Ph_2Hg gives the μ-η^1-phenyl complex $Os_3(CO)_{10}[\mu\text{-}\eta^2\text{-}\overline{C=N(CH_2)_3}](\mu\text{-}\eta^1\text{-}C_6H_5)$. This cluster transforms into the μ-η^1:η^6-phenyl cluster $Os_3(CO)_8[\mu\text{-}\eta^2\text{-}\overline{C=N(CH_2)_3}](\mu\text{-}\eta^1\text{:}\eta^6\text{-}C_6H_5)$ in refluxing octane. The molecular structure of this latter cluster was unequivocally

established by X-ray crystallography. Ambiguities associated with the location of the hydride ligands in $Os_3(CO)_9(\mu\text{-}H)_2[\mu\text{-}\eta^2\text{-}C{=}N(CH_2)_3]Br$ have been addressed by investigating the solution dynamics and X-ray structure (Fig. 7) of the related cluster $Os_3(CO)_9(\mu\text{-}H)_2\ \mu\text{-}\eta^2\text{-}C{=}NCH(Me)CH_2CH_2\ Br$. Carbon nitrogen disordering was eliminated by the introduction of the 2-methyl group [117].

The reaction of $Fe_3(CO)_{12}$ with thiophene and benzothiophene is accelerated by microwave heating when carried out with added Fe_3O_4. No desulfurization was observed [118]. The kinetics and mechanism for isomerization of $HRu_3(CO)_9(\mu_3\text{-}\eta^2\text{-}EtSCCMeCMe)$ to $Ru_3(CO)_9(\mu\text{-}SEt)(\mu_3\text{-}\eta^3\text{-}CCMeCHMe)$ have been reported. An intramolecular process involving significant Ru–Ru or C–S bond cleavage in the transition state is favored, on the basis of the reported activation parameters. The large activation volume rules out a rate-limiting step involving CO loss and C–H bond reductive elimination [119]. The difunctional ligands 2-mercaptobenzoic acid, 3-mercaptopropanoic acid and 2,6-dicarboxypyridine react with $Os_3(CO)_{10}(MeCN)_2$ to give the linked clusters $[Os_3(CO)_{10}H]_2L$. Full solution characterization and two X-ray structures are presented [120]. The electrochemical behavior of $[Fe_3(CO)_9(\mu_3\text{-}S)]^{2-}$ has been reinvestigated, allowing for the isolation of the new cluster $[Fe_5(CO)_{14}S_2]^{2-}$ and the known cluster $[Fe_6(CO)_{12}S_6]^{2-}$. X-ray crystallography has been employed in the structural analysis of each of these clusters. Bulk electrolytic oxidation of $[Fe_5(CO)_{14}S_2]^{2-}$ gives $[Fe_5(CO)_{14}S_2]^{-}$, whose ESR signal was recorded in solution. The one-electron oxidation is chemically reversible in CH_2Cl_2 but not in MeCN solution. It is demonstrated that oxidation of $[Fe_3(CO)_9(\mu_3\text{-}S)]^{2-}$ gives $[Fe_3(CO)_9(\mu_3\text{-}S)]$ and that it is this latter cluster that is involved in the formation of $[Fe_5(CO)_{14}S_2]^{n-}$ (where $n=0$–2) [121]. The protonation and ligand substitution chemistry in the triruthenium sulfonohydrazido-capped clus-

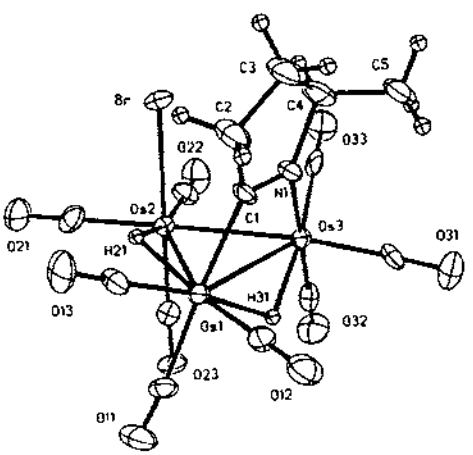

Fig. 7. X-ray structure of $Os_3(CO)_9(\mu\text{-}H)_2\ \mu\text{-}\eta^2\text{-}C{=}NCH(Me)CH_2CH_2\ Br$. Reprinted with permission from Organometallics. Copyright 1996 American Chemical Society.

ter $Ru_3(CO)_9(\mu_2\text{-}H)[\mu_3\text{-}\eta^2\text{-}H_2NNS(O)_2Mes]$ has been explored [122]. PPh_3 ligand substitution occurs in $Ru_3(CO)_9(\mu_2\text{-}H)(\mu_3\text{-}\eta^2\text{-}SCNHPhNPh)$ to give $Ru_3(CO)_{9-n}(PPh_3)_n(\mu_2\text{-}H)(\mu_3\text{-}\eta^2\text{-}SCNHPhNPh)$ (where $n = 1, 2$). Both clusters were fully characterized in solution and by X-ray crystallography. Thermolysis of the bis-phosphine cluster or the parent cluster in the presence of PPh_3 (2 equiv.) affords the sulfur-capped complex $Ru_3(CO)_7(PPh_3)(\mu_2\text{-}\eta^2\text{-}C_6H_5)(\mu_2\text{-}PPh_2)(\mu_3\text{-}S)$. The substitution reaction involving dppe produces $Ru_3(CO)_7(dppe)(\mu_2\text{-}H)(\mu_3\text{-}\eta^2\text{-}SCNHPhNPh)$, whose dppe ligand is bound *cis* to the μ_2-S moiety and *cis* to the μ_2-hydride ligand [123]. The synthesis and structural analysis of an electron-deficient Ru_3 cluster that contains a chiral sulfoximido capping ligand have been published. The reaction between $Ru_3(CO)_{12}$ and methylphenylsulfoximine produces $Ru_3(CO)_9(\mu_2\text{-}H)[\mu_3\text{-}NS(O)MePh]$ in good yields. It is shown that N–H bond activation of enantiomerically pure MePhS(O)NH does not affect the chirality of the sulfur stereocenter [124]. *N*-Sulfinylaniline, an SO_2 analog, reacts with $Ru_3(CO)_{12}$ in refluxing toluene to give low yields of $Ru_3(CO)_9(\mu_3\text{-}NPh)(\mu_3\text{-}S)$, $Ru_3(CO)_9(\mu_3\text{-}NPh)_2$, $Ru_4(CO)_{10}(\mu\text{-}CO)(\mu_4\text{-}\eta^2\text{-}SNPh)(\mu_4\text{-}S)$ and $Ru_4(CO)_{10}(\mu\text{-}CO)(\mu_4\text{-}\eta^2\text{-}SNPh)(\mu_4\text{-}NPh)$. Use of $Ru_3(CO)_{10}(MeCN)_2$ leads to $Ru_3(CO)_9(\mu_3\text{-}NPh)(\mu_3\text{-}S)$ as the major product in good yield. With the exception of the known cluster $Ru_3(CO)_9(\mu_3\text{-}NPh)_2$, all clusters were subjected to X-ray analysis. A mechanism accounting for the formation of $Ru_3(CO)_9(\mu_3\text{-}NPh)(\mu_3\text{-}S)$ and the results of variable-temperature ^{13}C NMR studies are presented [125]. The photochemical reactivity of the 2-mercaptopyridine-substituted clusters $[Os_3(CO)_{10}H]_2(\mu\text{-}SC_5H_3NCO_2)$, $Os_3(CO)_{10}H[SC_5H_3N(OH)]$ and $Os_3(CO)_{10}H(SC_5H_4N)$ has been studied. Photochemically induced decarbonylation readily occurs, and the pyridyl nitrogen moiety coordinates to the third osmium center in these clusters. The quantum yields for these reactions are reported. Two of the three products have had their structures established by X-ray crystallography [126]. $Ru_3(CO)_{12}$ in refluxing toluene reacts with diphenyl-2-thienylphosphine to give $Ru_3(CO)_9(\mu_2\text{-}H)(\mu_3\text{-}Ph_2PC_4H_2S)$ (major) and $Ru_3(CO)_8(\mu_2\text{-}H)(\mu_3\text{-}Ph_2PC_4H_2S)(Ph_2PC_4H_3S)$ (minor). The cyclometalated thiophene ring in the major product was verified by X-ray diffraction analysis (Fig. 8). This same cluster exhibits a dynamic interchange between the σ and η^2 interactions of the thienyl group, as determined by variable-temperature NMR measurements. Thermolysis of $Ru_3(CO)_9(\mu_2\text{-}H)(\mu_3\text{-}Ph_2PC_4H_2S)$ with $Ru_3(CO)_{12}$ produces the tetraruthenium clusters $Ru_4(CO)_{11}(\mu_4\text{-}PPh)(\mu_4\text{-}C_4H_2S)$ and $Ru_4(CO)_{11}(\mu_4\text{-}PPh)(\mu_4\text{-}C_6H_4)$. These products arise through the formal elimination of benzene and thiophene, respectively. The molecular structure of the latter Ru_4 cluster accompanies this report [127].

UV irradiation of $[Os(CO)_4(SnMe_2)]_2$ produces the tetraosmium cluster $Os_4(CO)_{14}(SnMe_2)_4$, whose X-ray structure shows an essentially planar Os_4Sn_4 core comprised of a central rhomboidal Os_2Sn_2 moiety with each Os atom part of two outer Os_2Sn triangles. Treatment of $[Os(CO)_4(SnMe_2)]_2$ with Me_3NO leads to $Os_4(CO)_{14}(\mu_3\text{-}O)_2(SnMe_2)_4$ in low yield. The solid-state structure of this cluster reveals a central six-membered $(OsOSn)_2$ ring to which are fused two OsOSnO rings. The outer rings share a common OsO edge with the central ring. The observed

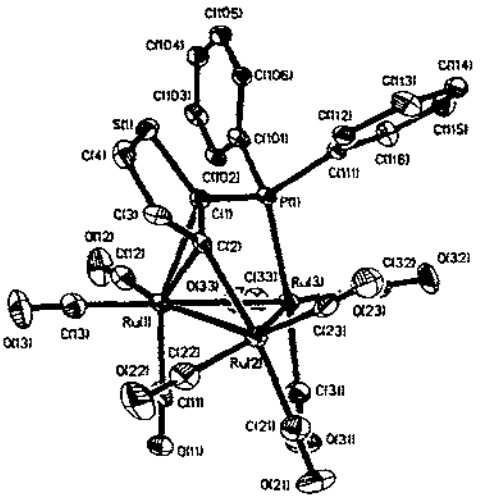

Fig. 8. X-ray structure of $Ru_3(CO)_8(\mu_2\text{-}H)(\mu_3\text{-}Ph_2PC_4H_2S)$. Reprinted with permission from Organometallics. Copyright 1996 American Chemical Society.

cluster structures are discussed relative to Polyhedral Skeletal Electron Pair theory [128]. The reactivity of $[Et_4N][Sb\{Fe(CO)_4\}_4]$ with alkyl halides and dihalides has been explored [129]. $Fe_2(CO)_6(\mu\text{-}Se)_2$ reacts with the diyne compounds HC≡CC≡CR (where R = TMS, $SnBu_3$) to yield $[Fe_2(CO)_6Se_2](\mu\text{-}s\text{-}trans\text{-}C_4H_2)$. The 1,3-butadiene ligand is coordinated to the Fe_2Se_2 core in a *trans* fashion, as determined by X-ray analysis [130]. $Ru_3(CO)_{12}$ reacts with allylbenzene or 4-phenylbut-1-ene to give the tetraruthenium clusters $Ru_4(CO)_{10}(C_9H_{10})$ and $Ru_4(CO)_{10}(C_9H_{12})$, respectively. The molecular structure of each cluster was crystallographically determined [131]. The isolation and characterization of the products formed from the reaction between $Os_3(CO)_{10}(\mu\text{-}H)_2(MeCN)_2$ and cyclohexa-1,3-diene are reported. Besides the formation of four known tetraosmium clusters possessing a cyclohexa-1,3-diene derived ligand, the new clusters $Os_4(CO)_{10}(\mu\text{-}H)(\mu_3\text{-}\eta^1\text{:}\eta^2\text{:}\eta^1\text{-}C_6H_8)(\eta^3\text{-}C_6H_9)$, $Os_4(CO)_{10}(\mu\text{-}H)_2(\eta^6\text{-}C_6H_5C_6H_9)$ and $Os_5(CO)_{13}(\mu\text{-}H)_2(\eta^4\text{-}C_6H_8)$ have been isolated. The molecular structure of each new cluster has been solved, and the ^1H NMR data on the first of these clusters, which possesses a cyclohexyne allyl moiety, are discussed. The hydrogenation and dehydrogenation steps observed in these reactions are contrasted with the chemistry found on metal surfaces [132].

Treatment of either $[Cp^*Ru(\mu_3\text{-}Cl)]_4$ or $Cp^*RuCl(\mu\text{-}Cl)_2RuCp^*Cl$ with H_2S gives the hydrosulfido-bridged complex $Cp^*RuCl(\mu\text{-}SH)_2RuCp^*Cl$. Thiols react with $[Cp^*Ru(\mu_3\text{-}Cl)]_4$ to produce $Cp^*RuCl(\mu\text{-}SR)_2RuCp^*Cl$ (where R = Et, tolyl), which upon reaction with Wilkinson's catalyst (2 equiv.) yields the triangular mixed-metal cluster $(Cp^*Ru)_2(\mu_2\text{-}H)(\mu_3\text{-}S)_2RhCl_2(PPh_3)$ [133]. Diferrocenyl dichalcogenides undergo reaction with $[Cp^*Ru(\mu_3\text{-}Cl)]_4$ to give the ferrocenylchalcogenolate-bridged ruthenium complexes $[Cp^*RuCl(\mu\text{-}EFc)]_2$ (where E = S, Se, Te). Sodium amalgam

reduction of these complexes in the presence of 1,3-butadiene leads to $[Cp^*Ru(\mu\text{-}EFc)]_2(\mu\text{-}s\text{-}trans\text{-}\eta^2\text{:}\eta^2\text{-}C_4H_6)$ [134].

Cluster expansion by metal fragment addition to *nido* clusters has been documented in the reaction of *nido* $Ru_3(CO)_9[\mu_3\text{-}PC(CO)Bu^t]_2$ with 12-valence electron fragments. Use of $Ru_3(CO)_{12}$ and $Fe_2(CO)_9$ allows for the isolation of the tetrametallic clusters $Ru_4(CO)_{10}(\mu\text{-}CO)[\mu_4\text{-}PC(CO)Bu^t]_2$ and $FeRu_3(CO)_{10}(\mu\text{-}CO)[\mu_4\text{-}PC(CO)Bu^t]_2$, respectively. Both clusters are coordinatively saturated given the presence of seven skeletal electron pairs and a *closo* M_4P_2 polyhedral core [135]. Thermolysis of $Ru_3(CO)_{12}$ with 1,3-COD affords the clusters $Ru_4(CO)_{12}(\mu_4\text{-}\eta^2\text{-}C_8H_{10})$ and $Ru_4(CO)_{12}(\mu_4\text{-}\eta^2\text{:}\eta^2\text{-}C_8H_{10})$. These isomeric clusters differ only in the overall electron donation from the C_8H_{10} to the cluster. The former cluster possesses 60 electrons while the latter cluster contains 62 electron. X-ray studies reveal that both polyhedral frameworks are based on a butterfly structure. The bonding interactions between the polyene ligand and the cluster have been investigated by extended Hückel MO calculations [136]. The 64-electron butterfly cluster $Ru_4(CO)_9(\mu\text{-}PPh_2)_2(C_2Bu^t)_2$, which was obtained from the thermolysis of $Ru_3(CO)_6(\mu\text{-}PPh_2)(C_2Bu^t)$, undergoes C–C bond coupling to give the diyne clusters $Ru_4(CO)_8(\mu\text{-}PPh_2)_2(C_4Bu^t_2)$ and $Ru_4(CO)_7(\mu\text{-}PPh_2)_2(C_4Bu^t_2)$. The structural identity of the diyne clusters was determined by X-ray crystallography [137]. The clusters $Ru_4(CO)_{13}(PNPr^i_2)$ and $Os_4(CO)_{13}(PNPr^i_2)$ have been synthesized from $[Ru_4(CO)_{13}]^{2-}$ and $[Os_4(CO)_{13}]^{2-}$. The latter reagent is prepared from $Os_3(CO)_{12}$ and $[Os(CO)_4]^{2-}$, providing a facile route to this dianion. Both tetrametallic clusters are decarbonylated to $M_4(CO)_{12}(PNPr^i_2)$, and which upon chromatography furnishes $[M_4(CO)_{12}(PO)]^-$. These clusters showing the coordination of a phosphorus monoxide moiety possess a square-pyramidal M_4P arrangement of atoms. X-ray crystallographic data indicate that considerable double-bond character is present in the P–O moiety. Fig. 9 shows the X-ray structure of $Os_4(CO)_{13}(PNPr^i_2)$ [138].

A review dealing with the intramolecular interactions and supramolecular organ-

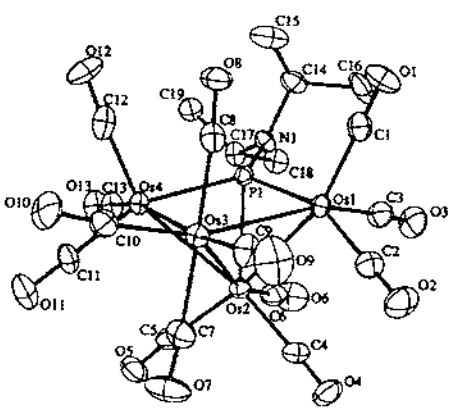

Fig. 9. X-ray structure of $Os_4(CO)_{13}(PNPr^i_2)$. Reprinted with permission from Organometallics. Copyright 1996 American Chemical Society.

ization in polynuclear clusters has appeared. The factors responsible for molecular cohesion of isomeric clusters have been evaluated [139]. A second crystal form of $Os_5(CO)_{16}(\mu\text{-}H)_2$ has been observed by X-ray diffraction analysis [140]. The ligand substitution reactivity of the square-pyramidal cluster $Fe_5(CO)_{15}C$ with several small P-donor ligands has been investigated. A rapid and reversible addition of L is observed via polyhedral cluster expansion to the butterfly adduct $Fe_5(CO)_{15}C(L)$. Slow CO loss follows to give the corresponding mono-substituted products $Fe_5(CO)_{14}C(L)$. Rate comparisons for cluster expansion are made to the analogous $Ru_5(CO)_{15}C$, with the Fe_5 cluster reacting ca. 10^3 slower due to its smaller size. Reactions with ligands having a Tolman cone angle >136 are much slower and do not afford isolable products [141]. Treatment of $Ru_5(CO)_{13}(\mu_5\text{-}C_2PPh_2)(\mu\text{-}PPh_2)$ with dppm gives the spiked butterfly cluster $Ru_5(CO)_{12}(dppm)(\mu_5\text{-}C_2PPh_2)(\mu\text{-}PPh_2)$, which contains a chelating dppm ligand. Reaction of the aminophosphine ligand $PPh_2(C_6H_4NH_2\text{-}2)$ with the same cluster produces $Ru_5(CO)_{10}(\mu\text{-}CO)(\mu_5\text{-}C_2H)(\mu\text{-}PPh_2)_2(\mu\text{-}PPh_2C_6H_4NH\text{-}2)$ as the major product. The deprotonated anilinophosphine ligand is coordinated to a triangulated square Ru_5 core. Use of the olefinic phosphine $PPh_2(C_6H_4CH{=}CH_2\text{-}2)$ leads to a number of products. The molecular structures of four clusters were established by X-ray crystallography [142]. The two clusters $Ru_5(CO)_{11}(\mu_5\text{-}C_2)(\mu\text{-}PPh_2)_2(\mu\text{-}Cl)_2$ and $Ru_5(CO)_{12}(\mu\text{-}H)[\mu_5\text{-}CC(PPh_2)](\mu\text{-}PPh_2)(\mu\text{-}Cl)$ are obtained from the reaction of $Ru_5(CO)_{13}(\mu_5\text{-}C_2PPh_2)(\mu\text{-}PPh_2)$ with 5-chloro-4-chloromethyl-2,4-dimethylpent-1-ene. Both clusters were structurally analyzed by X-ray diffraction methods. The former product represents the second known example of a cluster that contains a C_2 moiety coordinated to a pentagonal Ru_5 core [143]. Alkyne coupling reactions with a cluster-bound dicarbon moiety (C_2) are described. The alkynes PhC≡CR (where R = H, Ph) react with $Ru_5(CO)_{11}(\mu_5\text{-}C_2)(\mu\text{-}SMe)_2(\mu\text{-}PPh_2)_2$ to give $Ru_5(CO)_{10}(\mu_5\text{-}CCCPhCR)(\mu\text{-}SMe)_2(\mu\text{-}PPh_2)_2$. In the case of phenylacetylene, the pentagonal Ru_5 cluster core is retained, whereas an envelope-type core is found in the diphenylacetylene ligand reaction. The nature of the C–C bond coupling products was ascertained by X-ray crystallography [144]. The formation of butatrienylidene by Ru_5 clusters is described. Treatment of $Ru_5(CO)_{11}(\mu_5\text{-}C_2)(\mu\text{-}SMe)_2(\mu\text{-}PPh_2)_2$ with $(TMS)_2C_2$ yields $Ru_5(CO)_{10}(\mu_4\text{-}CCCCHTMS)(\mu_3\text{-}SMe)(\mu\text{-}SMe)(\mu\text{-}PPh_2)_2$ as a mixture of geometric isomers. Alkaline hydrolysis removes the TMS group and gives the corresponding butatrienylidene cluster. The latter cluster exhibits an open envelope conformation, as determined by X-ray analysis. Thermolysis of this same cluster under a CO purge at 80 °C affords $Ru_5(CO)_{11}(\mu_5\text{-}CCCCH_2)(\mu\text{-}SMe)_2(\mu\text{-}PPh_2)_2$, which is shown to possess a spiked rhomboidal Ru_5 frame [145].

A review discussing the synthesis, isolation and characterization of polynuclear arene clusters has been published [146]. The planar hexaosmium cluster $HOs_6(CO)_{20}(\mu\text{-}\eta^2\text{-}NC_5H_4CH{=}CH)$ has been isolated from the reaction between the alkylidyne cluster $H_2Os_3(CO)_9(\mu_3\text{-}NC_5H_4CH{=}CH_2)$ and $Os_3(CO)_{10}(MeCN)_2$. The 94-electron Os_6 cluster exhibits an unprecedented planar Os_6 geometry in which an open Os_3 chain is fused to an edge of an Os_3 triangle by two Os–Os bonds and one bridging hydride group [147]. The X-ray structure of $(\mu\text{-}H)Ru_6(CO)_{15}(PPh_3)(\mu_5\text{-}S)(\mu_3\text{-}\eta^2\text{-}SCNHPhNPh)$, which is obtained from the

reaction of the hexadecacarbonyl cluster and PPh_3, confirms the presence of a significant degree of cluster deformation upon substitution. The substitution chemistry using Me_2S, PBu_3, $P(OMe)_3$ and Bu^tNC with the same starting cluster was also examined and the site of ligand attachment discussed [148]. The synthesis and X-ray structure of $Os_6(CO)_{19}(\mu\text{-}CO)(\mu\text{-}H)(\eta^2\text{-}C_6F_5NNNC_6F_5)$ are reported. The isolated product originates from the intermediate cluster $Os_6(CO)_{20}(\mu\text{-}H)(MeCN)_2(\eta^2\text{-}C_6F_5NNNC_6F_5)$ [149]. Treatment of $[Os_3(CO)_{11}(H)]^-$ with cupric salts in CH_2Cl_2 gives several known cluster products, including the new cluster $Os_3(\mu\text{-}H)(CO)_{10}(\mu_4\text{-}\eta^3\text{-}CO_2)Os_3(\mu\text{-}H)(CO)_{10}$. This cluster has been fully characterized in solution and X-ray diffraction analysis, which confirms the presence of the μ_4-η^3-carboxylate moiety [150].

The synthesis, electrochemical behavior and X-ray structures of $[Fe_4N(CO)_{11}\{PPh(C_5H_4FeC_5H_5)_2\}]^-$, $[Fe_6N(CO)_{15}]^{3-}$ and $[Fe_6N(H)(CO)_{15}]^{2-}$ are presented. The synthesis of the ^{15}N-labeled hexairon clusters has allowed for the measurement of the NMR chemical shift and IR bands of the interstitial μ_6-N ligand [151]. The ultraviolet-laser-desorption mass spectra of $Ru_6C(CO)_{17}$, $Ru_6C(CO)_{14}(\eta^6\text{-}C_6H_5Me)$ and $Ru_6C(CO)_{12}(\eta^6\text{-}C_6H_4Me_2)(\mu\text{-}C_6H_7Me)$ have been recorded. The clustering process commonly found in such mass spectrometry studies is discussed [152]. Pentamethylcyclopentadiene reacts with the carbide cluster $Ru_6C(CO)_{17}$ to produce the chelated cluster $Ru_6C(CO)_{14}(\mu\text{-}\eta^1\text{:}\eta^5\text{-}CH_2C_5Me_5)$. Cp groups may be introduced into $Ru_6C(CO)_{17}$ to give $Ru_6C(CO)_{12}Cp_2$ by treatment with nickelocene in refluxing hexane. The NMR and IR data for both clusters are reported, and the molecular structure of each cluster was established by X-ray analysis [153]. A second solid-state isomer of $[PPN][Ru_6C(CO)_{15}(C_3H_5)]$ has been obtained from a hot methanol solution of the cluster. Both isomers of this cluster possess identical IR and variable-temperature ^1H and ^{13}C NMR spectra; however, the differences in the carbonyl stereochemistries are documented by X-ray crystallography [154]. Thermolysis of $Ru_6C(CO)_{17}$ with dimethyl cyclohexa-1,3-diene-1,4-dicarboxylate affords the isomeric cluster complexes $Ru_6C(CO)_{14}[\eta^6\text{-}C_6H_4(CO_2Me)_2\text{-}1,4]$ and $Ru_6C(CO)_{14}[\mu_3\text{-}\eta^2\text{:}\eta^2\text{:}\eta^2\text{-}C_6H_4(CO_2Me)_2\text{-}1,4]$. The solid-state architectures of these clusters and their potential use in copolymerization reactions are discussed [155]. Nitric oxide has been allowed to react with $[PPN]_2[Ru_6C(CO)_{16}]$ to yield the nitrosyl cluster $[PPN][Ru_6C(CO)_{15}(NO)]$ in good yield. Additional reaction with NO leads to the pentaruthenium cluster $Ru_5C(CO)_{14}(NO)(NO_2)$. The presence of the nitrosyl and nitrite groups was determined by X-ray analysis. Reaction of NO with the allyl cluster $[PPN][Ru_6C(CO)_{15}(C_3H_5)]$ gives both $Ru_6C(CO)_{14}(C_3H_5)(NO)$ and $Ru_5C(CO)_{11}(NO)_2(NO_2)$. The cluster $Ru_5C(CO)_{13}(C_3H_5)(NO_2)$ (Fig. 10) has been isolated from the reaction of $Ru_6C(CO)_{14}(C_3H_5)(NO)$ with NO [156].

Thermolysis of $Ru_3(CO)_{12}$ in ethanol gives the hydridoruthenium cluster $[Ru_{10}H_2(CO)_{25}]^{2-}$. Use of methanol and H_2O as solvent furnishes the high nuclearity cluster $[Ru_{11}H(CO)_{27}]^{3-}$. X-ray analysis of both clusters shows related metal cores, with the latter cluster being a square-faced capped congener of the Ru_{10} cluster. The ^1H NMR data and reactivity with $[Au(PPh_3)]^+$ are described [157]. The high yield synthesis of $[Ru_2(\mu\text{-}H)(\mu\text{-}NC_5H_4)_2(CO)_4(Py)_2][Ru_{10}(\mu\text{-}H)(\mu_6\text{-}C)(CO)_{24}]$ from

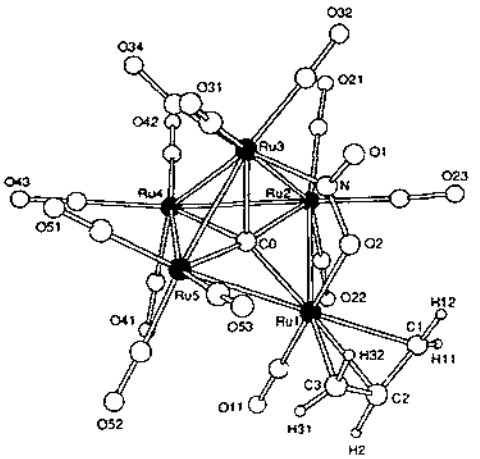

Fig. 10. X-ray structure of $Ru_4C(CO)_{13}(C_5H_4(NO_2)$. Reprinted with permission from Organometallics. Copyright 1996 American Chemical Society.

the thermolysis of $Ru_3(\mu\text{-}H)(\mu\text{-}NC_5H_4)(CO)_{10}$ is presented. When the same reaction is conducted in the presence of $[Ph_4P][BF_4]$, the corresponding Ru_{10} cluster may be isolated as the $[Ph_4P]^+$ salt in moderate yield. The phosphine substitution chemistry exhibited by the Ru_{10} cluster has been investigated. Hydride and CO ligand fluxionality in the new clusters has been examined by ^{13}C EXSY measurements [158]. $[Ph_4P][Ru_{10}(\mu\text{-}H)(\mu_6\text{-}C)(CO)_{24}]$ reacts with $P(OMe)_3$ (2 equiv.) to give a mixture of mono-, bis-, tris- and tetrakis-$P(OMe)_3$ substituted Ru_{10} clusters. This report includes the X-ray structure of $[Ph_4P][Ru_{10}(\mu\text{-}H)(\mu_6\text{-}C)(CO)_{22}\{P(OMe)_2\}_3]$, which reveals that the two $P(OMe)_3$ groups occupy apical sites on the cluster. Use of dppa (0.5 equiv.) affords the linked icosaruthenium cluster dianion $[\{Ru_{10}(\mu\text{-}H)(\mu_6\text{-}C)(CO)_{23}\}_2(\mu\text{-dppa})]^{2-}$ as the major product [159].

2.6. *Group 9 clusters*

The ligand stereochemistry about the clusters $M_3L_3(CO)_3$ (where M = Co, Rh; L = Cp, Cp*, η^5-Ind) and $Co_3Cp_3(\mu_3\text{-}\eta^2\text{:}\eta^2\text{:}\eta^2\text{-}RR'C_6H_4)$ (where R = R′ = H, Me, Et; R = Me, Et, Pr^i, R′ = H) has been examined by using MM3 calculations [160]. The triangular clusters $Cp^*_3M_3(\mu_3\text{-}CH)(\mu\text{-}H)$ (where M = Co, Ni) have been prepared from Cp*M(acac) and MeLi. Both clusters are paramagnetic. The 46-electron cobalt cluster possesses degenerate orbitals that are half-occupied, accounting for the observed paramagnetism. The 49-electron nickel cluster has a single electron in an a_2' orbital, as expected. The trihydride cluster $Cp^*_3Co_3(\mu_3\text{-}CH)(\mu\text{-}H)_3$ is obtained from the reaction of $Cp^*_3Co_3(\mu_3\text{-}CH)(\mu\text{-}H)$ and H_2. Bond-length comparisons between these clusters are made relative to the electron count [161]. Thermal and or photochemical activation of $(\eta^5\text{-}1,2,4\text{-}Bu^t_3C_5H_2)Co(CO)_2$ with white phosphorus leads to the trinuclear complexes $[(\eta^5\text{-}1,2,4\text{-}Bu^t_3C_5H_2)Co]_3P_8$ and $[(\eta^5\text{-}1,2,4\text{-}Bu^t_3C_5H_2)Co]_3P_{12}$. The molecular structure of the P_8 derivative has

been solved [162]. Nucleophilic attack on the face-capping ligand in $(CpCo)_3(\mu_3\text{-}\eta^2\text{:}\eta^2\text{:}\eta^2\text{-}p\text{-fluoro-}\alpha\text{-methylstyrene})$, which was prepared from the reaction between *p*-fluoro-α-methylstyrene and $CpCo(\mu\text{-}C_6Me_6)$, occurs when treated with hydride or phenyl anion. These anions react by way of fluoride displacement [163]. Metal versus ligand protonation has been explored in the clusters $(CpCo)_3(\mu_3\text{-}\eta^2\text{:}\eta^2\text{:}\eta^2\text{-arene})$ (where arene = isopropylbenzene, 1,4-diethylbenzene, 1,2-diphenylethane, 1,1-diphenylethane). These clusters are protonated at the three metals to give $[(\mu_3\text{-H})(CpCo)_3(\mu_3\text{-}\eta^2\text{:}\eta^2\text{:}\eta^2\text{-arene})]^+$. The X-ray structure of the 1,1-diphenylethane derivative (Fig. 11) confirms the site of protonation. Arene ligands bearing unsaturated substituents are protonated at the β-carbon of the side chain. The site-selective nature associated with these protonations is explained by extended Hückel MO calculations, using both charge and overlap control arguments [164].

$Co_2(CO)_8$ and perfluoro diphenyl sulfide react to give the sulfido-capped cluster $Co_3(CO)_8(C_6F_5)(\mu_3\text{-S})$. X-ray analysis shows that the C_6F_5 ligand binds to a single cobalt center by an aryl Co sigma bond [165]. The cluster $Co_3(CO)_9[\mu_3\text{-CSi(OH)}_3]$ has been the subject of an X-ray study, which has revealed an oval framework structure consisting of eight monomeric units. This cluster and a polyethylene glycol derivative were examined as catalysts in the hydroformylation of 1-hexene. Catalysis proceeds without an induction period and with high conversion and high chemoselectivity to the corresponding aldehydes [166]. Treatment of $Co_3(CO)_9[\mu_3\text{-CSi(OH)}_3]$ with EMe_3 (where E = Al, Ga, In) in THF leads to the group 13 heterosiloxanes $[Co_3(CO)_9\{\mu_3\text{-CSi(OE)}_3\cdot THF\}]_4$ in good yields. Full solution characterization and the X-ray structure of the Al complex are presented. The

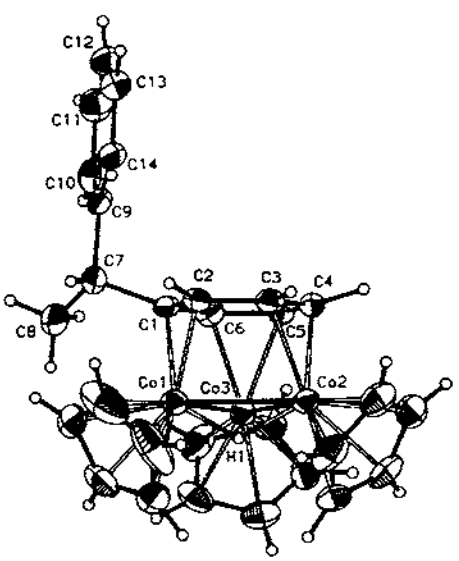

Fig. 11. X-ray structure of $[(\mu_3\text{-H})(CpCo)_3\{\mu_3\text{-}\eta^2\text{:}\eta^2\text{:}\eta^2\text{-}(Ph_2CHCH_3)\}]^+$. Reprinted with permission from Organometallics. Copyright 1996 American Chemical Society.

hydroformylation of 1-hexene has been investigated in order to identify the active catalyst species in solution. The Al- and Ga-containing heterosiloxanes are more active than the In analogue. The presence of $Co_2(CO)_8$ during hydroformylation suggests that cluster decomposition is occurring and that lower nuclearity species are presumably responsible for some of the observed hydroformylation activity [167].

The reaction between $Co_3(CO)_9(\mu_3\text{-}CFe)$ and the diphosphine ligand bped furnishes the cluster $Co_3(CO)_6[\mu_2\text{-}\eta^2{:}\eta^1\text{-}C(Fe)\overline{C{=}C(PPh_2)C(O)CH_2C(O)}](\mu_2\text{-}PPh_2)$. The precursor cluster $Co_3(CO)_7(bped)(\mu_3\text{-}CFe)$ was observed in solution by IR spectroscopy but was found to be unstable, transforming into the $Co_3(CO)_6$ cluster. The X-ray structure confirms the identity of the $Co_3(CO)_6[\mu_2\text{-}\eta^2{:}\eta^1\text{-}C(FC)\overline{C{=}C(PPh_2)C(O)CH_2C(O)}](\mu_2\text{-}PPh_2)$. Electrochemical analysis by cyclic voltammetry reveals the presence of three reversible, one-electron processes assignable to the 0/1−, 0/1 and 1/2 redox couples. The composition of the HOMO and LUMO was assessed by carrying out extended Hückel MO calculations [168]. The clusters $Co_3(CO)_9(\mu_3\text{-}CR)$ (where R = Me, CO_2Me) have been allowed to react with the unsaturated phosphine ligands $Ph_2PCH{=}CH_2$ and (*Z*)-$Ph_2PCH{=}CHPPh_2$. All clusters were characterized by spectroscopic methods and X-ray crystallography in the case of $Co_3(CO)_7[(Z)\text{-}Ph_2PCH{=}CHPPh_2](\mu_3\text{-}CCO_2Me)$ [169]. Face versus vertex coordination of tridentate crown thioethers in several $Co_3(CO)_6(\mu_3\text{-}CR)$ (where R = Cl, Me, Ph) has been explored. Six-membered crown thioethers coordinate to the axial sites of the cluster to give $Co_3(CO)_6(\mu_3\text{-crown})(\mu_3\text{-}CR)$, whereas the nine-membered crown ethers replace all three CO groups at a single cobalt center to produce $Co_3(CO)_5(\mu\text{-}CO)(crown)(\mu_3\text{-}CR)$. Seven X-ray structures are presented and the structural differences discussed [170]. The clusters $Co_3(CO)_{9-n}(PPh_3)_n[\mu_2\text{-}\eta^2{:}\eta^1\text{-}P(Ph)\overline{C{=}C(PPh_2)C(O)OC(O)}]$ (where $n = 0, 1$) have been prepared from the thermolysis reaction of $Co_3(CO)_9$(mesitylene) and the ligand bma. The X-ray structure of the PPh_3-substituted cluster (Fig. 12) confirms the P–Ph bond cleavage and transfer of the phenyl group to a transient μ_2-PPh_2 ligand to produce the PPh_3 ligand in $Co_3(CO)_6(PPh_3)[\mu_2\text{-}\eta^2{:}\eta^1\text{-}P(Ph)\overline{C{=}C(PPh_2)C(O)OC(O)}]$. Electrochemical comparisons between these clusters and the known carbene-bridged cluster $Co_3(CO)_6[\mu_2\text{-}\eta^2{:}\eta^1\text{-}C(Ph)\overline{C{=}C(PPh_2)C(O)OC(O)}](\mu_2\text{-}PPh_2)$ are discussed [171].

The $Rh_4(CO)_{12}$-catalyzed hydroformylation of 1-, 2- and 3-vinylpyrrole at 40 °C yields the corresponding branched aldehydes with high α-regioselectivity [172]. $Rh_4(CO)_{12}$ has been employed as a catalyst precursor in the double carbonylation of diiodomethane in the presence of triethylorthoformate to give diethylmalonate in good yield [173]. The cluster $Rh_4(CO)_{10}(\mu\text{-bpnap})$ was synthesized from $Rh_2(CO)_4Cl_2$ and bpnap under CO. The molecular structure was established by X-ray crystallography. The hydroformylation of 1-octene was investigated with this cluster as catalyst. A moderate *n*/*b* ratio was found for the product aldehydes [174]. The hydroformylation of (1*S*, 5*S*)-(−)- and (1*R*, 5*R*)-(−)-β-pinene has been studied

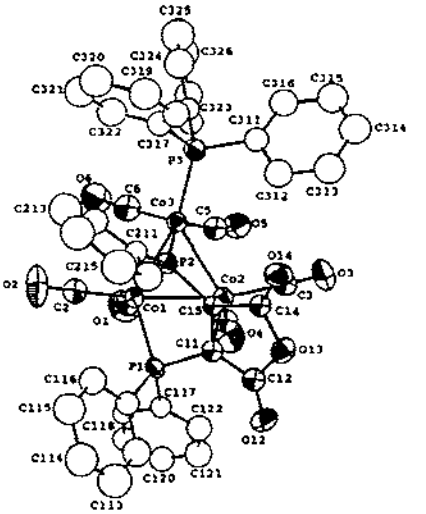

Fig. 12. X-ray structure of $Co_4(CO)_{11}(PPh_3)[\mu_2\text{-}\eta^2\text{:}\eta^1\text{-}P(Ph)C{=}C(PPh_3)C(O)OC(O)]$ Reprinted with permission from Organometallics. Copyright 1996 American Chemical Society.

by using catalyst mixtures of $Rh_4(CO)_{12}$ or $Rh_6(CO)_{16}$ and $Co_2(CO)_8$. High diastereoselectivity is observed [175]. The hydroformylation of simple olefins has been studied by using clusters supported on unfunctionalized inorganic carriers. The nature of the surface species and proposed reaction sequences are described [176]. The deuterioformylation of 1,1-diphenylethene using $Rh_4(CO)_{12}$ gives 3,3-diphenylpropanal-1,3-d_2, the monodeuterated olefin 1,1-diphenylethene-d_2 and the labeled normal aldehyde. ^2H NMR studies demonstrate that a tertiary alkyl rhodium intermediate is formed in a greater amount than the normal isomer, and which undergoes β-hydride elimination without formation of the branched aldehyde. It was concluded that any analysis based on the regioisomeric ratios of the product aldehydes may lead to erroneous conclusions regarding the importance of the pertinent metal alkyl intermediates [177].

Ligand substitution in $Co_4(CO)_{10}(\mu_4\text{-}PPh)_2$ with $PhPMe_2$ (2 equiv.) gives the corresponding bis-substituted cluster $Co_4(CO)_8(PhPMe_2)_2(\mu_4\text{-}PPh)_2$ as the major product. X-ray diffraction analysis shows that the $PhPMe_2$ groups adopt a 1,3-*cis* orientation about the cluster polyhedron. Generalizations pertaining to the regiochemistry and stereoselectivity in the substitution of two CO groups in this genre of cluster are discussed with respect to the capping μ_4-PPh moiety [178]. The reaction of $[RhCl(1,5\text{-}COD)]_2$ with *para*-toluidine and BuLi leads to $Rh_4(\mu\text{-}N\text{-}tolyl)_3(1,5\text{-}COD)_4$. This cluster is the first example of an μ_3-imido rhodium system. Here the two tolylimido ligands cap either side of a Rh_3 triangle by nitrogen coordination, with the ring of one phenyl group binding an isolated Rh(1,5-COD) fragment. The X-ray structure confirms the molecular structure of this cluster [179]. The reversible formation of raftlike imido-bridged rhodium clusters by the migration

of RhL_n^+ fragments has been described [180]. The synthesis and characterization of $Ir_4(CO)_5(\mu\text{-}CO)_3(\mu\text{-}PPh_2Py)(PPh_2Py)_2$, $Ir_4(CO)_5(\mu\text{-}CO)_3(\mu\text{-}PPhPy_2)(PPhPy_2)_2$ and $Ir_4(CO)_5(\mu\text{-}CO)_3(\mu\text{-}PPy_3)(PPy_3)_2$ from $Ir_4(CO)_{12}$ and pyridylphosphines are presented. The reactivity of these clusters with CO is discussed [181]. The first diimine complexes of $Ir_4(CO)_{12}$ have been prepared. Treatment of $[Ir_4(CO)_{11}X]^-$ (where X = Br, I) with aromatic diimines in the presence of silver(I) salts furnishes the clusters $Ir_4(CO)_{10}(N\text{–}N)$ (where N–N = 1,10-phen, 4,7-Me_2phen, 5,6-Me_2phen, 3,4,7,8-Me_4phen, bpy, 4,4′-Me_2-2,2′-bpy). The X-ray structures of the first and last of these derivatives reveal that the diimine ligands chelate to a basal iridium center [182]. Reduction of $[\{(Cp^*Rh)_2(\mu\text{-}CH_2)_2\}_2(\mu\text{-}S_4)]^{2+}$ with $NaBH_4$ leads to the dinuclear complex $(Cp^*Rh)_2(\mu\text{-}CH_2)_2(\mu\text{-}S_2)$, as determined by ^1H NMR and FAB mass spectrometry [183]. $[Ir_4(CO)_{11}Br][Et_4N]$ reacts with Ph_2PPy (2 equiv.) to give $Ir_4(CO)_{10}(Ph_2PPy)_2$. Both ligands act as monodentate P-bonded ligands that are coordinated to two of the basal iridium atoms in an axial and equatorial position. The fluxional behavior of these pyridylphosphine ligands was examined by variable-temperature ^{31}P NMR spectroscopy. The reactivity of this cluster with added $[Cu(MeCN)_4][BF_4]$ and $[Ag][PF_6]$ is discussed [184].

$Rh_6(CO)_{16}$-catalyzed carbonylation of 2-alkynylbenzaldehyde under water–gas shift conditions leads to the production of novel tricyclic lactones [185]. A report on the analysis of ^{13}C and ^{17}O chemical shift tensors of $Rh_6(CO)_{16}$ has appeared. The electronic structure of the Rh_6 cluster was investigated by using electron localization functions, which reveal that the bonding electrons are mainly localized on the unbridged octahedral faces [186]. The reaction between $Co_2(CO)_8$ and *p*-$(Cl_3C)_2C_6H_4$ affords the new cluster *p*-$[(OC)_9Co_3C]_2C_6H_4$. The related clusters $[(OC)_9Co_3CC(O)]C_6H_4\text{-}C_6H_4\text{-}[C(O)CCo_3(CO)_9]$ and *m*-$[(OC)_9Co_3CC(O)CH_2]_2C_6H_4$ have been synthesized by similar techniques. Cyclic voltammetric studies have been carried out and electronic communication through the benzene spacer of the first cluster has been observed [187].

Ethanol synthesis from CO_2 on a TiO_2-supported catalyst derived from $[PPN]_2[Rh_{10}Se(CO)_{22}]$ is reported. The EXAFS spectra of the supported catalysts were investigated under a variety of conditions [188].

2.7. Group 10 clusters

A publication discussing the recharacterization of the clusters $[\{Pt(diphosphine)(RNC)\}_2Pt]^{2+}$ has appeared. These compounds have been determined to be Pt–Hg–Pt mixed-metal systems. ICP emission spectroscopy was used to determine to ratio of the metal atoms [189]. The complex $[Pt_3(\mu\text{-}PPh_2)_2(C_6F_5)_4]$ reacts with *cis*-$Pt(C_6F_5)_2(THF)_2$ to give $[Pt_3(\mu\text{-}PPh_2)_2(C_6F_5)_5]^-$, whose X-ray structure shows the presence of an unusual μ_3-PPh(1,2-η^2-Ph)-K^3P phosphido ligand and semibridging C_6F_5 ligands [190]. The ability of halide ions to bind with the clusters $[Pd_3(\mu\text{-dppm})_3(CO)]^{2+}$ and $[PtPdCo(\mu\text{-dppm})_2(CO)_3(Bu^tNC)]^+$ has been examined by UV-vis spectroscopy. The binding varies as I > Br > Cl, with the Pd_3 cluster exhibiting the highest binding constant. MO calculations on $[Pd_2Co(\mu\text{-dppm})_2(CO)_3]^+$ have been carried out in order to predict the composition

of the lowest electronic bands in this and related clusters [191]. The self-assembled monolayers of 4-[μ_3-iodo-tris{bis(diphenylphosphino)methane}]-trinickel-isocyanophenylenesulfide have been examined by cyclic voltammetry. The rectification behavior exhibited by this and other structurally similar clusters is discussed [192]. The binding properties of unsaturated Pd_3 clusters may be altered by changing the nature of the diphosphine ligand employed. Use of the dpam ligand to give $[Pd_3(\mu\text{-dpam})_3(CO)]^{2+}$ has allowed for an increase in the size of the cavity in clusters of this genre. The binding constants for several neutral and anionic substrates have been measured by UV-vis spectroscopy. The larger cavity size of this new cluster has also been demonstrated by consideration of the solved X-ray structure [193]. A spectroelectrochemical study on the trinickel clusters $[Ni_3(\mu_3\text{-L})(\mu_3\text{-I})(\mu_2\text{-dppm})_3]^+$ (where L = various carbon capping ligands) has been carried out [194]. The photoinduced oxidative degradation of the unsaturated clusters $[M_3(\mu\text{-dppm})_3(CO)]^{2+}$ (where M = Pd, Pt) by chlorocarbons and chloride ions has been described. Detailed photochemical experiments have been conducted and the phototransformations occurring during the early stages of the reaction discussed [195]. CO reacts with the dinuclear complex $Pt_2[\mu_2\text{-P(Bu}^t)_2]_2(H)_2[P(Bu^t)_2H]_2$ to afford the new $Pt_2^{(I)}Pt^{(II)}$ triangular cluster $Pt_3[\mu\text{-P(Bu}^t)_2]_3(H)(CO)_2$. The X-ray structure of this 44-electron cluster is presented (Fig. 13), along with detailed multinuclear NMR data. A working mechanism leading to the formation of this Pt_3 cluster is discussed, and the reactivity of the cluster under high pressures of CO and phosphine ligands is described [196].

The synthesis and X-ray structure of the tetrapalladium cluster $[Pd(\mu\text{-Cl})\{\mu\text{-}(\sigma\text{-K-PhSCHCH}_2C_6F_5)\}]_4$ have been published [197].

Reduction of $PtCl_2(Me_2S)_2$ with excess $NaBH_4$ in the presence of dppp affords the cluster compound $Pt_6(\mu\text{-CO})_6(\mu\text{-dppp})_2(dppp)_2$ in high yield. This cluster contains two separate Pt_3 clusters bridged by two μ-dppp ligands. Reaction with either $[Tl][PF_6]$ or mercury leads to the cluster cryptate complexes $[TlPt_6(CO)_6(dppp)_3]^+$ and $HgPt_6(CO)_6(dppp)_3$, respectively. The X-ray structure of the thallium derivative

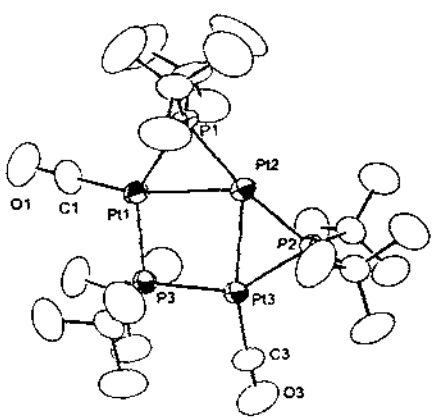

Fig. 13. X-ray structure of $Pt_3[\mu\text{-P(Bu}^t)_2]_3(H)(CO)_2$. Reprinted with permission from Inorganic Chemistry. Copyright 1996 American Chemical Society.

reveals that the Tl^+ ion is bound in sandwich fashion to all six platinum atoms [198]. A report describing the bicluster oxidative addition at $Pt_6(\mu\text{-}CO)_6(\mu\text{-}dppm)_3$ and $[Pt_6(CO)_6(\mu\text{-}dppm)_3]^{2+}$ has appeared. Here the formation and reactivity of the clusters $Pt_6(\mu_3\text{-}SnX_3)_2(\mu\text{-}CO)_6(\mu\text{-}dppm)_3$ (where X = F, Cl, Br) are discussed relative to intertriangular Pt–Pt bonding [199]. $NaBH_4$ reduction of $PtCl_2(Me_2S)_2$ in the presence of CO and diphosphine ligands furnishes the clusters $Pt_6(\mu\text{-}CO)_6(\mu\text{-}P\text{–}P)_2(P\text{–}P)_2$ (where P–P = dppe, dppp, dppb, dpppe, dpph). The trapping of Hg^{2+}, Tl^+ and $AuPPh_3^+$ ions is described. Extended Hückel MO calculations on both trigonal prism and trigonal antiprism cluster $HgPt_6$ geometries reveal that there is little barrier to rotation in these clusters, indicating that the observed solid-state structures are determined by steric and packing factors [200].

The "ship-in-bottle" synthesis of $[Pt_{15}(CO)_{30}]^{2-}$ encapsulated in ordered hexagonal mesoporous channels of FSM-16 is reported. This material was analyzed by X-ray powder patterns and EXAFS spectroscopy. High water–gas shift reactivity is reported for this cluster [201]. The synthesis and X-ray structure of the large nuclearity cluster $[Ni_{32}C_6(CO)_{36}]^{6-}$ have been published. This cluster is obtained by CO degradation of $[Ni_{38}C_6(CO)_{42}]^{6-}$ and from the thermal decomposition of $[Ni_{10}C_2(CO)_{16}]^{2-}$ in diglyme solvent at 110°C [202].

2.8. Group 11 clusters

The copper clusters $[Cu_3(dppm)_3(\mu_3\text{-}\eta^1\text{-}C{\equiv}CR)]^{2+}$ and $[Cu_3(dppm)_3(\mu_3\text{-}\eta^1\text{-}C{\equiv}CR)]^{+}$ (where R = Ph, Bu^t) have been prepared and their luminescence chemistry studied. The X-ray structure of $[Cu_3(dppm)_3(\mu_3\text{-}\eta^1\text{-}C{\equiv}CBu^t)][PF_6]_2$ accompanies this report [203]. The synthesis of the homoleptic copper(I) complexes $[Cu(SePy)]_4$ and $[Cu(SePy^*)]_4$ [where SePy* = (3-TMS)pyridine] has been described. X-ray analysis reveals that both clusters possess a tetrametallic core of copper(I) ions bound to two doubly bridging Se atoms and a pyridine nitrogen atom. The latter cluster decomposes at low temperature to give pure α-CuSe thin films [204]. The photolysis of $[Cu(C_6H_2Me_3\text{-}2,4,6)]_5$ in the presence of organic halides has been explored [205].

3. Heteronuclear clusters

3.1. Trinuclear clusters

$W(CO)_5(THF)$ reacts with $Fe_2(CO)_6(\mu\text{-}SeTe)$ and $Fe_2(CO)_6(\mu\text{-}SSe)$ to give the *nido* clusters $WFe_2(CO)_{10}(\mu_3\text{-}Se)(\mu_3\text{-}E)$ (where E = S, Te). These clusters were characterized in solution by IR and NMR (^{13}C, ^{77}Se, ^{125}Te) spectroscopies and by X-ray crystallography in the case of the Te-capped cluster. The X-ray structures of the known clusters $WFe_2(CO)_{10}(\mu_3\text{-}Se)_2$ and $MoFe_2(CO)_{10}(\mu_3\text{-}Se)_2$ are also presented [206]. The heterometallic clusters $(\mu_2\text{-}S_2)(Cp^*Ru)_2(\mu_3\text{-}S)(\mu_2\text{-}S_2)MS$ (where M = Mo, W) have been isolated from the reaction between $Cp^*RuCl(\mu\text{-}Cl)_2RuCp^*Cl$ and excess $[MS_4]^{2-}$. The molecular structure of each cluster was solved by X-ray analysis.

PEt_3 reacts with the WRu_2 cluster to give $Cp^*Ru(PEt_3)(\mu_2\text{-}S_2)W(\mu_2\text{-}S_2)RuCp^*(PEt_3)$ [207]. The synthesis and characterization of trinuclear clusters taining a M Hg M linkage (where M = Cr, Mo, W) have been published. These clusters may be isolated from the reaction between $[M(CO)_3(\eta^5\text{-}C_5H_4ZC_5H_4\text{-}\eta^5)M(CO)_3]^2$ [where $Z = C(O)CH_2CH_2C(O)$, $CH_2CH_2OCH_2CH_2$] and PhHgCl [208]. CO substitution in the mixed-metal cluster $(MeCp)MoFeCo(CO)_8(\mu_3\text{-}S)$ with dppe produces $(MeCp)MoFeCo(CO)_6(\mu\text{-dppe})(\mu_3\text{-}S)$. The dppe ligand is shown to bridge the Fe–Co bond by X-ray diffraction analysis [209]. The reaction of $(\mu\text{-}H)_2Fe_3(CO)_9(\mu_3\text{-Se})$ with $[CpW(CO)_3]_2$ in refluxing *m*-xylene gives two products, one of which is the cluster $(\mu\text{-}H)WFe_2(CO)_8Cp(\mu_3\text{-Se})$, whose X-ray structure was solved. The other product is presumed to be $W_2Fe(CO)_6Cp_2(\mu_3\text{-Se})$, on the basis of spectroscopic analyses and combustion data [210]. Treatment of $SFeCo_2(CO)_9$ with $[(RCp)Mo(CO)_3][Na]$ (where RCp = HCO, MeCO, EtOCO) yields the clusters $SMoFeCo(CO)_8(RCp)$. Reduction of the aldehyde and ketone side chains by $NaBH_4$ is described. The X-ray structure of the acetyl derivative is presented [211]. The barriers to vertex rotation in $FeCo_2(CO)_9S$ and $CpMoCo_2(CO)_8(CH)$ have been analyzed by extended Hückel MO calculations. Rotation of the $Fe(CO)_3$ moiety by 60° leads to a weakening of the M–M bonding interaction with the $FeCo_2$ triangle [212]. The μ_3-vinylidene clusters $Mo_2Ru(CO)_6Cp_2(\mu_3\text{-}C{\cdots}CHR')$ (where R' = H, Me, Ph, CO_2Me) have been synthesized from $Ru_3(CO)_{12}$ and $Cp_2Mo_2(CO)_4(\mu\text{-}HC{\equiv}CR')$. The X-ray structure of $Mo_2Ru(CO)_6Cp_2(\mu_3\text{-}C{-}CHMe)$ shows that the Mo_2Ru triangle is face-capped by the vinylidene ligand which is σ-bound to the two Mo centers and π-bound to the ruthenium atom. Also isolated from these reactions are the hexanuclear bis(alkylidyne) clusters $Mo_2Ru_4(CO)_{12}Cp_2(\mu_3\text{-}CH)(\mu_3\text{-}CR')$. In the case of R' = H, this represents the first example of the scission of ethyne into two methylidyne fragments at a metal cluster [213]. A study describing an approach to mixed-metal clusters containing selenolate and tellurolate ligands has been published. The X-ray structure of $(CO)_4Mn(\mu\text{-}TePh)_2Co(CO)(\mu\text{-}SePh)_3Mn(CO)_3$ is discussed [214]. Thiophenol reacts with the oxo-acetylide cluster $Cp^*W(O)Re_2(CO)_8(\mu\text{-}C{\equiv}CPh)$ to furnish the binuclear complex $Cp^*W(O)Re(CO)_4(\mu\text{-}H)(\mu\text{-}C{\equiv}CPh)$ in high yield [215].

Treatment of $Re_2(CO)_7(MeCN)(\mu\text{-}H)(\mu\text{-}C_2Ph)$ with $[Co(CO)_4]^-AuCl(PPh_3)$ gives the cluster $Re_2Au(CO)_8(PPh_3)(\mu\text{-}C_2Ph)$ as a minor by-product. The syn- of $Re_2Au(CO)_6(PPh_3)(\mu\text{-dppm})(\mu\text{-}C_2Ph)$ and $Re_2(CO)_6(\mu\text{-}H)[\mu\text{-}(PPh_2)_2CH]Au(PPh_3)](\mu\text{-}C_2Ph)$ are discussed. The metalated dppm ligand in the latter cluster was verified by spectroscopic methods. An analogous Re_3Rh cluster containing a $CH(PPh_2)_2$ ligand is also reported [216].

Metal triangle rotation in the solid state of $Fe_2Ru(CO)_{12}$ and $FeRu_2(CO)_{12}$ has been demonstrated by variable-temperature X-ray crystallography. The phase change from a noncentrosymmetric and ordered structure at low temperature to a disordered centrosymmetric phase at higher temperatures provides the evidence for triangle rotation in the solid state [217]. Variable-temperature X-ray diffraction and ^{13}C MAS NMR data are presented for $Fe_2Os(CO)_{12}$. The reported data support the existence of a low-energy process involving the in-plane rotation of the Fe_2Os triangle that occurs in steps of 60° within a relatively rigid icosahedral carbonyl manifold.

The higher energy fluxional process involves a localized axial equatorial exchange of CO groups on the $Os(CO)_4$ moiety. EXAFS spectra indicate that identical structures are present in the solid phase and THF solution [218]. The mixed-metal, mixed-chalcogenide cluster $CpFe_2Co(CO)_6(\mu_3\text{-}S)(\mu_3\text{-}Te)$ has been synthesized from $CpCo(CO)_2$ and $Fe_2(CO)_6(\mu\text{-}STe)$. The full solution characterization and the X-ray diffraction structure are discussed [219]. Photolysis of $[Cp^*Fe(\mu\text{-}NO)]_2$ with Cp*Co(ethylene) leads to NO transfer from iron to cobalt and formation of $Cp^*_3Co_3(\mu_3\text{-}NO)_2$ and $Cp^*_3Co_3(\mu_3\text{-}NO)(\mu_3\text{-}CMe)$. The latter cluster was examined by X-ray diffraction analysis, which revealed a statistical disordering of the μ_3-bridging groups. The unexpected cluster $Cp^*_3Co_3(\mu_3\text{-}CO)(\mu_3\text{-}O)$ was also observed, while the only containing iron product, $Cp^*_3Fe_3(\mu_3\text{-}NH)(\mu_3\text{-}NO)$, was isolated in low yield [220]. The four clusters $Cp(CO)_2Ru[\mu_3\text{-}\eta^1,\eta^2,\eta^3\text{-}C(O)CH{-}C{-}CH_2]Fe_2(CO)_6$, $(CO)_3Fe(\mu_2\text{-}CO)RuCp(\mu_2\text{-}CO)Fe(CO)_3(\mu_3\text{-}\eta^1\text{-}CCH{=}CH_2)$, $Cp(CO)_2Ru\{\mu_4\text{-}\eta^1,\eta^3,\eta^4,\eta^1\text{-}CH_2CCHC(CH)CH_2\}(CO)_3FeFe(CO)_2(\mu_2\text{-}CO)Ru(CO)Cp$ and $(CO)_3FeRu(CO)CpFe(CO)_3(\mu_3\text{-}\eta^1,\eta^1,\eta^3\text{-}CCHCH_2)$ have been prepared from the thermolysis reaction between $Fe_2(CO)_9$ and $CpRu(CO)_2(CH{\cdots}C{-}CH_2)$. Two X-ray structures and the reactivity of these clusters are described [221]. Several chiral clusters have been obtained from the reaction between $SFeCo_2(CO)_9$ and $[\{RC(O)Cp\}M(CO)_3]$ (where M = Mo, W; R = H, EtO) using electron-transfer-catalysis conditions [222]. The 1,5-COD and in $Fe_2(CO)_6(\mu_3\text{-}S)_2Pt(1,5\text{-}COD)$ is replaced by Ph_2PPy to afford $Fe_2(CO)_6(\mu_3\text{-}S)_2Pt(Ph_2PPy)_2$. X-ray analysis indicates that the Ph_2PPy ligands coordinate to the platinum center by the phosphorus atoms. Cyclic voltammetry studies and the results of extended Hückel MO calculations, which address the nature the HOMO and LUMO, are presented [223]. Various ferraboranes have n allowed to react with $Co_2(CO)_8$ to give mixed Fe/Co clusters. The new sters isolated include $Fe_2Co(CO)_9(\mu\text{-}CO)(BH_2)$, $FeCo_2(CO)_9(\mu\text{-}CO)(BH)$, $FeCo_2(CO)_9(BH)_2$ and $HFe_3Co(CO)_{12}(BH)$. A radical-based substitution mechanism is proposed for the observed $Co(CO)_x$ fragment addition and exchange reactions [224]. The synthesis of $Os_2Pt(CO)_8(PPh_3)$ from $Os_2(CO)_8(\mu\text{-}\eta^1,\eta^1\text{-}C_2H_4)$ and $Pt(PPh_3)_2(\eta^2\text{-}C_2H_4)$ is described. The molecular structure of the product (Fig. 14) shows an Os_2Pt triangle with the PPh_3 ligand bound to the platinum center. Variable-temperature NMR data indicate the existence of three isomers in solution as a result of PPh_3 redistribution about the cluster. The mechanisms and energetics of the isomerization sequences were determined by ^{31}P NMR selective inversion magnetization transfer experiments [225].

The synthesis and X-ray structure (NBD derivative) of $[(diene)Rh\{\mu\text{-}O(AuPPh_3)_2\}_2]^{2+}$ (where diene = NBD, 1,5-COD) are reported. The geometry of these double oxygen atom centered clusters having an unusual trigonal pyramidal oxygen is governed by the Au Au and Au Rh bonds [226]. The preption of the heterobridged heterotrinuclear clusters $[M(\mu\text{-}Pz)(\mu\text{-}PPh_2)(1,5\text{-}COD)]_2Pd$ (where M = Rh, Ir) has been published [227].

The reaction of *syn*-$[Pt_2(\mu\text{-}dpmp)_2(XylNC)_2]^{2+}$ with $[MCl(1,5\text{-}COD)]_2$ (where M = Rh, Ir) gives the linearly ordered Pt Pt M clusters $[Pt_2\{MCl(XylNC)\}(\mu\text{-}dpmp)_2(XylNC)]^{2+}$ and the asymmetrical A-frame clusters

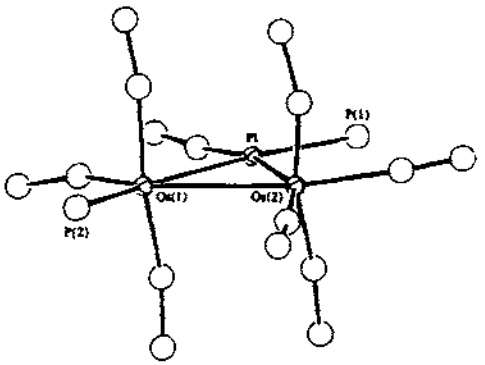

Fig. 14. X-ray structure of $Os_2Pt(CO)_8(PPh_3)$. Reprinted with permission from Organometallics. Copyright 1996 American Chemical Society.

$[Pt_2\{M(XylNC)\}(\mu\text{-}Cl)(\mu\text{-}dpmp)_2(XylNC)]^{2+}$. Three X-ray structures have been determined, and the existence of Pt–Pt and Pt–M d^9–d^9 covalent and $d^9 \leftarrow d^8$ dative bonds, respectively, are discussed [228]. Direct Ag···Pt_2 interactions in pentafluorophenyl A-frame complexes have been verified by X-ray crystallographic studies [229].

$Au_2Cl_2(dppf)$ reacts with Li_2S (1:1 ratio) to give $S(Au_2dppf)$, which has been allowed to react with neutral and cationic gold(I) fragments to yield various polynuclear complexes. The X-ray structures of $S(Au_2dppf)\cdot 2CHCl_3$, $[(\mu\text{-}Au_2dppf)\{S(Au_2dppf)\}_2][OTf]_2\cdot 8CHCl_3$ and $[S(AuPPh_2Me)_2(Au_2dppf)][ClO_4]_2\cdot 3CH_2Cl_2$ are reported [230]. The synthesis and characterization of trinuclear Au_2Ag and Au_2Cu complexes with mesityl bridging ligands have been published [231].

3.2. Tetranuclear clusters

Treatment of $Cp_2Ti(SH)_2$ with $[Rh(\mu\text{-}OMe)(tetrafluorobenzobarrelene)]_2$ yields the cluster $CpTi(\mu_3\text{-}S)_2[Rh(tetrafluorobenzobarrelene)]_3$. The X-ray structure was determined and the unusual structural parameters discussed relative to the deactivation of metal sulfide catalysts [232]. $Cp_2Ta(CH_2)(Me)$ has been allowed to react with $Ru_3(CO)_{12}$ to give $Cp_2(Me)Ta(\mu\text{-}O)Ru_3(C_4H_4)(CO)_9$, which contains a 4-carbon cumulene ligand that bridges the three ruthenium centers. The use of this early–late metal cluster in CO bond reduction and cleavage reactions is discussed [233].

The synthesis of $[Mo_3Re(CO)_{12}H_4]^-$ from $[ReH_9]^{2-}$ and $Mo(CO)_3(diglyme)$ has been published. The solid-state structure reveals a pseudo-tetrahedral arrangement of $M(CO)_3$ fragments, while variable-temperature NMR measurements indicate that the CO ligands are fluxional. The ancillary hydrides are static on the NMR time scale [234]. P–C bond activation has been observed during the thermolysis of $CpWIr_3(CO)_7(\mu\text{-}CO)_3(PPh_3)$. Isolated from the reaction are $CpWIr_3(CO)_4(\mu\text{-}CO)_3[\mu_3\text{-}\eta^2\text{-}PPh(C_6H_4)]$ (major product) and $CpWIr_3(CO)_{11}$ (minor product). Starting with the bis-substituted PPh_3 analogue gives the previous major product and its PPh_3-substituted analogue. The X-ray structures of both

PPh_3-activated clusters confirm the identity of these products [235]. The new cluster $Cp_2Mo_2Fe_2STe(CO)_7$ is obtained as the major product from a refluxing benzene solution containing $Fe_3(CO)_9(S)(Te)$ and $Cp_2Mo_2(CO)_6$. The X-ray structure of this and five other related chalcogenide-capped clusters are included in this report [236]. Coupling of phenylacetylene and CO is observed in the reaction between $[WOs_3(CO)_{13}(\mu\text{-}CO)(\mu\text{-}H)]$ and phenylacetylene. A moderate yield of $WOs_3(CO)_{12}(\mu\text{-}H)[\mu_3\text{-}\eta^3\text{-}C(H)C(Ph)C(OH)]$ is obtained. The spectroscopic and crystallographic data for this cluster are discussed [237]. A detailed investigation on the intermediates involved in the reaction of $CpWOs_3(CO)_{11}(\mu_3\text{-}CTol)$ with H_2 and H_2O is presented. Decarbonylation of $CpWOs_3(CO)_{11}(\mu_3\text{-}CTol)$ with Me_3NO, followed by reaction with H_2 and H_2O, produces $CpWOs_3(CO)_{10}(\mu_3\text{-}CTol)(\mu\text{-}H)_2$ and $CpWOs_3(CO)_{10}(\mu_3\text{-}CTol)(\mu\text{-}O)$, respectively. Thermolysis of the hydrido cluster with H_2O affords the hydrido oxo alkylidene cluster *syn*-$CpWOs_3(CO)_9(\mu_3\text{-}CHTol)(\mu\text{-}O)(\mu\text{-}H)$, where the tolyl group on the alkylidene ligand is oriented *syn* to the μ-oxo ligand. The tetrahedral cluster $CpWOs_4(CO)_{10}(\mu\text{-}O)(\mu_3\text{-}CTol)$ is obtained from the decarbonylation of the deca-carbonyl butterfly cluster. All clusters have been characterized by IR and NMR spectroscopies and mass spectrometry. The X-ray structures of two clusters were crystallographically solved [238]. The X-ray structure of $Mo_2Co_2(\mu\text{-}CO)_4(CO)_4Cp_2(\mu_4\text{-}Me_2C_2)$ is reported, along with the synthesis of related alkyne derivatives [239]. The tetrahedral clusters $Cp_2Mo_2Ru_2(\mu_3\text{-}S)_2(\mu\text{-}SR)_2(CO)_4$ have been synthesized from $Ru_3(CO)_{12}$ and $Cp_2Mo_2(\mu\text{-}S)_2(\mu\text{-}SR)_2$ in refluxing THF. Both Mo_2Ru faces are capped by the triply bridging sulfido ligands, as determined by the X-ray structure of the Pr^i derivative [240]. Dimerization of the diynyl ligand has been demonstrated in the reaction between $CpW(CO)_3(C{\equiv}CC{\equiv}CH)$ and $Ru_3[\mu_3\text{-}HC_2C{\equiv}C\{CpW(CO)_3\}](\mu\text{-}CO)(CO)_9$. The unusual WRu_3 cluster isolated was fully characterized in solution and its solid-state structure solved by X-ray analysis [241]. The synthesis of the butterfly cluster $Cp_2Mo_2Co_2(CO)_4(\mu_3\text{-}CPh)_2(\mu_4\text{-}C_2Ph_2)$ is described. The role of a C_4Ph_4 intermediate complex is considered, and the unequivocal identity of the product determined by X-ray diffraction analysis [242]. Thermolysis of $Ru_3(CO)_{11}[Ph_2PC_6H_5Cr(CO)_3]$ affords two isomers of the benzyne cluster $Ru_3(CO)_7(C_6H_4)[PPhC_6H_5Cr(CO)_3]_2$, while the osmium analogue decomposes to $Os_3(CO)_9(C_6H_4)[PC_6H_5Cr(CO)_3]$ and $Os_3(CO)_8(PhPC_6H_4)[Ph_2PC_6H_5Cr(CO)_3]$. The thermolysis reactions of the related isopropylphosphine complexes have also been examined. Four of the products were characterized by X-ray crystallography [243]. Site-selective substitution in $CpWIr_3(CO)_{11}$ by phosphine ligands has been observed. The course of these reactions was assessed by NMR spectroscopy and X-ray diffraction analysis. The X-ray structures of $CpWIr_3(CO)_7(\mu\text{-}CO)_3(PPh_3)$ (Fig. 15), $CpWIr_3(CO)_6(\mu\text{-}CO)_3(PPh_3)_2$ and $CpWIr_3(CO)_7(\mu\text{-}CO)_3(PMe_3)$ are included in this report [244].

The electrochemical properties of $[Mn_3(CO)_{12}(\mu_3\text{-}H)(\mu\text{-}HgM)][PPh_4]$ (where M = various metal carbonyl fragments), $[\{Mn_3(CO)_{12}(\mu_3\text{-}H)\}_2Hg]^{2-}$, $[\{Mn_3(CO)_{12}(\mu_3\text{-}H)Au\}_2(dppe)]^{2-}$ and $[\{Mn_3(CO)_{12}(\mu_3\text{-}H)Au\}_n(AuCl)_{3n}]^{n-}$ (where $n = 1$–3) have been investigated by cyclic voltammetry and coulometric methods. All clusters exhibit a quasi-reversible oxidation and an irreversible reduc-

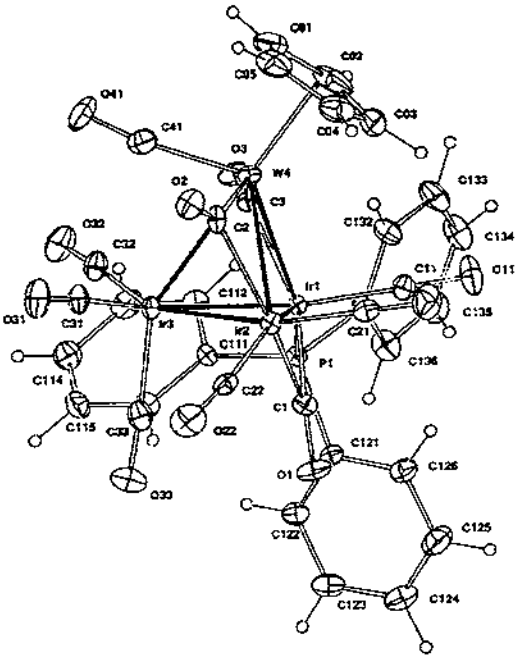

Fig. 15. X-ray structure of $CpWIr_3(CO)_4(\mu\text{-}CO)_4(PPh_3)$. Reprinted with permission from Organometallics. Copyright 1996 American Chemical Society

tion, with both redox responses being localized on the Mn_3Hg and Mn_3Au cores [245]. The synthesis and X-ray structure of the paramagnetic cluster $[\mu\text{-}Mn(THF)_2]_2Fe_2(CO)_8$ are reported [246]. Reaction of $[PPN][Fe_3(CO)_9\{CCOC(O)Me\}]$ with $[PPN][Re(CO)_5]$ affords the metalated acetylide cluster $[PPN][Fe_3(CO)_9\{CCRe(CO)_5\}]$, whose X-ray structure (Fig. 16) confirms the attack on the beta carbon of the CCOC(O)Me coordinated ligand [247].

The isomeric $Cp^*Ir(\eta^4\text{-}2,5\text{-dimethylthiophene})$ and $Cp^*Ir(C,S\text{-}2,5\text{-dimethylthiophene})$ complexes have been allowed to react with $Ru_3(CO)_{12}$. Both iridium complexes yield the CO-substituted cluster $Cp^*Ir(\eta^4\text{-}2,5\text{-dimethylthiophene})Ru_3(CO)_{11}$, in which the heterocyclic ligand is η^4-coordinated to the iridium center and S-coordinated to a ruthenium atom in the equatorial plane. The identity of this cluster was ascertained by X-ray diffraction analysis [248]. New rhenium platinum clusters exhibiting a spiked-triangular core have been synthesized from the reaction between $Re_2Pt(CO)_8(\mu\text{-}H)_2(1,5\text{-COD})$ and $[Re(CO)_5]$ or $[HRe_2(CO)_9]$. The X-ray structures of $[Re_2Pt(CO)_9(\mu\text{-}H)_2\{Re(CO)_5\}]$ and $[Re_2Pt(CO)_8(\mu\text{-}H)_2\{HRe_2(CO)_8\}]$ are presented, and the fluxional behavior of the ancillary hydride ligands has been investigated by variable-temperature NMR studies [249].

The new butterfly cluster $Ru_3IrH_3(CO)_{12}Cl$ has been prepared and the hydride ligands shown to bridge Ru Ru edges by X-ray crystallography [250].

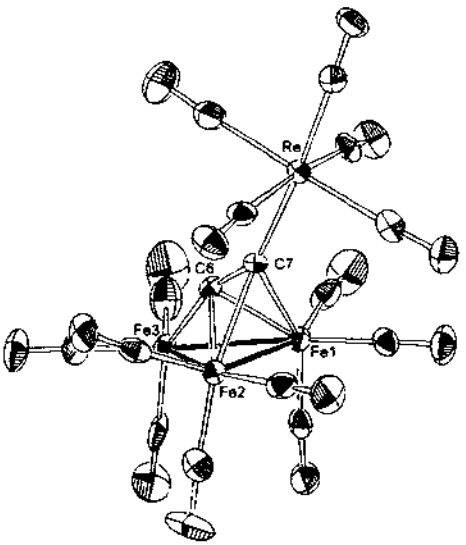

Fig. 16. X-ray structure of $[PPN][Fe_3(CO)_9\{CCRe(CO)_5\}]$. Reprinted with permission from Organometallics. Copyright 1996 American Chemical Society.

Treatment of $HRuCo_3(CO)_{12}$ and $H_3Ru_3Co(CO)_{12}$ with the tridentate phosphine ligand $HC(PPh_2)_3$ produces $HRuCo_3(CO)_9[HC(PPh_2)_3]$ and $H_3Ru_3Co(CO)_9[HC(PPh_2)_3]$, respectively. The P-ligand coordinates to a Co_3 face in the former cluster and to a Ru_2Co face in the latter cluster, as determined by X-ray analysis [251]. The reactivity of $HRuCo_3(CO)_9[HC(PPh_2)_3]$ and $H_3Ru_3Co(CO)_9[HC(PPh_2)_3]$ with PMe_2Ph has been studied and the resulting PMe_2Ph-substituted clusters fully characterized [252]. The tetranuclear cluster $Ru_2(CO)_6(\mu\text{-}PPh_2)(\mu\text{-}\eta^1,\eta^2_{\alpha,\beta}\text{:}\eta^2,\eta^2_{\gamma,\delta}\text{-}C{\equiv}C{-}C{\equiv}CBu^t)Co_2(CO)_6$ has been prepared and structurally characterized [253]. The bridging of a diallyl ligand derived by the unsymmetrical coupling of two allenyl groups has been found in $Cp_2Fe_2Ru_2(CO)_8(\mu_2\text{-}CO)(\mu_4\text{-}\eta^6\text{-}C_6H_6)$. This cluster, which was obtained from $CpRu(CO)_2(CH{-}C{\equiv}CH_2)$ and $Fe_2(CO)_9$, was structurally characterized [254]. The reactivity of $Cp^*Ru_3RhH(CO)_9(BH_2)$ with dppf and dppa has been examined, with the X-ray structure of $Cp^*Ru_3RhH_2(CO)_8(\mu\text{-dppf})(AuB)$, which was obtained from $Cp^*Ru_3RhH_2(CO)_8(\mu\text{-dppf})(BH)$ and $Au_2Cl_2(dppf)$, being reported in this publication [255]. Ferrocene chromophores have been introduced into Ru_3 and Os_3 clusters and examined by electrochemical and diffraction methods. The clusters studied have the form $M_3(CO)_{10}(\mu\text{-}H)[\mu\text{-}NC_5H_3C_6H_4(\eta^5\text{-}C_5H_4)Fe(\eta^5\text{-}Cp)]$ [256]. The air-stable clusters $HOs_3(CO)_{10}(O_2CC_5H_4FeC_5H_5)$ and $[HOs_3(CO)_{10}]_2(O_2CC_5H_4FeC_5H_4CO_2)$ have been prepared from $Os_3(CO)_{10}(MeCN)_2$ and the appropriate ferrocenecarboxylic acid. The electrochemical properties were examined by cyclic voltammetry and the molecular structures determined by X-ray crystallography [257]. The reaction between $Os_3(CO)_{10}(MeCN)_2$ and $Fe[C_5H_4(C_2TMS)]_2$ at room temperature affords $Os_3(CO)_{10}[\mu_3\text{-}\eta^2\text{-}Fe\{C_5H_4(C_2TMS)\}_2]$ and the decarbonylated product

$Os_3(CO)_9[\mu_3\text{-}\eta^4\text{-}Fe\{C_5H_4(C_2TMS)\}_2]$. The presence of a metallobutadienyl ligand in the latter cluster is supported by X-ray analysis. Cyclic voltammetry studies reveal a reversible one-electron oxidation at the ferrocene moiety and an irreversible two-electron reduction at the Os_3 core [258]. The known cluster $Os_3(CO)_{10}[(\eta^5\text{-}C_5H_5)FeC_5H_4CCH]$ and the new cluster $Os_3(CO)_9[\{(\eta^5\text{-}C_5H_5)FeC_5H_4CCH\}_2CO]$ have been obtained from the reaction between $Os_3(CO)_{10}(MeCN)_2$ and ethynylferrocene. The linking of the two ethynylferrocene groups by a metal carbonyl group affords a 2,6-bis(ferrocenyl)vinyl allyl ether, as determined by spectroscopic and crystallographic techniques [259]. The gold(I)–gold(III) complexes $S(Au_2dppf)[Au(C_6F_5)_3]_2$ and $S(AuPPh_3)_2[Au(C_6F_5)_3]_2$ have been synthesized and structurally characterized [260].

Treating $Ru_3(CO)_{12}$ with $[Rh(CO)_4]^-$ leads to the anionic cluster $[Ru_2Rh_2(CO)_{12}]^{2-}$. This anion reacts with acids and $AuPPh_3Cl$ to give $[Ru_2Rh_2H(CO)_{12}]^-$ (Fig. 17) and $[Ru_2Rh_2(AuPPh_3)(CO)_{12}]^-$, respectively. Whereas the parent cluster and the monohydride possess a tetrahedral Ru_2Rh_2 metallic core, the gold derivative exhibits a trigonal-bipyramidal frame with apical ruthenium and gold atoms. The fluxional behavior of these clusters was studied by ^{13}C NMR spectroscopy [261].

The ionic complexes $[Au_2(P\ P)_2][Co(CO)_4]_2$ are shown to be intermediates in the synthesis of Co_2Au_2 complexes. While the unobserved intermediate $[Au_2(\mu\text{-dppm})_2][Co(CO)_4]_2$ transforms into $Co_2Au_2(CO)_6(\mu\text{-dppm})_2$ and $[(OC)_4CoAu]_2(\mu\text{-dppm})$ in solution, the isolated ionic complex $[Au_2(\mu\text{-dppip})_2][Co(CO)_4]_2$ provides evidence for the proposed reaction mechanism [262]. The oxidatively induced reductive coupling of PPh_2 and Ph groups has been demonstrated in a Pt_3 cluster. Oxidation of $Pt_3(\mu\text{-}PPh_2)_3(Ph)(PPh_3)_2$ by I_2 gives $[Pt_3(\mu\text{-}I)(\mu\text{-}PPh_2)_2(PPh_3)_3][I]$, while reaction with AgO_2CCF_3 yields the Pt_3Ag cluster $Pt_3(\mu_3\text{-}AgO_2CCF_3)(\mu\text{-}PPh_2)_3(Ph)(PPh_3)_2$. Both clusters have been characterized by X-ray diffraction analysis, and in the case of the latter cluster a tetrahedral Pt_3Ag core is found [263].

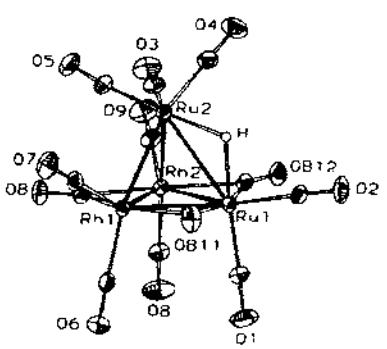

Fig. 17. X-ray structure of $[Ru_2Rh_2H(CO)_{12}]^-$. Reprinted with permission from Inorganic Chemistry. Copyright 1996 American Chemical Society.

3.3. Pentanuclear clusters

New polynuclear complexes are obtained from the reaction of $M_3(CO)_{12}$ (where M = Co, Rh) with $(\eta^6\text{-}PhCH_2Ph)Cr(CO)_3$. Fragmentation occurs with the cobalt cluster to give $Co_2(CO)_6(\mu_4\text{-}\eta^2\text{:}\eta^6\text{-}PhCH_2Ph)Cr(CO)_3$, while the rhodium cluster remains intact and yields $Rh_4(CO)_9(\mu_5\text{-}\eta^2\text{:}\eta^6\text{-}PhCH_2Ph)Cr(CO)_3$. An unusual interaction between the $Cr(CO)_3$ moiety and one of the rhodium atoms is found in the X-ray crystal structure. ^{13}C NMR spectroscopy indicates that the solid-state structure is maintained in solution [264]. The synthesis and X-ray structure of $MnFe_3(CO)_{11}(\mu_3\text{-}Se_2)(\mu_3\text{-}Te)_2$ are reported [265]. Decomposition of digold manganese clusters in the presence of $AuCl(PR_3)$ gives the unsaturated cluster $Mn_2Au_3[\mu\text{-}P(OEt)_2](CO)_6(PR_3)_2$ (where R = Ph, Et) in low yields. The X-ray structure of the phenyl derivative has been determined, and the reactivity of $[Mn_2\{\mu\text{-}P(OEt)_2\}\{\mu\text{-}\eta^2\text{-}OP(OEt)_2\}(CO)_6]^2$ in cluster build-up schemes discussed [266]. CO scission in $Cp_2W_2Ru_3(CO)_{12}$, which was prepared from $CpWRu_3(CO)_{12}H$ and $CpW(CO)_3H$, occurs in refluxing toluene to give the oxo-carbide complex $CpW(O)CpWRu_3(CO)_{11}(\mu_6\text{-}C)$ in 22% yield. The Cp* analogue displays similar chemistry. The X-ray structure of the Cp*-based oxo-carbide cluster reveals a wingtip-bridged butterfly arrangement of metal atoms, with the carbide ligand being linked to all five metal atoms. Since no CO_2 was observed in these reactions, a CO disproportionation sequence was ruled out. A mechanism with a putative $\mu_4\text{-}\eta^2\text{-}CO$ of $\mu_5\text{-}\eta^2\text{-}CO$ ligand is postulated [267]. The reaction of $(OC)_6Fe_2Se_2[\mu\text{-}HC\ C(C{\equiv}CMe)]$ with $Os_3(CO)_{10}(MeCN)_2$ gives $(OC)_6Fe_2Se_2(\mu\text{-}HC{-}CC\ CMe)Os_3(CO)_{10}$, whose X-ray structure accompanies this report [268]. The synthesis and reactions of $Ru_3(\mu\text{-}H)(\mu_3\text{-}\eta^1\text{:}\eta^2\text{:}\mu\text{-}\eta^2\text{-}HC_2C_2TMS)[Co_2(CO)_4(\mu\text{-dppm})](CO)_6$ and $Os_3(\mu_3\text{-}\eta^1\text{:}\eta^2\text{:}\mu\text{-}\eta^2\text{-}HC_2C_2TMS)[Co_2(CO)_6](\mu\text{-}CO)(CO)_9$ have been published [269]. The butterfly cluster $[Ru_4(CO)_{12}H(BH)]$ reacts with $[Cp^*RhCl_2]_2$ to give the boron-containing cluster $Ru_4RhCp^*(\mu\text{-}Cl)(CO)_{12}(B)$. The 78-electron cluster possesses an envelope or an edge-bridge square geometry, as determined by X-ray analysis. Carrying out the same reaction using $[Rh(NBD)Cl]_2$ affords the related Ru_4RhB cluster and a Ru_4Rh_2B cluster. The trapping of these Ru/Rh clusters with gold(I) phosphines is described and the data obtained from NMR studies discussed [270]. Use of the sandwich compound $Fe(\eta^5\text{-}C_5H_5)(\eta^5\text{-}P_3C_2Bu^t_2)$ as a ligand in the reaction with $[Ir_4(CO)_{11}Br]$ is discussed. Depending upon the ligand-to-cluster stoichiometry employed, the complexes $Ir_4(CO)_{11}[Fe(\eta^5\text{-}C_5H_5)(\eta^5\text{-}P_3C_2Bu^t_2)]$ and $HIr_4(CO)_{10}[\mu\text{-}Fe(\eta^5\text{-}C_5H_5)(\eta^5\text{-}P_3C_2)(CMe_2)Bu^t]Ir_4(CO)_{11}$ may be isolated. The oxidative addition of one of the methyls of a *t*-butyl group was ascertained by NMR spectroscopy (^1H, ^{31}P) and X-ray crystallography [271]. The preparation and fluxional properties of $[Ru_4Cu(CO)_{12}(\mu_3\text{-}H)_3]_2(\mu\text{-dppe})$ are described. ^{13}C NMR measurements indicate that the whole of each of the $[Ru_4Cu(CO)_{12}(\mu_3\text{-}H)_3]$ subunits undergoes fast rotation around the Cu–P bond [272]. The iridathiabenzene complex $Cp^*Ir(C,S\text{-}2,5\text{-}Me_2thiophene)$ reacts with $Co_4(CO)_{12}$ to furnish the clusters $Cp^*Ir(\eta^4\text{-}2,5\text{-}Me_2thiophene)Co_4(CO)_{11}$ and $[Cp^*Ir\{C(Me){=}CHCH{=}C(Me)\}$

$(\mu\text{-}CO)_2Co]_2$. The latter cluster derives from the former cluster, as shown by independent experiments using pure $Cp^*Ir(\eta^4\text{-}2,5\text{-}Me_2thiophene)Co_4(CO)_{11}$. The X-ray structure (Fig. 18) of this $IrCo_4$ cluster is presented [273].

3.4. Hexanuclear clusters

The catalytic behavior of SiO_2-grafted $[(\mu_3\text{-}C_4H\text{-})_2Rh]_2V_4O_{12}$ and $(CpRh)_4V_6O_{19}$ was investigated as molecular models for supported Rh catalysts for the oxidation of propene to acetone. These two systems exhibited high catalytic activity and were characterized by TPD methods and EXAFS and FT-IR spectroscopy. Several other zeolite-entrapped metal carbonyl clusters were also examined in C–C bond forming reactions [274]. The silica-supported carbide clusters $[Fe_5RhC(CO)_{16}]^-$ and $[Fe_4RhC(CO)_{14}]^-$ were studied as catalysts in CO hydrogenation and propene hydroformylation reactions. The thermal stability of these clusters on the silica support was explored and the resulting species examined by Mössbauer spectroscopy and electron microscopy [275]. Highly active bimetallic Fe–Ir–MgO catalysts have been prepared by the controlled reductive decomposition of physisorbed $[Fe_2Ir_4(CO)_{16}]^{2-}$ and $[Fe_2Ir_3(CO)_{12}]^{2-}$. The exact nature of the catalysts was determined by *in situ* DRIFTS characterization and by EXAFS spectroscopy [276].

The synthesis and structural characterization of $[Mo_2O_2(\mu\text{-}S)_2\{Fe_2S_2(CO)_6\}_2]^{2-}$ have been published. The mixed-metal cluster contains a *cis*-bis(oxomolybdenum) core that is bridged by two sulfido groups. Also reported are the X-ray structures of $[Mo_2O_2(\mu\text{-}O)(\mu\text{-}S)\{Fe_2S_2(CO)_6\}_2]^{2-}$ and $[Mo_4O_8(\mu\text{-}OMe)_2\{Fe_2S_2(CO)_6\}_2]^{2-}$. The reactivity of these clusters with sulfide reagents is discussed [277]. Treatment of $Cp_2Mo_2(CO)_4$ with $Ru_3(CO)_{12}$ in refluxing toluene affords the heterometallic carbide-oxo cluster $Cp_2Mo_2Ru_4(\mu_6\text{-}C)(\mu_6\text{-}O)(CO)_{12}$ in moderate yield. The X-ray structure shows the presence of two isomeric molecules in the unit cell. The polyhedral cores of these isomers are identical, but one molecule has two bridging CO groups on Mo–Ru edges while the other isomer has two additional CO groups

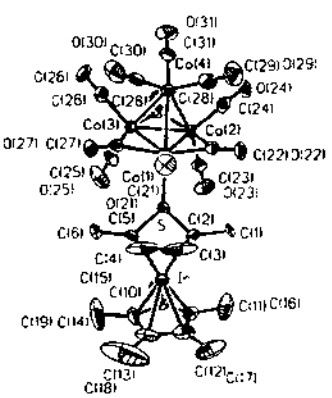

Fig. 18. X-ray structure of $Cp^*Ir(\eta^4\text{-}2,5\text{-}Me_2thiophene)Co_4(CO)_{11}$. Reprinted with permission from Organometallics. Copyright 1996 American Chemical Society.

weakly semibridging Ru–Ru edges [278]. $AuCl(PPh_3)$ $TlPF_6$ reacts with $[M_3(CO)_9(\mu\text{-}OEt)(\mu_3\text{-}OEt)_2]^-$ (where M = Mo, W) to give $M_3(CO)_9(AuPPh_3)_3(\mu\text{-}OEt)(\mu_3\text{-}OEt)_2$ in high yields. The solid-state structures of both M_3Au_3 clusters have been determined (Fig. 19) and are shown to be isomorphous. The fluxional behavior of these clusters is discussed and the valence isomerization pathways presented [279].

The clusters $Ir_4(CO)_{12-n}[Fe(\eta^5\text{-}C_5H_5)(\eta^5\text{-}P_3C_2Bu^t_2)]_n$ (where $n = 1, 2$) have been synthesized. C–H bond activation of the *t*-butyl group is also demonstrated [280]. $GeMe_2H_2$ undergoes reaction with $Fe_2[\mu_4\text{-}Ge]Co_3(CO)_{12}]^-$ to replace the μ-CO group on the Co–Co bond to give $Fe_2[\mu_4\text{-}Ge]Co_2(CO)_6(\mu\text{-}GeMe_2)]_2]^-$. The molecular structure was unambiguously established by X-ray analysis. Extended thermolysis of $Fe_2[\mu_4\text{-}Ge]Co_3(CO)_{12}]^-$ yields $Fe_2Co_4Ge_2(CO)_n$ (where $n = 19$ or 20), whose spectroscopic properties suggest a square-bipyramidal cluster with a $Fe_2Co_2Ge_2$ core [281]. Reaction of the carbide cluster $Os_5C(CO)_{15}$ with $Pd(PPh_3)_4$ and $PdCl_2(PPh_3)_2$ affords $Os_5PdC(CO)_{12}(\mu\text{-}CO)_2(PPh_3)_2$ and $Os_5PdC(CO)_{15}(\mu\text{-}Cl)_2(PPh_3)$, respectively. The former cluster contains a square-based pyramidal core of five osmium atoms and a face-capping $Pd(PPh_3)$ group, while the latter cluster possesses a butterfly polyhedron of four osmium atoms. The Pd atom bridges the wingtip atoms in this butterfly cluster with the remaining $Os(PPh_3)(CO)$ moiety being connected to the Pd apex [282]. The effect of the diphosphine ligand on the metal framework of carbido clusters has been demonstrated in the reaction between $[Fe_6C(CO)_{16}]^{2-}$ and Au(P–P) reagents. Use of $(AuCl)_2$(dppm) gives the hexametal cluster $Fe_4Au_2C(CO)_{12}$(dppm), whose structure (Fig. 20) was solved, while the analogous reagent $(AuCl)_2$(dppe) affords the 14-metal cluster

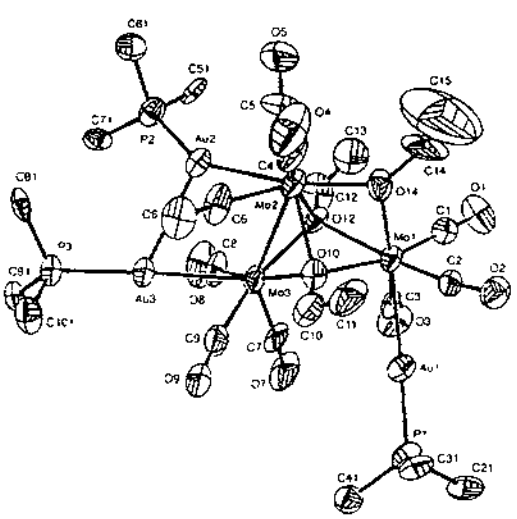

Fig. 19. X-ray structure of $Mo_3(CO)_9(AuPPh_3)_3(\mu\text{-}OEt)(\mu_3\text{-}OEt)_2$. Reprinted with permission from Organometallics. Copyright 1996 American Chemical Society.

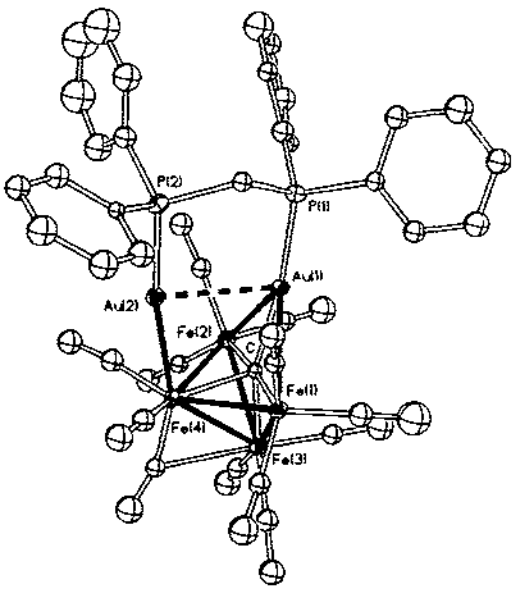

Fig. 20. X-ray structure of $Fe_4Au_2C(CO)_{12}$(dppm). Reprinted with permission from Organometallics. Copyright 1996 American Chemical Society.

$[\{Fe_6AuC(CO)_{16}\}_2(\mu\text{-dppe})]^{2-}$. The dppm-substituted cluster is a skeletal isomer of the known $Fe_4Au_2(CO)_{12}(PEt_3)_2$ cluster [283].

3.5. *Higher nuclearity clusters*

Redox condensation of $[PPN][Mn_2(CO)_8(\mu\text{-}PPh_2)]$ with $Au_2Cl_2(P\ P)$ (where P P = dppf, dppe) gives the clusters $[AuMn_2(CO)_8(\mu\text{-}PPh_2)]_2(\mu\text{-P P})$. The X-ray structure of the dppf derivative shows two Mn_2Au triangles that are ligated by the diphosphine ligand. This same cluster is cleaved by PPh_3 in refluxing THF or by $P(OEt)_3$ at room temperature to furnish the triangular clusters $Mn_2Au(CO)_8(\mu\text{-}PPh_2)(PR_3)$. Fenske Hall MO calculations have been carried out on several clusters and the overlap population of the Mn–Mn bond determined. The nature and strength of the bonding in the Mn_2Au fragment are discussed [284]. Sunlamp irradiation of $[PPN]_2[Re_6C(CO)_{19}]$ with $Mo(CO)_6$ or $Ru_3(CO)_{12}$ gives $[PPN]_2[Re_6C(CO)_{18}Mo(CO)_4]$ and $[PPN]_2[Re_6C(CO)_{18}Ru(CO)_3]$ in good yields. The X-ray structure of the Re–Mo cluster is composed of a Re_6C octahedral core and contains a face-capping $Mo(CO)_4$ fragment. The ancillary CO ligands undergo complete scrambling about the cluster polyhedron at ambient temperature, as judged by ^{13}C NMR analysis. ^{13}C NMR examination of the Re_6Ru cluster indicates that it adopts a structure similar to the Re_6Mo cluster. The redox properties of these clusters were examined by cyclic voltammetry, and the conditions necessary to bring about the decapping of the Mo fragment in the Re_6Mo cluster are discussed [285]. The low-yield synthesis of $Cp_3W_3Ir_3(\mu\text{-}H)(CO)_{12}$ from the thermolysis of

$Cp_2W_2Ir_2(CO)_{10}$ with Ph_3N is presented. The solid-state structure (Fig. 21) consists of a trigonal-bipyramidal $CpW[Ir(CO)_4]$ core that is bicapped by $CpW(CO)_2$ fragments [286].

Treatment of $[CpRu(MeCN)_3]^+$ with $[Os_5(CO)_{15}]^{2-}$ leads to the neutral heptanuclear cluster $Cp_2Os_5Ru_2(CO)_{15}$, whose X-ray structure reveals a metallic core containing a tricapped tetrahedral polyhedron [287]. The synthesis and X-ray structure of $Os_6Pd(CO)_{18}(bpy)$ have been published. This Os_6Pd cluster is obtained in moderate yield from the reaction of $Pd(bpy)(CO_2Me)_2$ with $Os_3(CO)_{10}(MeCN)_2$. Cyclic voltammetry reveals the presence of an irreversible oxidation wave at ca. 0.75 V and no reduction process. Use of $H_2Os_3(CO)_{10}$ in place of the bis(acetonitrile) cluster gives the pentanuclear cluster $[Pd(bpy)]_2Os_3(CO)_{10}$ [288]. The electrospray mass spectrometric studies on $[Fe_6C(CO)_{16}AuPPh_3]^-$ and other clusters are presented. These mass spectroscopic results are compared with those obtained by FAB-MS, and information on the strength of different M–M bonds discussed [289]. The dynamic behavior of the mixed-metal clusters $MM'Ru_4H_2(\mu\text{-dppf})(CO)_{12}$ (where M = M′ = Cu, Ag, Au; M = Cu, M′ = Au) have been examined by variable-temperature NMR measurements. The activation parameters for the various fluxional properties are reported, along with the X-ray structures of $Au_2Ru_4H_2(\mu\text{-dppf})(CO)_{12}$ and $CuAuRu_4H_2(\mu\text{-dppf})(CO)_{12}$ [290]. Facile Hg–C bond cleavage in $Hg(C{\equiv}CPh)_2$ has been utilized in the synthesis of mercury–osmium clusters. $Hg(C{\equiv}CPh)_2$ reacts with $H_2Os_3(CO)_{10}$ to give *cis*-$[Os_3(CO)_{10}(\mu\text{-}\eta^2\text{-}CH{=}CHPh)]_2(\mu_4\text{-}Hg)$. The thermal stability of these clusters was fully examined and the products characterized. The reaction of $H_2Os_3(CO)_{10}$ with $RHgC{\equiv}CHgR$ (where R = Ph, Me, Et) affords the clusters $[Os_3(CO)_{10}(\mu\text{-}\eta^2\text{-}CH{=}CH_2)](\mu_4\text{-}Hg)[Os_3(CO)_{10}(\mu\text{-}H)]$ and $[Os_3(CO)_{10}(\mu\text{-}\eta^2\text{-}CH{=}CH_2)]_2(\mu_4\text{-}Hg)$ [291].

The W(II)–W(III) cluster carboxylate complex $[Na][W_2(O_2CCo_3(CO)_9)_2(O_2CCF_3)_4(THF)_2]$ has been prepared and structurally characterized. On the basis of a distinctive EPR signal having a g value of 2.08, the complex may be regarded

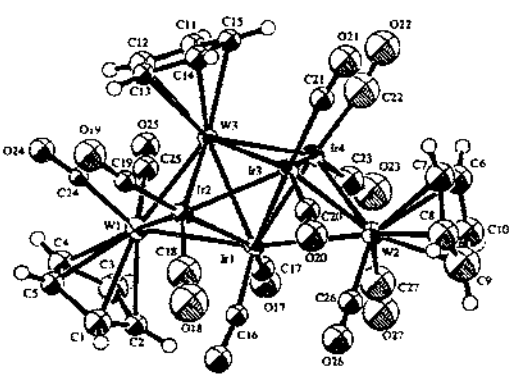

Fig. 21. X-ray structure of $Cp_2W_2Ir_2(\mu\text{-}H)_2(CO)_{12}$. Reprinted with permission from Organometallics. Copyright 1996 American Chemical Society.

as a mixed-valent W(II)–W(III) species [292]. The branched-type octanuclear sulfide complex $[Cp^*Rh(OEt)_3(\mu\text{-}WS_4)(CuCl)Cu]_2(\mu\text{-}Cl)_2$ has been synthesized and the cluster framework reactivity studied [293]. The synthesis and catalytic reactivity of supported Re/Ir catalysts prepared from $[Re_7IrC(CO)_{23}]^{2-}$ have been published. The final catalyst particle nanostructure is dependent on significant cluster fragmentation, followed by preferential nucleation at Ir centers [294]. The synthesis and X-ray structures of three clusters containing Au_2Ru_3 cores and the carbide cluster $Ru_6C(\mu\text{-}CO)_2(CO)_{14}[Au(PPh_3)]_2$ are reported. The gold fragments were introduced to the cluster by use of the trigold-oxonium cation $[O\{Au(PPh_3)\}_3]^+$ [295]. Density functional calculations on the clusters $[M_4\{Fe(CO)_4\}_4]^n$ (where M = Cu, Ag, Au) and $[Ag_{13}\{Fe(CO)_4\}_8]^n$ (where $n = 0$–5) have been carried out in order to study the electronic and geometric structure of these systems. The bonding in the silver clusters was found to be weaker than in the copper and gold derivatives [296]. An example of metalloselectivity in the reaction of $Cu_2Ru_6(\mu_6\text{-}C)(CO)_{16}(MeCN)_2$ with the thiacrown ether 1,5,9-trithiacyclododecane has been described. Extraction of the copper atoms by the thiacrown produces the salt complex $[Cu(\eta^3\text{-}12S3)(\eta^1\text{-}12S3)]_2[Ru_6(\mu_6\text{-}C)(CO)_{16}]$ in moderate yield. Variable-temperature NMR measurements confirm the dynamic process that serves to average the coordinated thiacrowns ($\eta^3 \rightleftharpoons \eta^1$). The molecular structure of the product was verified by X-ray crystallography [297].

Functionalization studies of the layer-segregated cluster $Pt_3Ru_6(CO)_{21}(\mu_3\text{-}H)(\mu\text{-}H)_3$ are reported. Deprotonation of this cluster affords the corresponding dianion, which after treatment with $[Cp^*Ir(MeCN)_3]^{2+}$ and HgI_2, gives $Pt_3Ru_6(CO)_{21}(\mu_3\text{-}Cp^*Ir)(\mu_3\text{-}H)_2$ and $[Pt_3Ru_6(CO)_{21}(\mu_3\text{-}HgI)(\mu_3\text{-}H)_2]^-$, respectively. The X-ray structures of both clusters (Fig. 22) are similar, with the heterometallic

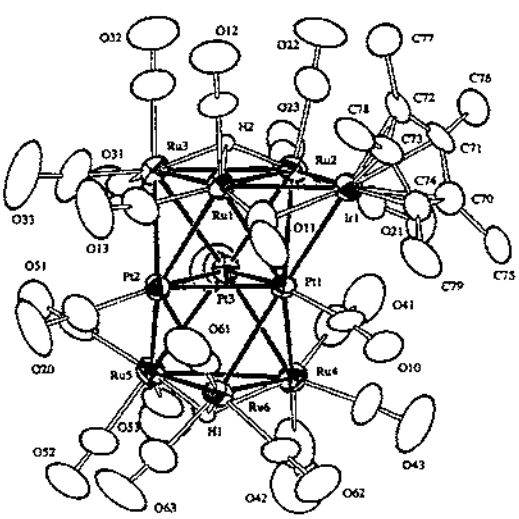

Fig. 22. X-ray structure of $Pt_3Ru_6(CO)_{21}(\mu_3\text{-}Cp^*Ir)(\mu_3\text{-}H)_2$. Reprinted with permission from Organometallics. Copyright 1996 American Chemical Society.

fragment serving to triply bridge one of the Ru_2Pt faces. The two ancillary hydrides are shown to adopt triply bridging positions on the two Ru_3 triangular faces [298].

The solid-state NMR examination of metal clusters containing interstitial hydride ligands is reported. Some of the complexes studied by ^1H and ^2H NMR spectroscopy include $[Rh_{13}H_x(CO)_{24}]^{(5-x)}$ (where $x=2,3$). $Ru_2Rh_2H_2(CO)_{12}$ and $[Co_6H(CO)_{15}]$ [299]. The tubular clusters $Os_{10}(CO)_{24}[Au(PPh_2R)]_4$ (where R = Me, Ph) have been synthesized and fully characterized. The inability of Polyhedral Skeletal Electron Pair Theory to accurately predict the observed 132-electron count is discussed with respect to the polarity of the heterometallic OsAu bonds [300]. Treatment of $[Ru_6C(CO)_{16}]^{2-}$ with CuCl affords the cluster $[\{Ru_6Cu_2C(CO)_{16}\}_2Cl]^{2-}$ in quantitative yield. The Ru_6 octahedra are linked together by a rectangular planar motif of copper atoms, as determined by X-ray diffraction analysis [301]. Sodium benzophenone reduction of $[PPN]_2[Os_{18}Hg_xC_2(CO)_{42}]$ (where $x=2$, 3) gives the hexaanionic cluster $[Os_{18}Hg_xC_2(CO)_{42}]^{6-}$, which was characterized by IR spectroscopy and by its chemical reactivity. Chromatographic work-up afforded the tetraanionic cluster $[Os_{18}HgC_2(CO)_{42}]^{4-}$ [302]. New titanium(IV) oxo alkoxy carboxylates have been prepared from $Ti(OR)_4$ and $Co_3(CO)_9(\mu_3\text{-}CCO_2H)$. The new complexes isolated and characterized include $Ti_6(\mu_3\text{-}O)_4(\mu\text{-}OEt)_8[\mu\text{-}(CO)_9Co_3(\mu_3\text{-}CCO_2)]_4$, $Ti_4(\mu_3\text{-}O)_4(OPr^i)_4[\mu\text{-}(CO)_9Co_3(\mu_3\text{-}CCO_2)]_4$ and $Ti_4(\mu_3\text{-}O)_4(OPh)_4[\mu\text{-}(CO)_9\text{-}Co_3(\mu_3\text{-}CCO_2)]_4$ [303]. The reaction between $[Ni_6(CO)_{12}]^{2-}$ and $Pd(PPh_3)_2Cl_2$ affords $[Pd_{33}Ni_6(CO)_{41}(PPh_3)_6]^{4-}$, whose pseudo-$D_{3h}$ hcp $Pd_{33}Ni_6$ core was confirmed by X-ray analysis. The 518-electron count found for this cluster is in agreement with PSEP Theory [304].

4. Abbreviations

acac	acetylacetonate
Ad	adamantyl
ampy	2-amino-6-methylpyridinate
binap	2,2′-bis(diphenylphosphino)-1,1′-binapthyl
bma	2,3-bis(diphenylphosphino)maleic anhydride
bped	4,5-bis(diphenylphosphino)-4-cyclopenten-1,3-dione
bpnap	2,2′-bis[(1,1′-biphenyl-2,2′-diyl)phosphite]-1,1′- binaphthyl
bpy	2,2′-bipyridine
COD	1,5-cyclooctadiene
Cp	cyclopentadienyl
Cp*	pentamethylcyclopentadienyl
Cy	cyclohexyl
DBU	1,8-diazabicyclo[5.4.0]undec-7-ene
dmpm	bis(dimethylphosphino)methane
dpam	$Ph_2AsCH_2AsPh_2$
dpmp	$(Ph_2PCH_2)_2PPh$
dppa	1,2-bis(diphenylphosphino)acetylene

dppb	1,4-bis(diphenylphosphino)butane
dppe	1,2-bis(diphenylphosphino)ethane
dppf	1,1′-bis(diphenylphosphino)ferrocene
dpph	1,6-bis(diphenylphosphino)hexane
dppip	diphenylphosphinoisopropane
dppm	bis(diphenylphosphino)methane
dppp	1,3-bis(diphenylphosphino)propane
Fc	ferrocenyl
MAS	magic angle spinning
Mes	mesityl
MeCp	methylcyclopentadienyl
PPN	bis(triphenylphosphine)iminium
Py	pyridine
Tol	tolyl
Xyl	2,6-xylyl

References

[1] R.W. Day, Diss. Abstr. B 56 (1996) 6104, DANN00365.
[2] M.A. Mansour, Diss. Abstr. B 57 (1996) 3730, DA9635564.
[3] G. Bhandari, Diss. Abstr. B 57 (1996) 3725, DA9632566.
[4] J. Chen, Diss. Abstr. B 3762 (1996) 3762, DANN96964.
[5] S.B. Falloon, Diss. Abstr. B 56 (1996) 4306, DA9541218.
[6] L. Hao, Diss. Abstr. B 56 (1996) 5483, DANN99256.
[7] Y. Wei, Diss. Abstr. B 56 (1996) 6741, DANN02612.
[8] G.N. Harakas, Diss. Abstr. B 57 (1996) 1788, DA9623841.
[9] P.D. Lane, Diss. Abstr. B 57 (1996) 2558, DA9624405.
[10] W. Paw, Diss. Abstr. B 56 (1996) 3757, DA9538116.
[11] F.J. Safarowic, Diss. Abstr. B 56 (1996) 3758, DA9538122.
[12] X. Qu, Diss. Abstr. B 56 (1996) 4310, DA9541248.
[13] R.L. Holliday, Diss. Abstr. B 56 (1996) 4878, DA9602265.
[14] J.F. Corrigan, Diss. Abstr. B 56 (1996) 5482, DANN99788.
[15] E.P. Boyd, Diss. Abstr. B 56 (1996) 6734, DA9612156.
[16] G. Proulx, Diss. Abstr. B 57 (1996) 1790, DA9621323.
[17] L.C.-F. Chao, Diss. Abstr. B 57 (1996) 1785, DANN05829.
[18] J.R. Eveland, Diss. Abstr. B 57 (1996) 3195, DA9631073.
[19] D.E. Gindelberger, Acta Cryst. C52 (1996) 2493.
[20] R. Andres, M. Galakhov, M.P. Gómez-Sal, A. Martín, M. Mena, C. Santamaría, J. Organomet. Chem. 526 (1996) 135.
[21] D. Osella, M. Ravera, C. Floriani, E. Solari, J. Organomet. Chem. 510 (1996) 45.
[22] C.D. Abernethy, F. Bottomley, A. Decken, T.S. Cameron, Organometallics 15 (1996) 1758.
[23] M.H. Chisholm, K.S. Kramer, J. Chem. Soc. Chem. Commun. (1996) 1331.
[24] Y. Shi, S. Lu, H. Gao, Q. Wu, N. Hu, J. Organomet. Chem. 514 (1996) 183.
[25] S. Poder-Guillou, P. Schollhammer, F.Y. Pétillon, J. Talarmin, S.E. Girdwood, K.W. Muir, J. Organomet. Chem. 506 (1996) 321.
[26] L.-C. Song, J.-Q. Wang, Q.-M. Hu, X.-Y. Huang, Polyhedron 15 (1996) 2453.
[27] R.E. Cramer, K. Yamada, H. Kawaguchi, K. Tatsumi, Inorg. Chem. 35 (1996) 1743.
[28] R. Seidel, B. Schnautz, G. Henkel, Angew. Chem., Int. Ed. Engl. 35 (1996) 1710.
[29] H.-J. Haupt, R. Wittbecker, U. Flörke, J. Organomet. Chem. 518 (1996) 213.

[30] C.V. Depree, L. Main, B.K. Nicholson, K. Roberts, J. Organomet. Chem. 517 (1996) 201.
[31] R.D. Adams, M. Huang, J.H. Yamamoto, L. Zhang, Chem. Ber. 129 (1996) 137.
[32] M.I. Bruce, P.J. Low, J. Organomet. Chem. 519 (1996) 221.
[33] R. Alberto, R. Schibli, P.A. Schubiger, U. Abram, R. Hübener, H. Berke, T.A. Kaden, J. Chem. Soc. Chem. Commun. (1996) 1291.
[34] H.C. Horng, C.P. Cheng, C.S. Yang, G.-H. Lee, Organometallics 15 (1996) 2543.
[35] T. Beringhelli, G. D'Alfonso, M.G. Garavaglia, J. Chem. Soc. Dalton Trans. (1996) 1771.
[36] T. Beringhelli, G. D'Alfonso, M. Freni, A.P. Minoja, Inorg. Chem. 35 (1996) 2393.
[37] M. Bergamo, T. Beringhelli, G. D'Alfonso, G. Ciani, M. Moret, A. Sironi, Organometallics 15 (1996) 3876.
[38] A. Sironi, Inorg. Chem. 35 (1996) 1725.
[39] D. Braga, F. Grepioni, E. Tedesco, K. Biradha, G.R. Desiraju, Organometallics 15 (1996) 2692.
[40] A.K. Hughes, K.L. Peat, K. Wade, J. Chem. Soc. Dalton Trans. (1996) 4639.
[41] F. Kakiuchi, M. Yamauchi, N. Chatani, S. Murai, Chem. Lett. (1996) 111.
[42] N. Chatani, T. Fukuyama, F. Kakiuchi, S. Murai, J. Am. Chem. Soc. 118 (1996) 493.
[43] S. Cenini, F. Ragaini, S. Tollari, D. Paone, J. Am. Chem. Soc. 118 (1996) 11964.
[44] M. Haukka, T. Venäläinen, P. Hirva, T.A. Pakkanen, J. Organomet. Chem. 509 (1996) 163.
[45] A.J. Blake, P.J. Dyson, P.E. Gaede, B.F.G. Johnson, S. Parsons, Organometallics 15 (1996) 4100.
[46] A.J. Arce, Y. De Sanctis, R. Machado, J. Manzur, M.V. Capparelli, Organometallics 15 (1996) 1834.
[47] A.J. Blake, P.J. Dyson, P.E. Gaede, B.F.G. Johnson, Inorg. Chim. Acta 241 (1996) 11.
[48] P.E. Gaede, B.F.G. Johnson, M. McPartlin, M.-A. Pearsall, J. Chem. Soc. Dalton Trans. (1996) 4621.
[49] P.E. Gaede, S. Parsons, B.F.G. Johnson, J. Chem. Soc. Dalton Trans. (1996) 3833.
[50] K.O. Kallinen, M. Ahlgrén, T.T. Pakkanen, T.A. Pakkanen, J. Organomet. Chem. 510 (1996) 37.
[51] M.-J. Arce, A.L. Viado, S.I. Khan, Y. Rubin, Organometallics 15 (1996) 4340.
[52] H.-F. Hsu, J.R. Shapley, J. Am. Chem. Soc. 118 (1996) 9192.
[53] F. Ragaini, Organometallics 15 (1996) 3572.
[54] S. Bhaduri, N. Sapre, P.G. Jones, J. Organomet. Chem. 509 (1996) 105.
[55] M.I. Bruce, B.C. Hall, B.W. Skelton, A.H. White, Aust. J. Chem. 49 (1996) 1019.
[56] M.C. Crossman, J. Fawcett, E.G. Hope, D.R. Russell, J. Organomet. Chem. 514 (1996) 87.
[57] S. Rivomanana, C. Mongin, G. Lavigne, Organometallics 15 (1996) 1195.
[58] V.N. Lebedev, D.F. Mullica, E.L. Sappenfield, F.G.A. Stone, Organometallics 15 (1996) 1669.
[59] Y.-H. Liao, D.F. Mullica, E.L. Sappenfield, F.G.A. Stone, Organometallics 15 (1996) 5102.
[60] T. Takemori, H. Suzuki, M. Tanaka, Organometallics 15 (1996) 4346.
[61] S. Aime, W. Dastrù, R. Gobetto, J. Krause, L. Matas, A. Viale, Organometallics 15 (1996) 4967.
[62] D. Osella, M. Ravera, M. Vincenti, M. Salmain, G. Jaouen, Organometallics 15 (1996) 3037.
[63] J.U. Köhler, J. Lewis, P.R. Raithby, Angew. Chem., Int. Ed. Engl. 35 (1996) 993.
[64] M.I. Bruce, N.N. Zaitseva, B.W. Skelton, A.H. White, Inorg. Chim. Acta 250 (1996) 129.
[65] K.J. Adams, J.J. Barker, S.A.R. Knox, A.G. Orpen, J. Chem. Soc. Dalton Trans. (1996) 975.
[66] V.V. Krivykh, O.A. Kizas, E.V. Vorontsov, F.M. Dolgushin, A.I. Yanovsky, Y.T. Struchkov, A.A. Koridze, J. Organomet. Chem. 508 (1996) 39.
[67] P. Grenouillet, C. de Bellefon, J. Organomet. Chem. 513 (1996) 155.
[68] F.J. Safarowic, J.B. Keister, Organometallics 15 (1996) 3310.
[69] J.A.K. Bauer, J.-H. Chung, E.P. Boyd, J. Liu, D.S. Strickland, H.-J. Kneuper, J.R. Shapley, S.G. Shore, Inorg. Chem. 35 (1996) 1405.
[70] B.K. Das, M.G. Kanatzidis, J. Organomet. Chem. 513 (1996) 1.
[71] C.J. Cardin, D.J. Cardin, M.A. Convery, M.M. Devereux, B. Twamley, J. Silver, J. Chem. Soc. Dalton Trans. (1996) 3145.
[72] R. Reina, O. Rossell, M. Seco, M.A. Pellinghelli, A. Tiripicchio, D. de Montauzon, Organometallics 15 (1996) 5347.
[73] W.K. Leong, F.W.B. Einstein, R.K. Pomeroy, Organometallics 15 (1996) 1589.
[74] C.J. Cardin, D.J. Cardin, M.A. Convery, Z. Dauter, D. Fenske, M.M. Devereux, M.B. Power, J. Chem. Soc. Dalton Trans. (1996) 1133.
[75] L. Xu, S.L. Gipson, Polyhedron 15 (1996) 2211.

[76] H. Adams, X. Chen, B.E. Mann, J. Chem. Soc. Dalton Trans. (1996) 2159.
[77] A.J. Deeming, C.M. Martin, J. Chem. Soc. Chem. Commun. (1996) 53.
[78] A.M.Z. Slawin, M.B. Smith, J.D. Woollins, J. Chem. Soc. Chem. Commun. (1996) 2095.
[79] R.A. Harding, A.K. Smith, J. Chem. Soc. Dalton Trans. (1996) 117.
[80] M.I. Bruce, N.N. Zaitseva, B.W. Skelton, A.H. White, J. Organomet. Chem. 515 (1996) 143.
[81] F.W. Heinemann, H.-C. Böttcher, J. Organomet. Chem. 526 (1996) 145.
[82] M.I. Bruce, P.A. Humphrey, B.W. Skelton, A.H. White, J. Organomet. Chem. 526 (1996) 85.
[83] Y.-Y. Choi, W.-Y. Wong, W.-T. Wong, J. Organomet. Chem. 518 (1996) 227.
[84] M.I. Bruce, P.A. Humphrey, B.W. Skelton, A.H. Allen, J. Organomet. Chem. 522 (1996) 259.
[85] H.-C. Böttcher, H. Thönnessen, P.G. Jones, R. Schmutzler, J. Organomet. Chem. 520 (1996) 15.
[86] R. Gobetto, C.G. Arena, D. Drommi, F. Faraone, Inorg. Chim. Acta 248 (1996) 257.
[87] T.J. Safarowic, D.J. Bierdeman, J.B. Keister, J. Am. Chem. Soc. 118 (1996) 11805.
[88] B.F.G. Johnson, J. Lewis, E. Nordlander, P.R. Raithby, J. Chem. Soc. Dalton Trans. (1996) 3825.
[89] M. Koike, D.H. Hamilton, S.R. Wilson, J.R. Shapley, Organometallics 15 (1996) 4930.
[90] B.F.G. Johnson, J. Lewis, E. Nordlander, S.M. Owen, P.R. Raithby, J. Chem. Soc. Dalton Trans. (1996) 1567.
[91] B.F.G. Johnson, J. Lewis, L. Nordlander, P.R. Raithby, J. Chem. Soc. Dalton Trans. (1996) 755.
[92] H.-G. Ang, K.-W. Ang, S.-G. Ang, A.L. Rheingold, J. Chem. Soc. Dalton Trans. (1996) 3131.
[93] H.-G. Ang, S.-G. Ang, Q. Zhang, J. Chem. Soc. Dalton Trans. (1996) 2773.
[94] H.-G. Ang, S.-G. Ang, Q. Zhang, J. Chem. Soc. Dalton Trans. (1996) 3843.
[95] H.G. Ang, S.G. Ang, S.W. Du, B.H. Snow, A.L. Rheingold, J. Organomet. Chem. 510 (1996) 13.
[96] H. Shen, S.G. Bott, M.G. Richmond, Inorg. Chim. Acta 241 (1996) 71.
[97] P. Baistrocchi, M. Careri, D. Cauzzi, C. Graiff, M. Landfranchi, P. Manini, G. Predieri, A. Tiripicchio, Inorg. Chim. Acta 252 (1996) 367.
[98] L.-P. Lorenz, W. Pohl, K. Polborn, Chem. Ber. 129 (1996) 11.
[99] H. Shen, S.G. Bott, M.G. Richmond, Inorg. Chim. Acta 247 (1996) 161.
[100] K.K. Hong, W.T. Wong, Inorg. Chem. 35 (1996) 5393.
[101] K.K.H. Lee, W.T. Wong, J. Chem. Soc. Chem. Commun. (1996) 3911.
[102] K.K.H. Lee, W.T. Wong, J. Chem. Soc. Dalton Trans. (1996) 1707.
[103] J.-K. Shen, F. Basolo, P. Nombel, N. Lugan, G. Lavigne, Inorg. Chem. 35 (1996) 755.
[104] W. Imhof, J. Chem. Soc. Dalton Trans. (1996) 1429.
[105] H.G. Ang, L.L. Koh, G.Y. Yang, J. Chem. Soc. Dalton Trans. (1996) 1573.
[106] W.-Y. Wong, W.-T. Wong, J. Chem. Soc. Dalton Trans. (1996) 1853.
[107] B.K.-M. Bui, W.-T. Wong, J. Chem. Soc. Dalton Trans. (1996) 2177.
[108] H.G. Ang, L.L. Koh, S.G. Ang, S.Y. Ng, G.Y. Yang, J. Chem. Soc. Dalton Trans. (1996) 4083.
[109] J.-T. Hung, S. Kumaresan, L.-C. Lin, Y.-S. Wen, L.-K. Liu, K.-L. Lu, J.R. Hwu, Organometallics 15 (1996) 5605.
[110] J.A. Cabeza, I. del Rio, J.M. Fernández-Colinas, V. Riera, Organometallics 15 (1996) 449.
[111] J.A. Cabeza, I. del Rio, A. Llamazares, V. Riera, J. Organomet. Chem. 511 (1996) 103.
[112] J.A. Cabeza, M.A. Martínez-García, V. Riera, S. García-Granda, J.F. Van der Maelen, J. Organomet. Chem. 514 (1996) 197.
[113] P.L. Andreu, J.A. Cabeza, I. del Rio, V. Riera, C. Bois, Organometallics 15 (1996) 3084.
[114] M.P. Cifuentes, M.G. Humphrey, B.W. Skelton, A.H. White, J. Organomet. Chem. 513 (1996) 201.
[115] K.A. Azam, R. Dilshad, S.E. Kabir, K. Khatoon, L. Nessa, M.M. Rahman, E. Rosenberg, M.B. Hursthouse, K.M.A. Malik, A.J. Deeming, J. Chem. Soc. Dalton Trans. (1996) 1731.
[116] S.E. Kabir, D.S. Kolwaite, E. Rosenberg, L.G. Scott, T. McPhillips, R. Duque, M. Day, K.I. Hardcastle, Organometallics 15 (1996) 1979.
[117] S.E. Kabir, E. Rosenberg, J. Stetson, M. Yin, J. Ciurash, K. Mnatsakanova, K.I. Hardcastle, H. Noorani, N. Movsesian, Organometallics 15 (1996) 4473.
[118] K. Singh, W.R. McWhinnie, H.L. Chen, M. Sun, T.A. Hamor, J. Chem. Soc. Dalton Trans. (1996) 1545.
[119] W. Paw, D.K. Bower, D.J. Bierdeman, J.B. Keister, E.M. Schulman, J. Coord. Chem. 39 (1996) 199.
[120] E.W. Ainscough, A.M. Brodie, R.K. Coll, A.J.A. Mair, J.M. Waters, J. Organomet. Chem. 509 (1996) 259.

[121] F. Calderoni, F. Demartin, M.C. Iapalucci, F. Laschi, G. Longoni, P. Zanello, Inorg. Chem. 35 (1996) 898.
[122] G. Rheinwald, H. Stoeckli-Evans, G. Süss-Fink, J. Organomet. Chem. 512 (1996) 27.
[123] L.A. Hoferkamp, G. Rheinwald, H. Stoeckli-Evans, G. Süss-Fink, Organometallics 15 (1996) 704.
[124] G. Süss-Fink, G. Rheinwald, H. Stoeckli-Evans, C. Bolma, D. Kaufmann, Inorg. Chem. 35 (1996) 3081.
[125] W.-Y. Yeh, C. Stern, D.F. Shriver, Inorg. Chem. 35 (1996) 7857.
[126] E.W. Ainscough, A.M. Brodie, R.K. Coll, T.G. Kotch, A.J. Lees, A.J.A. Mair, J.M. Waters, J. Organomet. Chem. 517 (1996) 173.
[127] A.J. Deeming, S.N. Jayasuriya, A.J. Arce, Y. De Sanctis, Organometallics 15 (1996) 786.
[128] W.K. Leong, F.W.B. Einstein, R.K. Pomeroy, Organometallics 15 (1996) 1582.
[129] M. Shieh, C. Sheu, L.-F. Ho, J.-J. Cherng, L.-F. Jang, C.-H. Ueng, S.-M. Peng, G.-H. Lee, Inorg. Chem. 35 (1996) 5504.
[130] P. Mathur, A.K. Dash, M.M. Hossain, C.V.V. Satyanarayana, B. Verghese, J. Organomet. Chem. 506 (1996) 307.
[131] P.E. Gaede, S. Parsons, B.F.G. Johnson, J. Chem. Soc. Dalton Trans. (1996) 4629.
[132] B.F.G. Johnson, C.M. Martin, A.J. Blake, D. Reed, D. Braga, F. Grepioni, J. Chem. Soc. Dalton Trans. (1996) 2165.
[133] K. Hashizume, Y. Mizobe, M. Hidai, Organometallics 15 (1996) 3303.
[134] H. Matsuzaka, J.-P. Qü, T. Ogino, M. Nishio, Y. Nishibayashi, Y. Ishii, S. Uemura, M. Hidai, J. Chem. Soc. Dalton Trans. (1996) 4307.
[135] P.E. Gaede, B.F.G. Johnson, J.F. Nixon, M. Nowotny, S. Parsons, J. Chem. Soc. Chem. Commun. (1996) 1455.
[136] D. Braga, F. Grepioni, D.B. Brown, B.F.G. Johnson, M.J. Calhorda, Organometallics 15 (1996) 5723.
[137] Y. Chi, A.J. Carty, P. Blenkiron, E. Delgado, G.D. Enright, W. Wang, S.-M. Peng, G.-H. Lee, Organometallics 15 (1996) 5269.
[138] W. Wang, J.F. Corrigan, S. Doherty, G.D. Enright, N.J. Taylor, A.J. Carty, Organometallics 15 (1996) 2770.
[139] D. Braga, F. Grepioni, J. Chem. Soc. Chem. Commun. (1996) 571.
[140] W.K. Leong, F.W.B. Einstein, R.K. Pomeroy, Acta Cryst. C52 (1996) 1607.
[141] A.J. Pöe, Y. Zheng, Inorg. Chim. Acta 252 (1996) 311.
[142] C.J. Adams, M.I. Bruce, B.W. Skelton, A.H. White, J. Organomet. Chem. 513 (1996) 255.
[143] C.J. Adams, M.I. Bruce, B.W. Skelton, A.H. White, J. Organomet. Chem. 506 (1996) 191.
[144] C.J. Adams, M.I. Bruce, B.W. Skelton, A.H. White, J. Chem. Soc. Chem. Commun. (1996) 969.
[145] C.J. Adams, M.I. Bruce, B.W. Skelton, A.H. White, J. Chem. Soc. Chem. Commun. (1996) 2663.
[146] B.F.G. Johnson, P.J. Dyson, C.M. Martin, J. Chem. Soc. Dalton Trans. (1996) 2395.
[147] W.-Y. Wong, W.-T. Wong, J. Organomet. Chem. 513 (1996) 27.
[148] L.A. Hoferkamp, G. Rheinwald, H. Stoeckli-Evans, G. Süss-Fink, Organometallics 15 (1996) 1122.
[149] H.G. Ang, L.L. Koh, G.Y. Yang, J. Chem. Soc. Chem. Commun. (1996) 1075.
[150] W.G.-Y. Ho, W.-T. Wong, Polyhedron 15 (1996) 165.
[151] R.D. Pergola, C. Bandini, F. Demartin, E. Diana, L. Garlaschelli, P.L. Stanghellini, P. Zanello, J. Chem. Soc. Dalton Trans. (1996) 747.
[152] M.J. Dale, P.J. Dyson, B.F.G. Johnson, P.R.R. Langridge-Smith, H.T. Yates, J. Chem. Soc. Dalton Trans. (1996) 771.
[153] V.S. Kaganovich, M.I. Rybinskaya, Z.A. Kerzina, F.M. Dolgushin, A.I. Yanovsky, Y.T. Struchkov, P.V. Petrovskii, J. Kivikoski, J. Valkonen, K. Laihia, J. Organomet. Chem. 518 (1996) 115.
[154] T. Chihara, K. Komori, H. Ogawa, Y. Wakatsuki, J. Organomet. Chem. 515 (1996) 27.
[155] A.J. Edwards, B.F.G. Johnson, S. Parsons, D.S. Shephard, J. Chem. Soc. Dalton Trans. (1996) 3837.
[156] T. Chihara, K. Sawamura, H. Ikezawa, H. Ogawa, Y. Wakatsuki, Organometallics 15 (1996) 415.
[157] P.J. Bailey, M.A. Beswick, B.F.G. Johnson, J. Lewis, M. McPartlin, P.R. Raithby, M.C.R. de Arellano, J. Chem. Soc. Dalton Trans. (1996) 3515.
[158] M.P. Cifuentes, M.G. Humphrey, B.W. Skelton, A.H. White, J. Organomet. Chem. 507 (1996) 163.
[159] M.P. Cifuentes, M.G. Humphrey, A.C. Willis, J. Organomet. Chem. 513 (1996) 85.

[160] P. Mercandelli, A. Sironi, J. Am. Chem. Soc. 118 (1996) 11548.
[161] M.E. Smith, R.A. Andersen, Organometallics 15 (1996) 2680.
[162] O.J. Scherer, G. Berg, G. Wolmershäuser, Chem. Ber. 129 (1996) 53.
[163] H. Wadepohl, T. Borchert, H. Pritzkow, J. Organomet. Chem. 516 (1996) 187.
[164] H. Wadepohl, M.J. Calhorda, M. Herrmann, C. Jost, P.E.M. Lopes, H. Pritzkow, Organometallics 15 (1996) 5622.
[165] G. Gervasio, S. Vastag, G. Bor, G. Natile, L. Markó, Inorg. Chim. Acta 251 (1996) 35.
[166] U. Ritter, N. Winkhofer, H.-G. Schmidt, H.W. Roesky, Angew. Chem., Int. Ed. Engl. 35 (1996) 524.
[167] U. Ritter, N. Winkhofer, R. Murugavel, A. Voigt, D. Stalke, H.W. Roesky, J. Am. Chem. Soc. 118 (1996) 8580.
[168] H. Shen, S.G. Bott, M.G. Richmond, Inorg. Chim. Acta 250 (1996) 195.
[169] G.A. Acum, M.J. Mays, P.R. Raithby, G.A. Solan, J. Organomet. Chem. 508 (1996) 137.
[170] C. Renouard, G. Rheinwald, H. Stoeckli-Evans, G. Süss-Fink, D. Braga, F. Grepioni, J. Chem. Soc. Dalton Trans. (1996) 1875.
[171] C.-G. Xia, K. Yang, S.G. Bott, M.G. Richmond, Organometallics 15 (1996) 4480.
[172] R. Settambolo, A. Caiazzo, R. Lazzaroni, J. Organomet. Chem. 506 (1996) 337.
[173] M. Cheong, M.-N. Kim, J.Y. Shim, J. Organomet. Chem. 520 (1996) 253.
[174] B. Moasser, W.L. Gladfelter, Inorg. Chim. Acta 242 (1996) 125.
[175] F. Azzaroni, P. Biscarini, S. Bordoni, G. Longoni, E. Ventutini, J. Organomet. Chem. 508 (1996) 59.
[176] M. Lenarda, L. Storaro, R. Ganzerla, J. Mol. Catal. A 111 (1996) 203.
[177] R. Lazzaroni, G. Uccello-Barretta, S. Scamuzzi, R. Settambolo, A. Caiazzo, Organometallics 15 (1996) 4657.
[178] W.H. Watson, A. Nagl, M.-J. Don, M.G. Richmond, J. Chem. Crystallogr. 26 (1996) 75.
[179] C. Tejel, Y.-M. Shi, M.A. Ciriano, A.J. Edwards, F.J. Lahoz, L.A. Oro, Angew. Chem., Int. Ed. Engl. 35 (1996) 633.
[180] C. Tejel, Y.-M. Shi, M.A. Ciriano, A.J. Edwards, F.J. Lahoz, L.A. Oro, Angew. Chem., Int. Ed. Engl. 35 (1996) 1516.
[181] K. Wajda-Hermanowicz, F. Pruchnik, M. Zuber, J. Organomet. Chem. 508 (1996) 75.
[182] R. Ros, R. Bertani, A. Tassan, D. Braga, F. Grepioni, E. Tedesco, Inorg. Chim. Acta 244 (1996) 11.
[183] T. Nishioka, S. Nakamura, Y. Kaneko, T. Suzuki, I. Kinoshita, S. Kiyooka, K. Isobe, Chem. Lett. (1996) 911.
[184] C.G. Arena, D. Drommi, F. Faraone, M. Lanfranchi, F. Nicolò, A. Tiripicchio, Organometallics 15 (1996) 3170.
[185] T. Sugioka, S.-W. Zhang, N. Morii, T. Joh, S. Takahashi, Chem. Lett. (1996) 249.
[186] M. Kaupp, Chem. Ber. 129 (1996) 527.
[187] S. Onaka, M. Otsuka, S. Takagi, K. Sako, J. Coord. Chem. 37 (1996) 151.
[188] H. Kurakata, Y. Izumi, K. Aika, J. Chem. Soc. Chem. Commun. (1996) 389.
[189] T. Tanase, Y. Yamamoto, R.J. Puddephatt, Organometallics 15 (1996) 1502.
[190] E. Alonso, J. Forniés, C. Fortuño, A. Martín, A.G. Orpen, J. Chem. Soc. Chem. Commun. (1996) 231.
[191] P.D. Harvey, K. Hierso, P. Braunstein, X. Morise, Inorg. Chim. Acta 250 (1996) 337.
[192] J.I. Henderson, S. Feng, G.M. Ferrence, T. Bein, C.P. Kubiak, Inorg. Chim. Acta 242 (1996) 115.
[193] T. Zhang, M. Drouin, P.D. Harvey, J. Chem. Soc. Chem. Commun. (1996) 877.
[194] J. Washington, C.P. Kubiak, Can. J. Chem. 74 (1996) 2503.
[195] P.D. Harvey, R. Provencher, J. Gagnon, T. Zhang, D. Fortin, K. Hierso, M. Drouin, S.M. Socol, Can. J. Chem. 74 (1996) 2268.
[196] P. Leoni, S. Manetti, M. Pasquali, A. Albinati, Inorg. Chem. 35 (1996) 6045.
[197] A.C. Albéniz, P. Espinet, Y.-S. Lin, A.G. Orpen, A. Martín, Organometallics 15 (1996) 5003.
[198] L. Hao, J.J. Vittal, R.J. Puddephatt, Inorg. Chem. 35 (1996) 269.
[199] G.J. Spivak, L. Hao, J.J. Vittal, R.J. Puddephatt, J. Am. Chem. Soc. 118 (1996) 225.
[200] L. Hao, J.J. Vittal, R.J. Puddephatt, Organometallics 15 (1996) 3115.
[201] T. Yamamoto, T. Shido, S. Inagaki, Y. Fukushima, M. Ichikawa, J. Am. Chem. Soc. 118 (1996) 5810.

[202] F. Calderoni, F. Demartin, M.C. Iapalucci, G. Longoni, Angew. Chem., Int. Ed. Engl. 35 (1996) 2225.
[203] V.W.-W. Yam, W.-K. Lee, K.-K. Cheung, B. Crystall, D. Phillips, J. Chem. Soc. Dalton Trans. (1996) 3283.
[204] Y. Cheng, T.J. Emge, J.G. Brennan, Inorg. Chem. 35 (1996) 7339.
[205] V.W.-W. Yam, W.-K. Lee, K.K. Cheung, H.-K. Lee, W.-P. Leung, J. Chem. Soc. Dalton Trans. (1996) 2889.
[206] P. Mathur, P. Sekar, C.V.V. Satyanarayana, M.F. Mahon, J. Chem. Soc. Dalton Trans. (1996) 2173.
[207] Y. Mizobe, M. Hosomizu, Y. Kubota, M. Hidai, J. Organomet. Chem. 507 (1996) 179.
[208] L.-C. Song, Y.-B. Dong, Q.-M. Hu, J. Sun, Organometallics 15 (1996) 1954.
[209] Q.-L. Wang, S.-N. Chen, X. Wang, G.-M. Wu, W.-H. Sun, H.-Q. Wang, S.-Y. Yang, Polyhedron 15 (1996) 2613.
[210] S.N. Konchenko, A.V. Virovets, S.V. Tkachev, V.I. Alekseev, N.V. Podberezskaya, Polyhedron 15 (1996) 1221.
[211] W. Heping, Y. Yuanqi, Y. Qingchuan, Polyhedron 15 (1996) 43.
[212] K.L. Malisza, L. Li, M.J. McGlinchey, Can. J. Chem. 74 (1996) 1021.
[213] H. Adams, L.J. Gill, M.J. Morris, Organometallics 15 (1996) 4182.
[214] W.-F. Liaw, C.-Y. Chuang, W.-Z. Lee, C.-K. Lee, G.-H. Lee, S.-M. Peng, Inorg. Chem. 35 (1996) 2530.
[215] H.-L. Wu, G.-L. Lu, Y. Chi, L.J. Farrugia, S.-M. Peng, G.-H. Lee, Inorg. Chem. 35 (1996) 6015.
[216] M.I. Bruce, P.J. Low, B.W. Skelton, A.H. White, J. Organomet. Chem. 515 (1996) 65.
[217] D. Braga, L.J. Farrugia, A.L. Gillon, F. Grepioni, E. Tedesco, Organometallics 15 (1996) 4684.
[218] L.J. Farrugia, A.M. Senior, D. Braga, F. Grepioni, A. G. Orpen, J.G. Crossley, J. Chem. Soc. Dalton Trans. (1996) 631.
[219] P. Mathur, P. Sekar, C.V.V. Satyanarayana, M.F. Mahon, J. Organomet. Chem. 522 (1996) 291.
[220] J. Müller, I. Sonn, T. Akhnoukh, J. Organomet. Chem. 506 (1996) 113.
[221] C.E. Shuchart, M. Calligaris, M.R. Churchill, P. Faleschini, R.F. See, A. Wojcicki, Inorg. Chim. Acta 243 (1996) 109.
[222] H.-P. Wu, Y.-Q. Yin, Q.-C. Yang, Inorg. Chim. Acta 245 (1996) 143.
[223] M.-J. Don, K. Yang, S.G. Bott, M.G. Richmond, J. Coord. Chem. 40 (1996) 273.
[224] C.S. Jun, A.K. Bandyopadhyay, T.P. Fehlner, Inorg. Chem. 35 (1996) 2189.
[225] J. Cooke, R.E.D. McClung, J. Takats, R.D. Rogers, Organometallics 15 (1996) 4459.
[226] H. Shan, P.R. Sharp, Angew. Chem., Int. Ed. Engl. 35 (1996) 635.
[227] M.T. Pinillos, A. Elduque, E. Berkovich, L.A. Oro, J. Organomet. Chem. 509 (1996) 89.
[228] T. Tanase, H. Toda, K. Kobayashi, Y. Yamamoto, Organometallics 15 (1996) 5272.
[229] J.M. Casas, L.R. Falvello, J. Formiés, A. Martin, Inorg. Chem. 35 (1996) 7867.
[230] F. Canales, M.C. Gimeno, A. Laguna, P.G. Jones, J. Am. Chem. Soc. 118 (1996) 4839.
[231] M. Contel, J. Garrido, M.C. Gimeno, P.G. Jones, A. Laguna, M. Laguna, Organometallics 15 (1996) 4939.
[232] R. Atencio, M.A. Casado, M.A. Ciriano, F.J. Lahoz, J.J. Pérez-Torrente, A. Tiripicchio, L.A. Oro, J. Organomet. Chem. 514 (1996) 103.
[233] G. Proulx, R.G. Bergman, J. Am. Chem. Soc. 118 (1996) 1981.
[234] J.W. Freeman, A.M. Arif, R.D. Ernst, Inorg. Chim. Acta 250 (1996) 15.
[235] S.M. Waterman, V.-A. Tolhurst, M.G. Humphrey, B.W. Skelton, A.H. White, J. Organomet. Chem. 515 (1996) 89.
[236] P. Mathur, M.M. Hossain, S.B. Umbarkar, C.V.V. Satyanarayana, A.L. Rheingold, L.M. Liable-Sands, G.P.A. Yap, Organometallics 15 (1996) 1898.
[237] J.W.-S. Hui, W.-T. Wong, Polyhedron 15 (1996) 541.
[238] J.T. Park, J.-H. Chung, H. Song, K. Lee, J.-H. Lee, J.-R. Park, I.-H. Suh, J. Organomet. Chem. 526 (1996) 215.
[239] H. Adams, N.A. Bailey, L.J. Gill, M.J. Morris, F.A. Wildgoose, J. Chem. Soc. Dalton Trans. (1996) 1437.
[240] H. Adams, N.A. Bailey, S.R. Gay, L.J. Gill, T. Hamilton, M.J. Morris, J. Chem. Soc. Dalton Trans. (1996) 2403.

[241] M.I. Bruce, B.W. Skelton, A.H. White, N.N. Zaitseva, J. Chem. Soc. Dalton Trans. (1996) 3151.
[242] H. Adams, L.J. Gill, M.J. Morris, J. Chem. Soc. Dalton Trans. (1996) 3909.
[243] W.R. Cullen, S.J. Rettig, H. Zhang, Inorg. Chim. Acta 251 (1996) 53.
[244] S.M. Waterman, M.G. Humphrey, V.-A. Tolhurst, B.W. Skelton, A.H. White, D.C.R. Hockless, Organometallics 15 (1996) 934.
[245] O. Rossell, M. Seco, G. Segalés, R. Mathieu, D. de Montauzon, J. Organomet. Chem. 509 (1996) 241.
[246] G.N. Harakas, B.R. Whittlesey, J. Am. Chem. Soc. 118 (1996) 4210.
[247] D.M. Norton, R.W. Eveland, J.C. Hutchison, C. Stern, D.F. Shriver, Organometallics 15 (1996) 3916.
[248] J. Chen, V.G. Young Jr., R.J. Angelici, Organometallics 15 (1996) 2727.
[249] M. Bergamo, T. Beringhelli, G. D'Alfonso, G. Ciani, M. Moret, A. Sironi, Organometallics 15 (1996) 1637.
[250] A.C. Härkönen, M. Ahlgrén, T.A. Pakkanen, J. Pursiainen, J. Organomet. Chem. 519 (1996) 205.
[251] H.J. Kakkonen, M. Ahlgrén, J. Pursiainen, T.A. Pakkanen, J. Organomet. Chem. 507 (1996) 147.
[252] H.J. Kakkonen, M. Ahlgrén, T.A. Pakkanen, J. Pursiainen, J. Organomet. Chem. 518 (1996) 203.
[253] P. Blenkiron, J.F. Corrigan, D. Pilette, N.J. Taylor, A.J. Carty, Can. J. Chem. 74 (1996) 2349.
[254] M.R. Churchill, R.F. See, C.E. Shuchart, A. Wojcicki, J. Organomet. Chem. 512 (1996) 189.
[255] J.R. Galsworthy, C.E. Housecroft, A.L. Rheingold, J. Chem. Soc. Dalton Trans. (1996) 2917.
[256] W.-Y. Wong, W.-T. Wong, J. Chem. Soc. Dalton Trans. (1996) 3209.
[257] S.-M. Lee, K.-K. Cheung, W.-T. Wong, J. Organomet. Chem. 506 (1996) 77.
[258] L.P. Clake, J.E. Davies, P.R. Raithby, G.P. Shields, J. Chem. Soc. Dalton Trans. (1996) 4147.
[259] S.L. Ingham, B.F.G. Johnson, P.R. Raithby, K.J. Taylor, L.J. Yellowlees, J. Chem. Soc. Dalton Trans. (1996) 3521.
[260] F. Canales, M.C. Gimeno, A. Laguna, P.J. Jones, Organometallics 15 (1996) 3412.
[261] A. Fumagalli, D. Italia, M.C. Malatesta, G. Ciani, M. Moret, A. Sironi, Inorg. Chem. 35 (1996) 1765.
[262] A. Pons, O. Rossell, M. Seco, X. Solans, M. Font-Bardia, J. Organomet. Chem. 514 (1996) 177.
[263] C. Archambault, R. Bender, P. Braunstein, A. De Cian, J. Fischer, J. Chem. Soc. Chem. Commun. (1996) 2729.
[264] S.P. Tunik, P.N. Shipil, A.V. Vlasov, V.R. Denisov, A.B. Nikol'skii, F.M. Dolgushin, A.I. Yanovsky, Y.T. Struchkov, J. Organomet. Chem. 515 (1996) 11.
[265] P. Mathur, P. Sekar, J. Chem. Soc. Chem. Commun. (1996) 727.
[266] X.-Y. Liu, V. Riera, M.A. Ruiz, A. Tiripicchio, M. Tiripicchio-Camellini, Organometallics 15 (1996) 974.
[267] C.-J. Su, P.-C. Su, Y. Chi, S.-M. Peng, G.-H. Lee, J. Am. Chem. Soc. 118 (1996) 3289.
[268] P. Mathur, M.M. Hossain, A.L. Rheingold, J. Organomet. Chem. 507 (1996) 187.
[269] M.I. Bruce, P.J. Low, A. Werth, B.W. Skelton, A.H. White, J. Chem. Soc. Dalton Trans. (1996) 1551.
[270] A.D. Hattersley, C.E. Housecroft, A.L. Rheingold, J. Chem. Soc. Dalton Trans. (1996) 603.
[271] M.H.A. Benvenutti, P.B. Hitchcock, J.F. Nixon, M.D. Vargas, J. Chem. Soc. Chem. Commun. (1996) 441.
[272] T. Adatia, I.D. Salter, Polyhedron 15 (1996) 597.
[273] J. Chen, V.G. Young Jr., R.J. Angelici, Organometallics 15 (1996) 1414.
[274] M. Ichikawa, W. Pan, Y. Imada, M. Yamaguchi, K. Isobe, T. Shido, J. Mol. Catal. A 107 (1996) 23.
[275] V.I. Kovalchuk, N.M. Mikova, N.V. Chesnokov, L.V. Naimushina, B.N. Kuznetsov, J. Mol. Catal. A 107 (1996) 329.
[276] R. Ugo, C. Dossi, R. Psaro, J. Mol. Catal. A 107 (1996) 13.
[277] D.E. Barber, R.F. Bryan, M. Sabat, K.S. Bose, B.A. Averill, Inorg. Chem. 35 (1996) 4635.
[278] H. Adams, L.J. Gill, M.J. Morris, Organometallics 15 (1996) 464.
[279] J.T. Lin, C.C. Yu, C.H. Lo, S.Y. Wang, T.Y.R. Tsai, M.M. Chen, Y.S. Wen, K.J. Lin, Organometallics 15 (1996) 2132.
[280] M.H.A. Benvenutti, P.B. Hitchcock, J.F. Nixon, M.D. Vargas, J. Chem. Soc. Dalton Trans. (1996) 739.

[281] S.G. Anema, K.M. Mackay, B.K. Nicholson, J. Chem. Soc. Dalton Trans. (1996) 3853.
[282] J. Wing-Sze, W.-T. Wong, J. Chem. Soc. Dalton Trans. (1996) 2887.
[283] O. Rossell, M. Seco, G. Segalés, B.F.G. Johnson, P.J. Dyson, S.L. Ingham, Organometallics 15 (1996) 884.
[284] P.M.N. Low, A.L. Tan, T.S.A. Hor, Y.-S. Wen, L.-K. Liu, Organometallics 15 (1996) 2595.
[285] G. Hsu, S.R. Wilson, J.R. Shapley, Inorg. Chem. 35 (1996) 923.
[286] S.M. Waterman, M.G. Humphrey, D.C.R. Hockless, Organometallics 15 (1996) 1745.
[287] J. Lewis, C.A. Morewood, P.R. Raithby, M.C.R. de Arellano, J. Chem. Soc. Dalton Trans. (1996) 4509.
[288] S. Chan, S.-M. Lee, Z. Lin, W.-T. Wong, J. Organomet. Chem. 510 (1996) 219.
[289] M. Ferrer, R. Reina, O. Rossell, M. Seco, G. Segalés, J. Organomet. Chem. 515 (1996) 205.
[290] I.D. Salter, V. Sik, S.A. Williams, T. Adatia, J. Chem. Soc. Dalton Trans. (1996) 643.
[291] Y.-K. Au, W.-T. Wong, J. Chem. Soc.,Dalton Trans. (1996) 899.
[292] V. Calvo-Perez, T.P. Fehlner, A.L. Rheingold, Inorg. Chem. 35 (1996) 7289.
[293] S. Ogo, T. Suzuki, Y. Ozawa, K. Isobe, Inorg. Chem. 35 (1996) 6093.
[294] M.S. Nashner, D.M. Somerville, P.D. Lane, D.L. Adler, J.R. Shapley, R.G. Nuzzo, J. Am. Chem. Soc. 118 (1996) 12964.
[295] M.I. Bruce, E. Horn, P.A. Humphrey, E.R.T. Tiekink, J. Organomet. Chem. 518 (1996) 121.
[296] K. Albert, K.M. Neyman, G. Pacchioni, N. Rösch, Inorg. Chem. 35 (1996) 7370.
[297] R.D. Adams, R. Layland, K. McBride, Organometallics 15 (1996) 5425.
[298] R.D. Adams, T.S. Barnard, J.E. Cortopassi, L. Zhang, Organometallics 15 (1996) 2664.
[299] T. Eguchi, B.T. Heaton, R. Harding, K. Miyagi, G. Longoni, J. Nähring, N. Nakamura, H. Nakayama, T.A. Pakkanen, J. Pursiainen, A.K. Smith, J. Chem. Soc. Dalton Trans. (1996) 625.
[300] Z. Akhter, S.L. Ingham, J. Lewis, P.R. Raithby, Angew. Chem., Int. Ed. Engl. 35 (1996) 992.
[301] M.A. Beswick, J. Lewis, P.R. Raithby, M.C.R. de Arellano, J. Chem. Soc. Dalton Trans. (1996) 4033.
[302] L.H. Gade, B.F.G. Johnson, J. Lewis, M. McPartlin, I.J. Scowen, J. Chem. Soc. Dalton Trans. (1996) 597.
[303] X. Lei, M. Shang, T.P. Fehlner, Organometallics 15 (1996) 3779.
[304] M. Kawano, J.W. Bacon, C.F. Campana, L.F. Dahl, J. Am. Chem. Soc. 118 (1996) 7869.